THE JOURNAL OF THE AMERICAN CERAMIC SOCIETY, NOVEMBER 1, 1943

THE JOURNAL

OF THE

AMERICAN CERAMIC SOCIETY

DECEMBER 1, 1943

MONTHLY PUBLICATION DEVOTED TO THE ARTS AND SCIENCES RELATED TO THE SILICATE INDUSTRIES

TABLE OF CONTENTS

Vol. 26 December, 1943 No. 12

THE JOURNAL

The Vitreous State 393–98

By M. L. Huggins, K.-H. Sun, and Alexander Silverman

Experimental Studies of Temperature Gradients in Glasses of Various Colors 398–404

By H. H. Holscher, R. R. Rough, and J. H. Plummer

Electrically Fused Forsterite-Olivine, I–II 405–13

By the Electrothermal Section of the Electrotechnical Laboratory

Duplication of Chrome-Brown Electrical Porcelain Glazes with Nonessential Materials 414

By R. B. Fuller and A. S. Watts

Author Index to *The Journal* 415–16

Subject Index to *The Journal* 416–24

Footnote Citations Index to *The Journal* 424–29

Publication Office: 20th & Northampton Sts., Easton, Pa.
Editorial Office: 2525 N. High St., Columbus 2, Ohio
Committee on Publications: J. D. Sullivan, *Chairman*; H. H. Blau, R. L. Stone, J. J. Canfield, H. Thiemecke, and R. C. Purdy, *ex officio*.
Entered as second-class matter at the post office at Easton, Pa., under the act of March 3, 1879. Published monthly.
Subscription fifteen dollars ($15.00) a year. Single numbers $1.50
(Foreign and Canadian postage, 50¢ additional on subscriptions)
(Copyright 1943, American Ceramic Society, Inc.)

Second Ceramic War Conference

FORTY-SIXTH ANNUAL MEETING

The American Ceramic Society, Inc.

Hotel William Penn, Pittsburgh, Pa.

April 2, 3, 4, and 5, 1944

Only Eight Weeks Remain in Which to Assemble the Program

"If the clock's ticking off its minutes does not stimulate the lazy, weary, or ambitionless man to accomplishment, the rolling years ultimately will overtake him while he is yet empty handed."—Dr. Dugald C. Jackson, "Biography of Frank Julian Sprague," Scientific Monthly, November, 1943.

Not Lazy, weary, or ambitionless

yet some will procrastinate

The Clock Ticks Off Time The World Moves On

The War Will End, Finding Many Unprepared

It Is Important That Ceramists Be Prepared

THE JOURNAL
OF
THE AMERICAN CERAMIC SOCIETY

Vol. 26 December 1, 1943 No. 12

THE VITREOUS STATE*

By Maurice L. Huggins,† Kuan-Han Sun,† and Alexander Silverman‡

Abstract

The difficulty of defining the vitreous state in a rigorous manner, the existence of many borderline cases, and the theoretical requirements which must be met if a substance is to be vitreous are discussed. Silicate glasses and certain other typical classes of vitreous substances are treated in some detail with especial reference to the relation between their structures and vitreous properties.

I. General Considerations

If a substance possesses a degree of rigidity comparable to that possessed by typical crystalline substances yet lacks the dependence on direction (characteristic of the crystalline state) of such properties as hardness, rate of growth and solution, and sometimes refractive index, it is said to be in the vitreous state.

From the structural point of view, the vitreous state of matter may be defined, alternatively, as that state in which the arrangement of the component atoms, ions, or molecules possesses a permanence similar to that in the crystalline state and a randomness similar to that characteristic of liquids.

The terms "vitreous substance," "vitreous solid," "amorphous solid," "supercooled liquid," "glass," and "plastic" may be considered to be practically synonymous. The term used by a given author at a given time is largely a matter of preference, depending in part on the type of characteristic property (e.g., rigidity, lack of directional properties, method of production) which it is desired to emphasize.

A rigorous definition of a vitreous substance is impossible without the introduction of purely arbitrary quantitative limiting values for the rigidity (or viscosity) and the dependence of various properties on direction or for the degree of permanence and lack of order in the atomic distribution. Rather than introduce such arbitrariness, it seems better to consider the term vitreous merely as a convenient descriptive adjective, realizing that there are many borderline cases to which the term may be applied or not as convenient.

On raising the temperature, most vitreous solids are transformed to liquids; the transformation, however, is gradual rather than sharp as is the change from the crystalline to the liquid states. A vitreous substance in the transition range has properties intermediate between those characteristic of an amorphous solid and those characteristic of a liquid. It may be described either as a very viscous liquid or as a plastic solid as suits one's fancy.

As examples of substances intermediate between vitreous solids and crystalline solids, glasses that are inhomogeneous and show a tendency toward crystallization and organic long-chain polymers, which have been given directional properties by stretching or cold drawing, may be mentioned.

Looking at the subject from an atomic point of view, the reasons for the existence of many borderline cases are obvious. Like atoms (or ions or groups of atoms) tend to be surrounded by other atoms (or ions or atomic groups) in a like manner. In any condensed system, that is, crystalline solid, vitreous solid, or liquid, there tends to be a regularity in the atomic distribution immediately surrounding each atom (or ion or group of atoms). If in addition to the local regularity there is also a long-distance regularity, the substance is crystalline; if not, it is a vitreous solid or a liquid, depending on the degree of permanence of the long-distance structure, which is a function of temperature.

A crystalline arrangement of atoms or molecules has (at least nearly always) a lower energy than a noncrystalline arrangement, although the difference is usually not large. If the interatomic (or interionic or intermolecular) forces tending to maintain a momentarily existing long-distance structure are small enough, the thermal vibrations of the atoms will cause the struc-

* Presented at the Forty-Fifth Annual Meeting, The American Ceramic Society, Pittsburgh, Pa., April 20, 1943 (Glass Division). Received April 3, 1943.

Communication No. 919 from the Kodak Research Laboratories. This paper is an abridgment of a portion of an article to be published soon in Volume V of Colloid Chemistry, Theoretical and Applied, edited by Jerome Alexander.

† Eastman Kodak Company, Rochester, N. Y.

‡ Department of Chemistry, University of Pittsburgh, Pittsburgh, Pa.

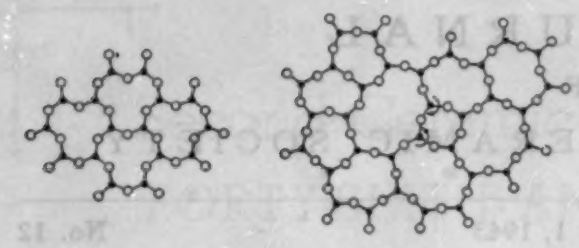

FIG. 1.—Two dimensional representations of (*a*) crystalline and (*b*) vitreous SiO_2 structures (after Zachariasen[8(a)] and Warren[7(a)]).

ture to change rapidly to a different structure and the substance is a liquid. If the substance is then cooled rapidly to a temperature such that the average kinetic energy tending to change the structure is considerably smaller than the energy humps tending to prevent rearrangement to a crystalline structure, a vitreous solid results. If, on the other hand, the cooling takes place sufficiently slowly and if the energy of a structure having long-distance regularity is enough lower than the energy of any other structure, a crystalline substance is produced. The existence of vitreous substances is thus closely related to the strengths of the interatomic, interionic, and intermolecular forces and to the rate of cooling from the liquid state.

In general, a substance tends to be a solid if interatomic bonds, strong enough to resist breaking by thermal collisions, form a three-dimensional network structure extending throughout the mass. If a regular network structure has a considerably lower energy than any irregular structure, the solid tends to be crystalline. It tends to be amorphous, however, if different arrangements have practically equal energy.

In silicate glasses, the strongest interatomic forces are usually those between adjacent silicon and oxygen atoms. Because of these forces, each silicon is bonded tetrahedrally to four oxygens and each oxygen to one or two silicons (usually in addition to one or more other metallic atoms). In most ordinary glasses, the ensemble of Si—O bonds forms a network structure. The rings of which this network may be considered to be composed are of various sizes, partly because of the effects of the other atoms of various sizes and coordination numbers and partly because the energy of the network depends only slightly on the ring-size distribution (see Fig. 1). The fact that different relative orientations of practically equal stability are possible for the two Si—O bonds extending from many of the oxygen atoms contributes both to the irregularity of distribution of ring sizes and to the irregularity in shape of the rings of the same size.

At sufficiently high temperatures, such as those at which the glass was made, the viscosity is that of an ordinary liquid; the network is continually being broken and re-formed with a change of configuration. This change necessitates the breaking and re-formation of Si—O bonds.

As the temperature is lowered, the rate of breaking of Si—O bonds rapidly becomes smaller and the viscosity greatly increases. Within the temperature range in which the viscosity is rapidly changing (or at any higher temperature), the structure existing at any instant is far from regular because the differences in energy between different configurations (different sizes of rings, etc.) for each small region of the structure are small in relation to the thermal energy available.

On further cooling, practically no Si—O bonds are broken, and in this respect the structure remains fixed. Other changes having smaller activation energies continue to occur at temperatures somewhat below the range of rapid viscosity increase. These include the breaking and making of other metal—oxygen bonds and changes of orientation of Si—O bonds in the silicate net insofar as possible without breaking any of these bonds or changing Si—O—Si bond angles too greatly from their most stable values. Those changes are preferred over changes in the opposite direction, which result in a decrease in (free) energy.

If the cooling takes place very slowly through each temperature range in which the rate of shift for a given type of structure change is rapidly decreasing, approximate equilibrium with respect to each of these types of changes can be maintained. In those types of subsystems in which one of two alternative distributions is considerably more stable than the other, practically all will have the more stable distribution when the temperature is reached at which the rate of shift becomes negligible. Slow cooling over all of these critical regions therefore produces a glass at room temperature that approaches the lowest possible energy, that is, maximum stability. Rapid cooling through any of the critical regions results in the "freezing in" of some relatively unstable atomic distributions, which causes strains and inhomogeneities. The tendency to relieve these strains to give a thermodynamically more stable structure produces slow internal changes which persist over a long period of time.

Very slow cooling through temperatures only slightly below those at which the glass is fluid favors the production and growth of crystalline regions in the mass, but the importance of this tendency is greatly dependent on the composition. Such crystalline regions, especially if the crystal structure is quite anisotropic with strength and other properties varying greatly with direction, may be very deleterious, producing inhomogeneity and other undesirable properties in the final product.

II. Vitreous Sulfur and Selenium

In this and the following sections, some typical substances and types of substances which form vitreous solids will be discussed, with emphasis on the structural relationships.

Among the elements known in the vitreous state are sulfur and selenium. According to the Lewis theory of valence and atomic structure,[1] these elements would be expected to form either rings or very long chains, each atom in either case (except for the few terminal

[1] G. N. Lewis, Valence and Structure of Atoms and Molecules, pp. 94–95. Reinhold Publishing Corp., New York, 1923.

atoms of the long chains) being bonded to two others, with a bond angle at least roughly approximating the tetrahedral angle (110°). This expectation has been verified by X-ray work on the crystalline forms of the elements.[2]

Amorphous sulfur and selenium can be obtained by rapidly cooling the liquids after heating at a temperature sufficient to break the rings. The amorphous substances contain long chains of atoms[3] and probably also rings of various sizes. These chains and rings have many different configurations because of the nearly equal stability of various orientations of each single bond relative to each of the two adjacent bonds. This picture is consistent with the rubberlike elasticity of amorphous sulfur at ordinary temperatures and of amorphous selenium at somewhat higher temperatures, a property now known to be due to the entropy decrease occurring when randomly kinked chains become more or less straightened out and mutually aligned when the material is stretched.[4] The elasticity disappears as the temperature is lowered (as in the case of rubber) because the thermal motions of the atoms become insufficient to produce the changes of orientation at a sufficiently rapid rate.

III. Vitreous Silica

The structure of vitreous silica, SiO_2, will be discussed in this section. Reasoning from the Lewis theory of valence,[5] each silicon atom in silicon dioxide should be tetrahedrally bonded to four oxygen atoms and each oxygen should be bonded to two silicons by bonds making approximately tetrahedral angles with each other. These conclusions have been verified by the results of X-ray studies of quartz[6] and vitreous silica.[7]

Because of the possibility, without much energy change, of different orientations of each Si—O bond relative to the other Si—O bond leading from the same oxygen atom, many different atomic arrangements satisfying the bond requirements just mentioned have nearly the same stability. The most stable of these at room temperature is that of quartz, but at much higher temperatures many less regular structures must exist in equilibrium with each other (see Fig. 1). A change from one of these structures to another involves (in most instances) the breaking of relatively strong Si—O bonds. The activation energy for this change is large, so large in fact that the rate must be negligibly slow at ordinary temperatures. Sudden cooling of the melt, through the temperature range within which this rate is not negligible, therefore "freezes in" the irregular arrangements, producing silica glass.

IV. Other Oxide Glasses

Other pure oxides which have yielded glasses on rapid cooling from the molten state include the following: B_2O_3,[8] GeO_2,[8] ZrO_2,[9] P_2O_5,[8] As_2O_3,[8] As_2O_5,[8(a,c)] Sb_2O_3,[8(a)] and Bi_2O_3.[10] Possibly P_2O_3,[8(a)] V_2O_5,[8] and Sb_2O_5[8(a)] should also be included in this list. In all of these substances in both the crystalline and vitreous states, rather strong metal—oxygen electronpair bonds would theoretically be expected. Except in ZrO_2, the existence of two such bonds would be expected, extending approximately at tetrahedral angles from each oxygen atom (or, in P_2O_3, As_2O_3, Sb_2O_3, and V_2O_3, from most of the oxygen atoms). The crystal structures of most of

---

[2] (*a*) B. E. Warren and J. T. Burwell, "Structure of Rhombic Sulfur," *Jour. Chem. Phys.*, **3** [1] 6–8 (1935).
(*b*) J. T. Burwell, "Unit Cell and Space Group of Monoclinic Sulfur," *Z. Krist.*, **A97** [1–2] 123–24 (1937).
(*c*) H. P. Klug, "X-Ray Study of Red Monoclinic Selenium; Proof of Existence of Two Red Monoclinic Varieties of Selenium," *ibid.*, **A88** [2] 128–35 (1934); *Ceram. Abs.*, **13** [9] 244 (1934).
(*d*) M. K. Slattery, "Crystal Structure of Metallic Selenium and Tellurium," *Phys. Rev.*, **21** [3] 378–79 (1923).
(*e*) M. K. Slattery, "Crystal Structure of Metallic Tellurium and Selenium and of Strontium and Barium Selenide," *ibid.*, **25** [3] 333–37 (1925).
(*f*) A. J. Bradley, "Crystal Structures of Rhombohedral Forms of Selenium and Tellurium," *Phil. Mag.*, **48** [285] 477–96 (1924).

[3] K. H. Meyer and Y. Go, "Sur le soufre filiforme et sa structure," *Helv. Chim. Acta*, **17**, 1081–93 (1934).

[4] (*a*) K. H. Meyer, G. von Susich, and E. Valkó, "Die elastischen Eigenschaften der organischen Hochpolymeren und ihre kinetische Deutung," *Kolloid-Z.*, **59** [2] 208–16 (1932).
(*b*) W. F. Busse, "Physical Structure of Elastic Colloids," *Jour. Phys. Chem.*, **36** [12] 2862–79 (1932).
(*c*) E. Karrer, "Kinetic Theory of Elasticity of Highly Elastic Gels," *Phys. Rev.*, **39** [5] 857 (1932).

[5] (*a*) M. L. Huggins, "Crystal Structure of Quartz," *Phys. Rev.*, **19** [4] 363–68 (1922).
(*b*) See also p. 94 of reference 1.

[6] (*a*) R. E. Gibbs, "Variation with Temperature of the Intensity of Reflection of X-Rays from Quartz and Its Bearing on Crystal Structure," *Proc. Roy. Soc.* [London], **A107** [743] 561–70 (1925).
(*b*) R. E. Gibbs, "Structure of α-Quartz," *ibid.*, **A110** [754] 443–55 (1926).
(*c*) W. H. Bragg and R. E. Gibbs, "Structure of α- and β-Quartz," *ibid.*, **A109** [751] 405–27 (1925); *Ceram. Abs.*, **5** [5] 167 (1926).
(*d*) R. W. G. Wyckoff, "Crystal Structure of High-Temperature (β) Modification of Quartz," *Amer. Jour. Sci.*, **11**, 101–12 (1926).
(*e*) R. W. G. Wyckoff, "Kriterien für hexagonale Raumgruppen und die Kristallstruktur von β-Quartz," *Z. Krist.*, **A63** [V–V1] 507–37 (1926).
(*f*) See also reference 5 (*a*).

[7] (*a*) B. E. Warren, "X-Ray Diffraction of Vitreous Silica," *Z. Krist.*, **A86** [5–6] 349–58 (1933); *Ceram. Abs.*, **14** [4] 91 (1935).
(*b*) B. E. Warren and J. Biscoe, "Structure of Silica Glass by X-Ray Diffraction Studies," *Jour. Amer. Ceram. Soc.*, **21** [2] 49–54 (1938).

[8] (*a*) W. H. Zachariasen, "Atomic Arrangement in Glass," *Jour. Amer. Chem. Soc.*, **54** [10] 3841–51 (1932); *Ceram. Abs.*, **12** [4] 145 (1933).
(*b*) G. W. Morey, Properties of Glass, pp. 74–75. Amer. Chem. Soc. Monograph Series, Reinhold Publishing Corp., New York, 1938. 561 pp.; *Ceram. Abs.*, **18** [2] 48 (1939).
(*c*) G. Hägg, "Vitreous State," *Jour. Chem. Phys.*, **3** [1] 42–49 (1935); *Ceram. Abs.*, **14** [7] 161 (1935).

[9] (*a*) W. M. Cohn, "Über die Herstellung von Zirkondioxydglas mit Hilfe des Straubelschen Sonnenspiegels (Development of Zirconium Glass with the Help of the Straubel Sun Mirror)," *Ber. deut. keram. Ges.*, **12** [3] 118–22 (1931); *Ceram. Abs.*, **10** [9] 631 (1931).
(*b*) W. M. Cohn, "Crystal Modifications of Zirconia; Clear, Fused Zirconia Produced in the Sun Furnace," *Trans. Electrochem. Soc.*, **68**, 65–71 (1935); *Ceram. Abs.*, **18** [9] 244 (1939).

[10] J. T. Randall and H. P. Rooksby, "X-Ray Diffraction and Structure of Glasses," *Jour. Soc. Glass Tech.*, **17** [67] 287–95 (1933); *Ceram. Abs.*, **13** [3] 56 (1934).

TABLE I

N_{Si}	s	f_0	f_1	f_2	f_3	f_4	Diagrammatic representation
0.250	0	1	0	0	0	0	+
0.250–0.286	0–1	$\frac{2}{N_{Si}} - 7$	$8 - \frac{2}{N_{Si}}$	0	0	0	+ and ++
0.286	1	0	1	0	0	0	++
0.286–0.333	1–2	0	$\frac{2}{N_{Si}} - 6$	$7 - \frac{2}{N_{Si}}$	0	0	++···+(chains), with or without (rings)
0.333	2	0	0	1	0	0	Rings and/or infinitely long chains
0.333–0.400	2–3	0	0	$\frac{2}{N_{Si}} - 5$	$6 - \frac{2}{N_{Si}}$	0	Network, composed of ···+··· and ···+···, with or without rings
0.400	3	0	0	0	1	0	Network, composed of ···+···
0.400–0.500	3–4	0	0	0	$\frac{2}{N_{Si}} - 4$	$5 - \frac{2}{N_{Si}}$	Network, composed of ···+··· and ···+···
0.500	4	0	0	0	0	1	Network, composed of ···+···

these compounds have been determined and have been found to agree with these theoretical expectations. According to both the theory and the crystal structure results, three or more of the oxygen atoms surrounding each atom of the more metallic element are bonded also to other "metal" atoms. This permits a three-dimensional network structure and such a structure doubtless exists in these glasses. The randomness of the atomic arrangements in the glasses results from the possibility of different relative orientations of the two bonds connecting each oxygen to other atoms and from a randomness in the distribution of the bridging and nonbridging oxygens in those instances in which all of the oxygens surrounding each "metal" atom are not also bonded to other atoms.

V. Silicate Glasses

In most silicates, both crystalline and vitreous, the silicon—oxygen bonds are much stronger than any others present. (B—O and perhaps Al—O bonds are comparable in strength, but these bonds will be neglected here to simplify the discussion.) In agreement with theoretical expectation, it has been found that in silicate crystals each silicon is tetrahedrally surrounded by four oxygens and that each oxygen is bonded to either one or two silicons. Evidence regarding the structure of silicate glasses favors the assumption that a similar state of affairs also exists in these silicates.

The SiO_4 tetrahedra may be classified as types 0, 1, 2, 3, and 4, on the basis of the number of oxygens shared with other silicons. At least in crystals and glasses in which there are no other bonds comparable in strength with the Si—O bonds, it seems reasonable to assume that for greatest stability only types designated by adjacent numbers (0 and 1 or 1 and 2 or 2 and 3 or 3 and 4, but not 0 and 2 or 1 and 3, etc.) can exist together in a given sample. In other words, two SiO_4 tetrahedra of types 1 and 3 (having one and three oxygens shared), for example, would tend to react together in such a way as to produce two tetrahedra of type 2. The authors know of no contradictions to this generalization among silicate crystals. Among glasses some deviations might be expected, especially if the composition is such that nearly all of the tetrahedra are of a single type; for instance, a glass having nearly all of type 2 might well have some of type 1 and some of type 3. Some conclusions based on this generalization are nevertheless of interest and may be considered to be approximately correct.

For this purpose, a quantity N_{Si} may be used. This is defined as the ratio of the number of silicon atoms to the number of oxygen atoms in the glass (or crystal). It may be computed[11(a)] from the weight fractions (f_M) of the different oxide components (having formulas M_mO_n and molecular weights W_M) by means of relation (1).

$$N_{Si} = \frac{f_{Si}/W_{Si}}{\sum n_M f_M / W_M} = \frac{f_{Si}/60.06}{\sum n_M f_M / W_M} \qquad (1)$$

N_{Si} and s, the average number of oxygen atoms of each SiO_4 tetrahedron which are shared with other silicons, are related by equation (2).

$$s = 8 - \frac{2}{N_{Si}} \qquad (2)$$

Table I gives both the values of s and of $f_0, f_1 \ldots f_4$, the fractions of the SiO_4 tetrahedra which are of types 0, 1...4, respectively, for various compositions (N_{Si} values) and composition ranges, assuming the preceding generalization to be strictly correct.

In the right-hand column of Table I, the silicate structures present are symbolized diagrammatically. The crosses represent SiO_4 tetrahedra as follows: + denotes SiO_4^{-4} ions, having the "dot formula" (*A*) and ++ denotes $Si_2O_7^{-6}$ ions, having the dot formula (*B*).

(*A*)

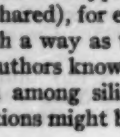

(*B*)

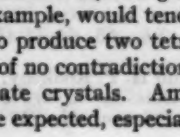

Except for pure SiO_2 (N_{Si} equals 0.50), each aggregation of silicon and oxygen atoms, joined together through Si—O bonds, is negatively charged, the magnitude of the charge being given by the formula $Si_xO_y^{(4x-2y)-}$. This charge is balanced by positively charged ions, such as Na^+, Ca^{++}, Al^{+++}, also present in the structure. The distribution of the positive ions, although important in determining the properties of the glass, will not be discussed at this time.

It must be emphasized that the distributions of silicon and oxygen atoms indicated in Table I at best are only approximate, limiting distributions. The energy change for the reaction between a type 1 tetrahedron and a type 3 tetrahedron to give two type 2 tetrahedra, for instance, is probably not large. At any temperature at which the rate of this reaction would not be negligible, the equilibrium distribution probably would contain a considerable fraction of types 1 and 3 coexisting in the same sample. Glasses having $N_{Si} \leqq 0.333$ would therefore be expected to have some branched chains, and those having $N_{Si} \geqq 0.333$ would be expected to have some chains with loose ends. The relative numbers of tetrahedra of the different types are certainly affected also by the kinds and numbers of other atoms or ions present, especially by those (B, Al) having the strongest attractions for the oxygens.

In spite of these limitations, it is felt by the authors that the dependence of structure on composition indicated in Table I is approximately correct and will prove useful in future discussions of the dependence of the properties of silicate glasses on their compositions. Considerations such as these in fact have already proved helpful in leading to reasonably satisfactory treatments of the dependence of the densities,[11] refractive indices,[12] and dispersions[13] of silicate glasses on their compositions.

The conclusions regarding the structure of silicate glasses containing no atoms, other than Si, which form strong electronpair bonds to oxygen, are readily generalized, on the basis of similar assumptions, to other mixed oxide glasses, both those containing silicon plus other elements such as boron, phosphorus, and germanium, and those containing no silicon.

VI. Glasses Containing Hydrogen Bridges

Many organic and inorganic hydroxy compounds form glasses in which the molecular or ionic units are held together by OHO hydrogen bridges.[14] Typical examples are glucose,

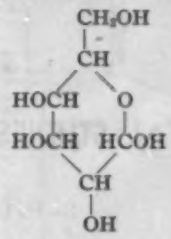

polyvinyl alcohol,

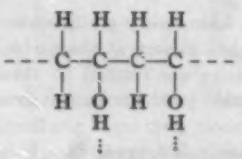

and glacial phosphoric acid, one of the forms of metaphosphoric acid. The last-named substance, the authors believe, consists of long chains,

kinked in a more or less random manner and connected to each other by means of the hydrogens. Some closed rings may also be present.

The possibilities of different orientations of the OHO bridges relative to the adjacent C—O or P—O bonds and of considerable variation in bond angles at (and within) these bridges, as well as other factors, help to produce an amorphous rather than a crystalline structure. The forces tending to prevent rearrangement of a momentarily existing structure are much less than for silicate glasses; the substances are therefore fluid at much lower temperatures. This condition greatly simplifies the investigation of the variation of various properties with temperature through the transition region between liquid and glass.

VII. Organic Polymers

Polyvinyl alcohol is but one of many organic polymers containing long chains which are kinked in a random manner, provided they have not been extended and oriented by stretching of the material. Such substances are rigid solids if the activation energies for rearrangement of the atomic positions are large relative to kT. They are soft and nonrigid if these activation energies are roughly equal to or are smaller than kT. They show rubberlike elasticity if (1) most of the atoms have considerable freedom of motion, being restricted

---

[11] (*a*) M. L. Huggins, "Density of Silicate Glasses as Function of Composition," *Jour. Optical Soc. Amer.*, **30** [9] 420–30 (1940); *Ceram. Abs.*, **20** [2] 41 (1941).
(*b*) M. L. Huggins and K.-H. Sun, "Calculation of Density and Optical Constants of a Glass from Its Composition in Weight Percentage," *Jour. Amer. Ceram. Soc.*, **26** [1] 4–11 (1943).

[12] (*a*) M. L. Huggins, "Refractive Index of Silicate Glasses as Function of Composition," *Jour. Optical Soc. Amer.*, **30** [10] 495–504 (1940); *Ceram. Abs.*, **20** [2] 41–42 (1941).
(*b*) See also reference 11(*b*).

[13] (*a*) M. L. Huggins, "Dispersion of Silicate Glasses as Function of Composition," *Jour. Optical Soc. Amer.*, **30** [11] 514–18 (1940); *Ceram. Abs.*, **20** [4] 88 (1941).
(*b*) M. L. Huggins, K.-H. Sun, and D. O. Davis, "Dispersion of Silicate Glasses as Function of Composition, II," *Jour. Optical Soc. Amer.*, **32** [12] 635–50 (1942); *Ceram. Abs.*, **22** [2] 30 (1943).
(*c*) See also reference 11(*b*).

[14] M. L. Huggins, "Hydrogen Bridges in Organic Compounds," *Jour. Org. Chem.*, **1** [5] 407–56 (1936).

only by small energy humps, yet (2) long-distance displacements are prevented by the existence of a three-dimensional network of strong bonds, capable of being broken only if large energy humps are passed over. Without such a network, these substances exhibit plastic flow rather than long-range elasticity.

EASTMAN KODAK COMPANY
ROCHESTER, NEW YORK

EXPERIMENTAL STUDIES OF THE TEMPERATURE GRADIENTS IN GLASSES OF VARIOUS COLORS*

BY H. H. HOLSCHER, R. R. ROUGH, AND J. H. PLUMMER

ABSTRACT

Laboratory gradients are presented for glasses of different colors and coloring agents when heated at the surface to a temperature of 2615°F. The gradients in commercial tanks are related to these laboratory-tank experiments. Ferrous iron and chromic oxide yield the largest gradients, whereas selenium, cerium, and very small amounts of cobalt give small gradients. Ferric iron gives a large gradient and manganese a relatively low gradient. Iron sulfur ambers are intermediate. Visible color or color intensity is no indication of the temperature gradients.

I. Introduction

In the melting of glass, the penetration of heat through the surface down to deeper sections is very important. In certain colors, the penetration is only a fraction of what it is in others, that is, the temperature gradient down through the glass may be very steep. Certain colored glass tanks are therefore usually shallower than flint tanks but the bottom tank block lasts much longer. Because of the rapid temperature drop down through the glass, difficulties resulting from the freezing of throats and from devitrification and stones are a major consideration. Stones may form because parts of the glass are below the liquidus temperature, and they may be slow to redissolve, moreover, because of the existing lower over-all temperatures. Sump or submarine throats are not advisable in such cases.

All of these factors are significant if maximum output is to be obtained from a unit and particularly for tanks in which both flint and colored glasses are to be melted. A furnace designed for one certain color is at a disadvantage for melting other colors.

Because a knowledge of the effects of different coloring agents also becomes important, a study was made of gradients existing in a small laboratory furnace and their relation to large tank furnace gradients. The authors also were seeking the most advantageous coloring agents from the standpoint of reducing the gradient.

The literature reveals studies on this subject, most of which are sketchy in nature. Differences in radiating power of various colored glasses were studied by Kitaĭgorodskiĭ and Solomin,[1] who listed the infrared transmission of a group of glasses with 2% of various coloring agents added in the order of flint (least radiating), manganese purple, ferric oxide, cobalt oxide, and ferrous oxide. They also discussed the relation of the rate of setting of the glass to its radiating power.

Turner and Winks[2] had previously suggested that the apparent difficulty of casing colorless glass by cobalt blue glass was a result of a change of setting rate caused by color or radiating properties.

Burch and Babcock[3] studied this problem and related setting rate to machine speed. An amber glass set up 5% faster than a flint glass and a medium green glass 8% faster than the flint. Machine speeds followed in relative order, in fact, almost in quantitative order. The obvious interpretation is that the higher the radiating power, the higher the gradient to be expected down through the glass in a melter.

Eitel and Lange[4] rated four glasses in the order of radiating power as flint (least), brown, green, and blue-green (highest).

Studies on luminous flames have shown similar effects. Schwalbe[5] compared luminous and nonluminous flames

---

* Presented at the Forty-Fifth Annual Meeting, The American Ceramic Society, Pittsburgh, Pa., April 21, 1943 (Glass Division). Received April 20, 1943.

[1] I. I. Kitaĭgorodskiĭ and N. W. Solomin, "Rate of Setting of Glass During Working," *Jour. Soc. Glass Tech.*, **18** [72] 323–35 (1934); *Ceram. Abs.*, **14** [8] 187 (1935).

[2] W. E. S. Turner and F. Winks, "Casing of Colorless by Cobalt Blue Glass: I, Thermal Expansion," *Jour. Soc. Glass Tech.*, **12** [45] 57–82 (1928); *Ceram. Abs.*, **8** [1] 24 (1929).

[3] O. G. Burch and C. L. Babcock, "Effect of Glass Color on Setting Rates in Manufacture of Glass Bottles," *Jour. Amer. Ceram. Soc.*, **21** [10] 345–51 (1938).

[4] W. Eitel and B. Lange, "Determining Radiating Power of Glass," *Glastech. Ber.*, **10** [2] 78–80 (1932); *Ceram. Abs.*, **11** [6] 358 (1932).

[5] (*a*) F. G. Schwalbe, "Depth of Heat Penetration in Molten Glass with Luminous and Nonluminous Flames," *Ind. Heating*, **2** [2] 99–102; [3] 153–54; [4] 209–10 (1935); *Ceram. Abs.*, **14** [8] 185 (1935).

(*b*) F. G. Schwalbe, "Control for Luminous Flame Firing in Glass Furnaces," *Jour. Amer. Ceram. Soc.*, **23** [6] 173–78 (1940).

and calculated the amount of energy penetrating the glass based on infrared transmissions at room temperature. He gives a few measurements at the surface and at depths in amber and flint glass, and he reports a drop of 200°F. through 36 in. of flint glass and a drop of 560°F. through 18 in. of amber glass. Similar scattered measurements are also noted by Gehlhoff and Thomas[6] and by the same writers and Schneekloth.[7]

Halle, Preston, and Turner[8] report gradients and gas consumption in a small experimental furnace for flint, amber, and iron-manganese green glasses as follows:

	°F./in.*	Gas required (ft.³/min.)†
Flint	27	7.5
Amber	72	6.0
Green	135	5.3

* From 3 to 4 in. depth (no insulation).
† To hold surface temperature of 2552°F.

From cooling rate data, they list several glasses in order of radiation as follows:

	Fe_2O_3	MnO_2
Flint	0.07	
Cobalt blue	0.22	(0.46 CoO)
C-S amber	0.2	
Fe-Mn light amber	2.88	3.28
Fe-Mn green	1.57	2.30
Fe-Mn dark amber	4.60	5.10

These same experimenters also show the relation between surface temperature under constant gas consumption to be flint 2552°, amber 2606°, and green 2660°F.

Shute and Badger[9] studied the iron oxide glasses with results as follows:

Fe_2O_3 (%)	Gradient (°F./in.)
0.035	19
0.135	25
0.335	30
0.535	39
1.035	46

Information on the infrared transmission of various glasses is also available to the reader.[10]

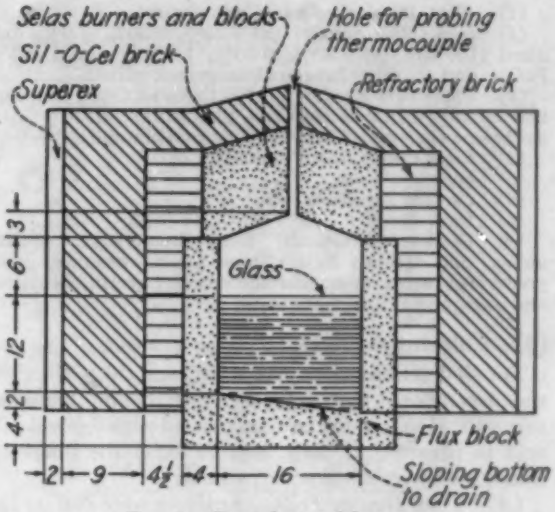

FIG. 1.—Experimental furnace.

II. Experimental Procedure

(1) Experimental Setup

The glasses were melted in a small furnace in which the side walls were well insulated (Fig. 1). The body of glass was 16 in. square and 12 in. deep, weighing about 400 lb. The furnace was made of flux block, 4 in. thick on the sides, and 4½ in. of fire-clay brick, and was insulated on all sides with 9-in. super Sil-O-Cel brick plus 2-in. Superex block. The heavy insulation was used to minimize the amount of lateral heat flow. The bottom was uninsulated. The furnace was fired by four Selas K–670 radiant burners set at an angle as shown in Fig. 1. A 1-in. hole in the center of the crown allowed a porcelain pyrometer tube to be raised or lowered as desired. Exhaust was obtained through the side, 4 in. above the glass and about 16 sq. in. in area.

A closed-end porcelain tube, ¾ in. in diameter, was used for probing to the bottom of the furnace. For the "surface reading," the surface was just touched, which resulted in surface tension that pulled the glass up about the closed end of the tube. Although this method gives some error of locating the surface reading, it was the most accurate method known. On darker colored glasses, this thermocouple reading checked closely with an optical pyrometer reading on the surface. Gradients were taken only after the surface was free from all foam and bubbles. Probes were taken every inch or so to allow a curve to be plotted.

(2) Glasses Used

The following composition was used on all experimental glasses: SiO_2 74.0, Na_2O 16.0, CaO 10.0, and Fe_2O_3 (by analysis) 0.035%.

The surface temperature was adjusted to 2615°F. under a combustion condition of 0 to 2% of excess air except in one series (reduced iron) in which 0 to 1% of air deficiency was used. The amount of gas necessary to hold this temperature was also determined.

The following glasses were studied and are reported herein:

[6] G. Gehlhoff and M. Thomas, "Temperature Measurement in Glass Furnaces," *Glastech. Ber.*, **4** [6] 210–19 (1926); *Ceram. Abs.*, **6** [7] 271 (1927).

[7] G. Gehlhoff, W. Schneekloth, and M. Thomas, "Currents and Temperatures in Glass Tanks," *Glastech. Ber.*, **9** [1] 22–29 (1931); *Ceram. Abs.*, **10** [7] 491 (1931).

[8] R. Halle, Eric Preston, and W. E. S. Turner, "Distribution of Temperature in Molten Masses of Colored and Colorless Glass," *Jour. Soc. Glass Tech.*, **23** [97] 171–96 (1939); *Ceram. Abs.*, **19** [4] 89 (1940).

[9] R. L. Shute and A. E. Badger, "Effect of Iron Oxide on Melting of Glass," *Jour. Amer. Ceram. Soc.*, **25** [August 1, No. 12] 355–57 (1942).

[10] (*a*) Glastechnische Tabellen, pp. 457–82.
(*b*) W. W. Coblentz, W. B. Emerson, and M. B. Long, "Spectroradiometric Investigation of the Transmission of Various Substances," *Nat. Bur. Standards, Sci. Paper*, No. 325, 24 pp. (Aug. 8, 1918).

(*1*) *Flint, Decolorized and Undecolorized.*
(*2*) *Iron Oxide Series:* (*a*) 0.25%, 0.50%, 1.0%, oxidized (100%); (*b*) 0.25%, 0.50%, 1.0%, reduced (65% FeO); and (*c*) miscellaneous iron greens, mixed.
(*3*) *Chromium greens:* 0.25% Cr_2O_3 as Cr_2O_3 plus carbon; 0.25% Cr_2O_3 as $Na_2Cr_2O_7$ plus sulfur; 0.20% Cr_2O_3 as chrome ore; and 0.14% Cr_2O_3 as iron chromite.
(*4*) *Light Cobalt Blue:* 0.003% CoO.
(*5*) *Selenium Pink.*
(*6*) *Cerium Titanium Topaz.*
(*7*) *Dark Purple:* 1.2% MnO_2.
(*8*) *Commercial Glasses:* flint, decolorized; pyrites amber, plus carbon; light chrome green, chromite; light green, iron manganese; chrome emerald green, chromite; and dark green, iron manganese.

(3) Colorant Analyses*

For all determinations except FeO and CeO_2, the glass was decomposed with HF just under boiling temperature with HNO_3 as oxidant and fumed with less volatile acid in presence of boric acid to expel the fluorides. Blank tests were made when necessary.

(*A*) *Total Iron as Fe_2O_3:* Analyses were run on the HCl solution of perchlorate residue without precipitation and re-solution of R_2O_3. Colorimetric determinations were made by the thiocyanate method when the total iron was less than 0.1%; otherwise, determination was made by reduction with $SnCl_2$, followed by potentiometric titration with ceric sulfate.

(*B*) *Chromic Oxide:* Analyses were run on the solution boiled with concentrated perchloric acid, cooled, reduced with an excess of ferrous ammonium sulfate, and back-titrated with potassium dichromate in the presence of phosphoric acid. The indicator was sodium diphenylamine sulfonate.

(*C*) *Manganese Oxide:* After expelling most of the HF with phosphoric acid, the manganese was oxidized to permanganate by boiling in a solution containing phosphoric acid, sulfuric acid, boric acid (to complex the residual fluoride), and sodium periodate. Excess periodate was precipitated with mercuric nitrate and filtered through a fritted glass funnel. The permanganate in the solution was reduced with an excess of ferrous ammonium sulfate and back-titrated with potassium permanganate.

(*D*) *Ferrous Oxide:* The glass was decomposed with HF and H_2SO_4 at room temperature under cover of CO_2 in a polystyrene flask. Free fluoride ions were complexed by addition of a great excess of boric acid crystals. Ferrous oxide (FeO) was then titrated with ceric sulfate with a microburet, using orthophenanthroline ferrous complex as indicator.

(*E*) *Ceric Oxide:* If no color developed when the indicator was added in a determination of FeO, the solution was titrated to the appearance of color with ferrous ammonium sulfate. The oxidation equivalent was taken to be excess ceric ion and calculated as CeO_2.

(*F*) *Ferric Oxide:* Ferric iron was calculated from the results of total iron and ferrous iron determinations.

III. Discussion

(1) Iron Series

First efforts to obtain the iron yellows were not successful because of insufficient oxidation. On the basis of color, the use of arsenic pentoxide, antimony pentoxide, ammonium sulfate, and sodium nitrate was unsatisfactory. The sulfates were ineffective as indicated by color, and the sodium nitrate and arsenic and antimony pentoxides were only partially effective. When ceric hydrate was tried in amounts three times the weight of the iron oxide, yellow colors with no tint of green were obtained.

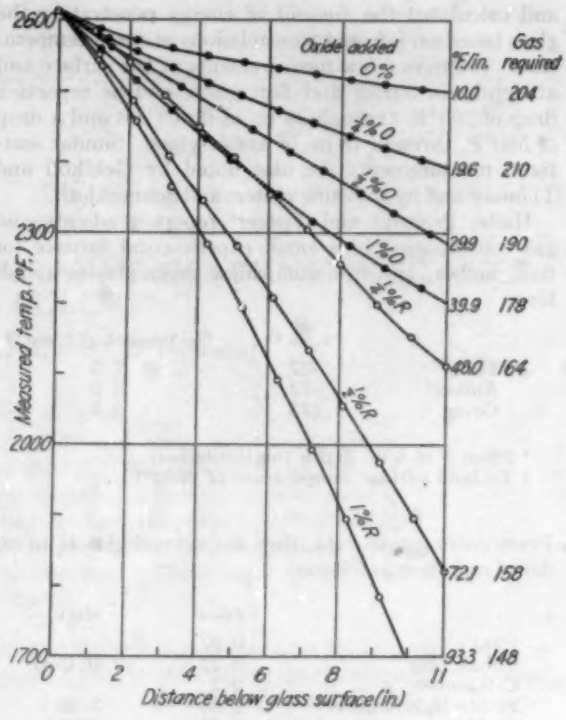

FIG. 2.—Iron oxide glasses; *R* curves, reduced; *O* curves, oxidized.

Analyses were made for excess ceric oxide because it was assumed that there would be no ferrous oxide in its presence. These analyses are shown in Table I. Total iron as ferric oxide was also determined. The colors of these oxidized iron glasses were, respectively, faint yellow (1/4%), a straw yellow (1/2%), and a light straw amber (1%).

The question may well be raised as to whether the ceric hydrate alone would affect the temperature gradient. Two melts with 0.1 and 1% of ceric hydrate (no added iron oxide) were made up. The first was colorless, and the 1% glass was a faint yellow. Its effect on the gradient was considered negligible, particularly in view of the gradient obtained on the topaz glass (see section III (4)) whose content of CeO_2 is within the same range.

The reduced iron series samples were made by adding carbon in an amount equal to 40% of the iron oxide used. These were melted under 0 to 1% of air deficiency. The analyses indicated about 65% of the total iron to be present in the ferrous state. These glasses were, respectively, aqua (1/4%), medium greenish aqua (1/2%), and dark greenish blue (1%) in color.

* Analyses by Paul Close and F. R. Bacon.

TABLE I

GLASSES COLORED WITH IRON OXIDE*

Series	Ingredients added (%)			Analysis				Gradient	Gas required
	Fe_2O_3	$Ce(OH)_4$	Coal	FeO	Fe_2O_3	Total Fe as Fe_2O_3	CeO_2		
Oxidized	0.25	0.78			0.29	0.29	0.03	19.6	210
	0.50	1.56			0.55	0.55	0.16	29.9	190
	1.00	3.12			1.02	1.02	0.32	39.3	178
Partially oxidized	0.25			0.11	0.13	0.25		39.5	173
	0.50	0.91		0.07	N.d.†	N.d.†		35.1	170
Reduced	0.25		0.10	0.15	0.12	0.29		48.0	164
	0.50		0.19	0.35	0.16	0.55		72.1	158
	1.00		0.38	0.60	0.23	1.00		93.3	148
Flint				N.d.†		0.035		10.3	204

* Combustion atmosphere: 0 to 0.2% excess air except reduced iron glasses which were under 0 to 1% air deficiency.
† Not determined.

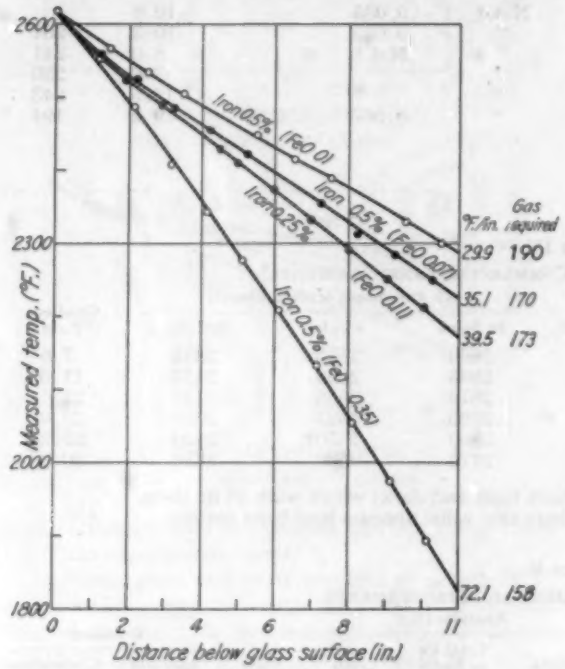

FIG. 3.—Ferrous-ferric glasses.

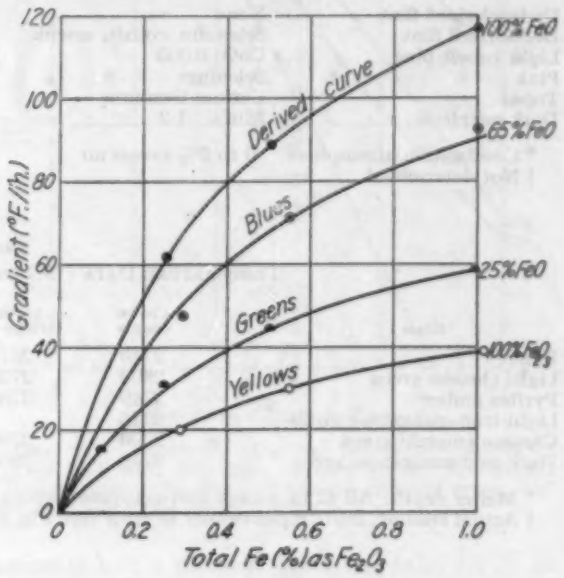

FIG. 4.—Iron oxide glasses.

The results given in Table I are plotted in Fig. 2, and these data show that the iron blues have gradients approximately 2.4 times those of the iron yellow gradients (Fig. 4). From these two experimental curves, a derived curve, which represents all of the iron in the ferrous state, was calculated. This is the top curve in Fig. 4. From the two extreme curves, a curve representing 25% of the iron in the ferrous state is shown. This is more or less typical of the condition existing in the greater share of the glasses which have been studied (unless a reducing agent such as carbon or sulfur has been added to the batch).

Figure 3 shows some interesting curves representing various degrees of reduction and the pronounced effect on the gradient. The gas consumption figures decrease as the gradient decreases.

The obvious conclusion is that iron oxide is a powerful colorant and materially reduces the temperature through the glass. Ferrous iron exerts much more influence than ferric iron.

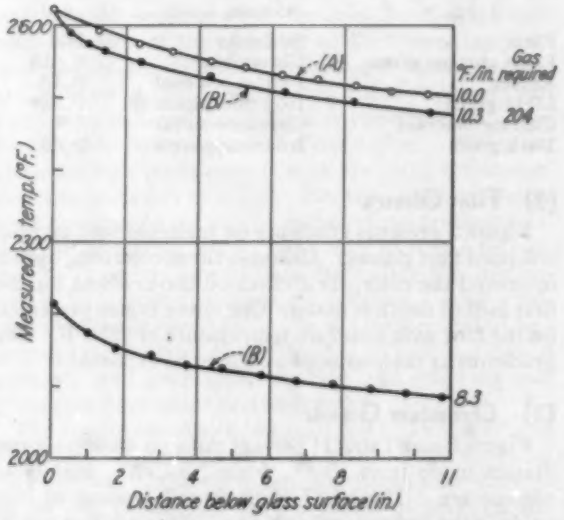

FIG. 5.—Flint glasses; curve *A*, undecolorized flint; curves *B*, decolorized flint.

TABLE II
GLASSES COLORED WITH CHROMIUM COMPOUNDS (MEDIUM GREENS)*

Coloring agents	Analysis (%) FeO	Fe_2O_3	Total Fe as Fe_2O_3	Cr_2O_3	Gradient	Gas required
Chrome ore	0.046	0.15	0.20	0.20	54	187
		Theoretical				
0.25 Cr_2O_3–0.09 C (%)			0.04	0.25	50	186
0.38 $Na_2Cr_2O_7$–0.04 S (%)			0.04	0.25	49	177

* Combustion atmosphere: 0 to 2% excess air.

TABLE III
MISCELLANEOUS COLORED GLASSES*

Color	Coloring agents (%)	Analysis (%) FeO	Fe_2O_3	MnO	Gradient	Gas required
Undecolorized flint	None	N.d.†	0.035		10.0	
Decolorized flint	Selenium, cobalt, arsenic	"	0.035		10.3	204
Light cobalt blue	CoO 0.003	"	N.d.†		8.0	241
Pink	Selenium	"	"		7.8	230
Topaz	Cerium-titanium	"	"		12.5	243
Dark purple	MnO_2 1.2	"	0.067	0.86	19.3	194

* Combustion atmosphere: 0 to 2% excess air.
† Not determined.

TABLE IV
TEMPERATURE DATA (°F.) FOR COMMERCIAL TANK GRADIENTS*

Glass	Crown couple	Optical bridge wall	Thermocouple reading (depth) In flame	1½ in.	26½ in.	Gradient (°F./in.)
Flint	2710	2670	2860	2655	2465	7.6
Light chrome green	2800	2730	2885	2630	2355	11.0
Pyrites amber	2740	2700	2810	2655	2115	21.6
Light iron-manganese green	2715		2795	2625	2050	23.0
Chrome emerald green	2790	2760	2880	2650†	2020	25.2
Dark iron-manganese green	2740	2690	2775	2500	1730	30.8

* Melter depth: All 42 in. except iron-manganese greens (both light and dark) which were 36 in. deep.
† Actual reading, 2675°F., obviously in error (see Fig. 9 where this value appears best from curve).

TABLE V
LABORATORY VERSUS COMMERCIAL MEASUREMENTS

Glass	Coloring agents	Analysis (%) FeO	Fe_2O_3	Total Fe as Fe_2O_3	Cr_2O_3	MnO	Gradient Laboratory	Commercial
Flint	Se-Co-As	N.d.		0.035			10.3	7.6
Light chrome green	Chromite	0.013	0.057	0.072	0.016		18.7	11.0
Amber	Pyrites-sea coal	0.15	0.01	0.18			50	21.6
Light green	Iron-manganese	0.23	0.65	0.90		0.92	66	23.0
Chrome emerald	Chromite-sulfur	0.12	0.09	0.22	0.14		71	25.2
Dark green	Iron-manganese	0.63	1.6	2.3		0.97	98	30.8

(2) Flint Glasses

Figure 5 presents gradients on undecolorized and decolorized flint glasses. Although the decolorizing agents improved the color, their effect on the gradient for the first inch of depth is noted. One curve is also presented on the flint with a surface temperature of 2210°F. The gradient has been reduced as was to be expected.

(3) Chromium Greens

Figure 6 and Table II present data on medium green glasses made from Cr_2O_3, from $Na_2Cr_2O_7$, and from chrome ore. The effect of the small amount of iron oxide in the chrome ore is obvious. The gradient resulting from ¼% of Cr_2O_3 in the glass is about the same as that obtained for the glass containing ¼% of iron blue. The visible color intensity, however, is considerably greater.

(4) Miscellaneous Glasses

Cobalt blue (0.003% of cobalt oxide), approximately a sky blue color, yielded a gradient smaller than that of flint glass (Fig. 7 and Table III). The same gradient was observed for selenium pink glass. Both of these glasses gave results of about 8°F. per in. of gradient as compared with 10°F. for flint glass. The visible color or transmission is obviously no criterion of the infrared transmission. Some experimenters may question these

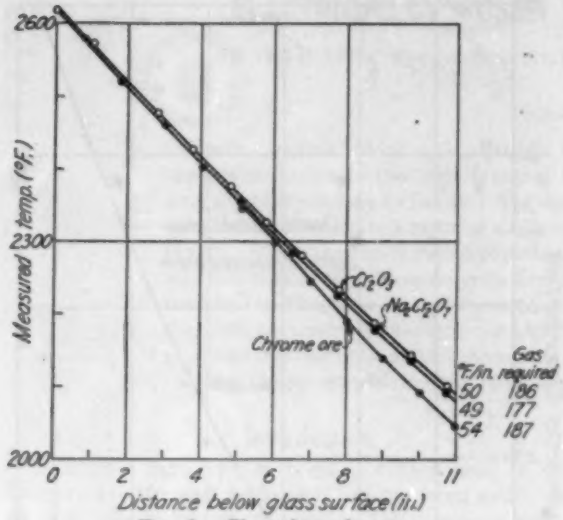

FIG. 6.—Chromium glasses.

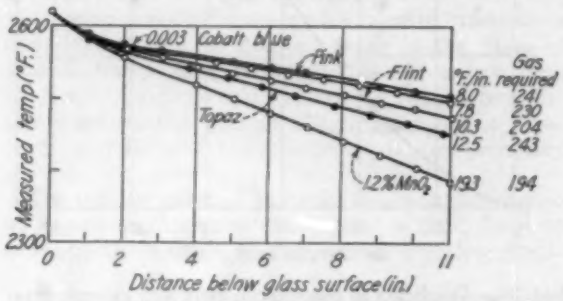

FIG. 7.—Miscellaneous glasses.

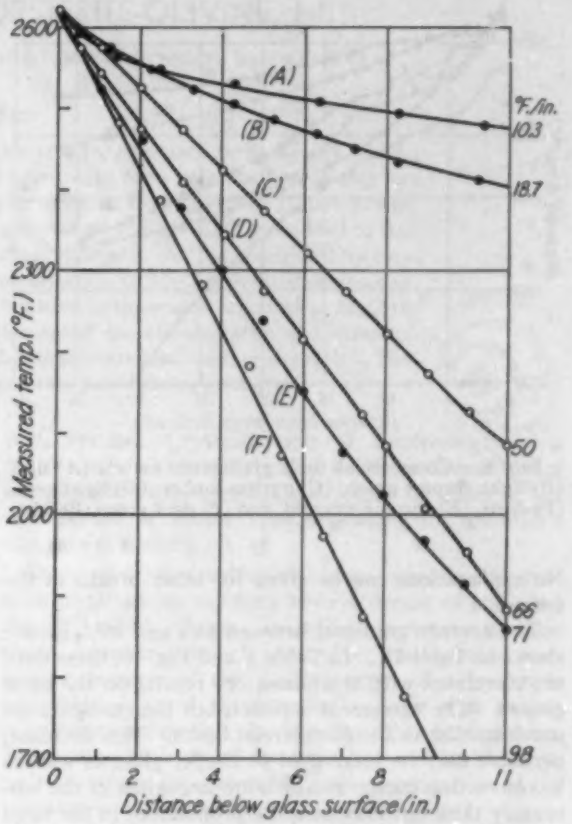

FIG. 8.—Commercial glasses (laboratory furnace): curves (*A*) flint, (*B*) light chrome green, (*C*) amber, (*D*) light green (Fe-Mn), (*E*) chrome emerald green, and (*F*) dark green (Fe-Mn).

results although they are definite and are many times that of the experimental error.

The topaz glass yielded a gradient of about 12°F. per in., which is slightly greater than that for flint glass. The manganese purple glass was quite deep in color, but it yielded a rather low gradient (19°F. per in.).

Visible color is no criterion of gradient, as has been shown in section III (1); a comparison of the topaz glass (with a gradient of 12.5° F. per in.) with a 1% ferric oxide glass (with a gradient of 40°F. per in.) further illustrates this fact. The colors do not match, but they agree in intensity and both are yellows. A similar comparison can be made for the cobalt blue glass (with a gradient of 8°F. per in.) and the 0.5% ferrous blue glass (48°F. per in.).

(5) Commercial Glasses

The laboratory results are shown in Table V and Fig. 8. No comment is necesary other than that there is a wide range of gradients.

(6) Commercial Tank Gradients*

Commercial tank gradients were taken with a water-cooled thermocouple assembly, 11 ft. long, inserted down through the crown in a commercial tank. The assembly held a platinum protection tube, $^1/_8$ in. in diameter and 5 in. long, into which was inserted a platinum-platinum rhodium thermocouple. This latter was connected to the compensating lead wire within the water-cooled section. The distance from the water-cooled portion of the assembly to the measuring junction was $4^1/_2$ in. Thermocouple sheath blocks, located in the center of the crown between the second and third ports, were removed, and the water-cooled assembly was lowered into the furnace with a chain block. When the platinum tube made contact with the glass, the immersion was recorded as $^1/_2$ in. Because there is always some doubt as to the exact location of the probe in relation to the surface, $^1/_2$ in. is as close as it can be estimated. Readings were taken only after the thermocouple had shown constant temperature. Such readings were made every inch near the surface and at less frequent intervals at greater depths. The water-cooled assembly was graduated in inches and reference was given to a fixed point on the crown.

The results are shown in Fig. 9 and in Tables IV and V. There are undoubtedly two errors in this work, (*a*) the proximity of the water-cooled section to the thermocouple and (*b*) the presence of batch or foam on the surface. The latter error probably caused the erratic results on amber glass at levels from $2^1/_2$ to 9 in. deep.

* These results were obtained in cooperation with R. D. Duff and O. W. Pfeifer at the Owens-Illinois factory, Streator, Illinois.

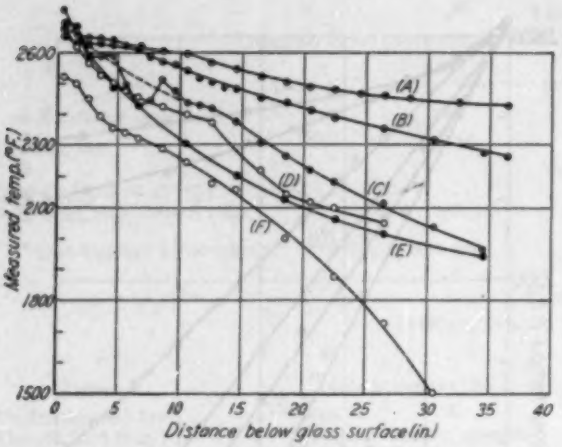

FIG. 9.—Commercial tank gradients: curves (*A*) flint, (*B*) light chrome green, (*C*) pyrites amber, (*D*) light green (Fe-Mn), (*E*) chrome emerald, and (*F*) dark green (Fe-Mn).

No explanations can be given for other breaks in the curves.

The average gradients between $1^1/_2$ and $26^1/_2$ in. are shown in Table IV. In Table V and Fig. 10, these data are correlated with the laboratory results on the same glasses. The agreement is direct, but the gradients are much smaller in the commercial tanks. This decrease, perhaps, may be attributed to deeper glass as well as to convection currents, which are negligible in the laboratory tank but may be quite pronounced in the large commercial tank.

IV. Results and Conclusions

(1) Temperature-gradient tests on iron glasses with iron in the reduced state indicate the gradients to be about three times as great as in the ferric state.

(2) Chromium oxide glasses (up to 0.25% Cr_2O_3) have about the same gradient as equivalent percentages of ferrous oxide.

(3) Manganese does not increase the gradient as much as other oxides giving similar visible color intensities.

(4) A small amount of cobalt yields a sky blue color but decreases rather than increases the flint gradient; similar results are found with a selenium pink.

(5) Decolorization of flint glass increases the gradient in the first inch of the glass surface with little effect at lower depths.

(6) Colors can be near matches although the glasses have radically different gradients; the visible color or color intensity likewise is no criterion of the gradient expected.

(7) A crude relationship exists between the gradient and the amount of gas consumed to maintain a 2615°F. surface temperature; the higher the gradient, the lower the amount of gas required; under similar gas consumption, the higher the gradient, the higher the surface temperature.

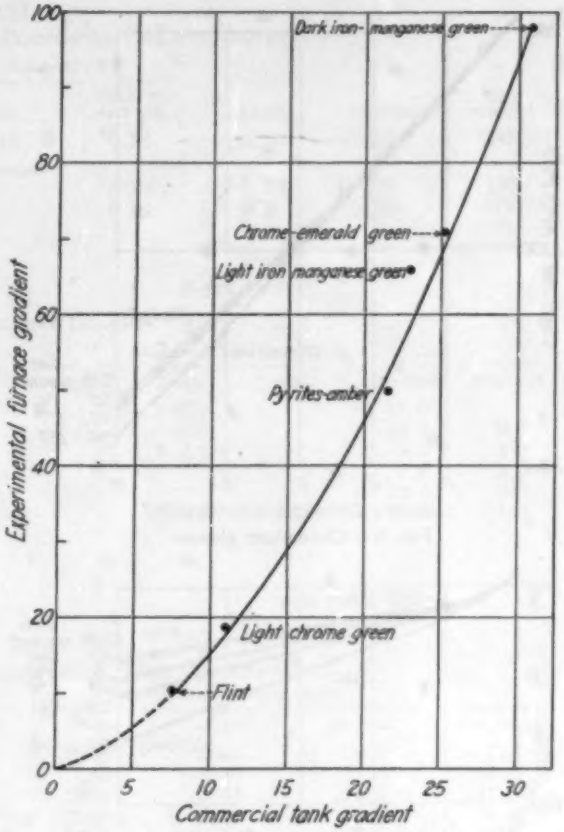

FIG. 10.—Gradients in commercial tank and experimental furnace (°F. per in.).

(8) There is a direct relation between the laboratory gradients presented here and those existing in commercial furnaces.

(9) The development of colors with lowered gradients is to be desired in conjunction with this work.

The relationship, if any exists, between the gradients and other melting problems, such as the amount of gas required, surface temperature, loads possible, devitrification and stone losses, and stone solution are being studied.

Acknowledgment

The authors wish to acknowledge the assistance and contributions of R. D. Duff and O. W. Pfeifer of the Streator, Illinois, factory.

GENERAL RESEARCH LABORATORY
OWENS-ILLINOIS GLASS COMPANY
TOLEDO, OHIO

ELECTRICALLY FUSED FORSTERITE-OLIVINE, I–II*

By the Electrothermal Section of the Electrotechnical Laboratory†

Abstract

North Carolina olivine was melted in the electric arc-resistance furnace, with simultaneous reduction of the iron (fayalite) components, to form a product consisting essentially of crystalline forsterite. The forsterite obtained from olivine by reduction was contaminated by clinoenstatite or a siliceous glass unless MgO or CaO was added to the charge. Silica, present in excess of orthosilicate proportions, was not eliminated by carbon reduction. Simultaneous reduction or vaporization of MgO prevented increase in the MgO to SiO_2 ratio by carbon reaction. Addition of theoretical amounts of MgO to the melt to produce forsterite completely eliminated the clinoenstatite and siliceous glass and resulted in an abrupt increase in high-temperature load-bearing strength. The presence of lime was detrimental to high-temperature load-bearing strength.

I. Introduction

Relatively pure forsterite has not been used in refractories in the past because it has not been available in quality and quantity suitable for practical tests. Forsterite does not occur naturally in a pure form, but, in isomorphous combination with fayalite, tremendous quantities appear as dunite olivine in the State of Washington[1] and in the Appalachian Mountain areas of North Carolina and Georgia.[2] The eastern deposits are located strategically within reach of Pittsburgh and Birmingham, the principal steel-producing centers.

The melting point of forsterite has been determined by Bowen and Andersen[3] to be 1890° ± 20°C. (Fig. 1) in connection with their study of the complete MgO–SiO_2 system. Crystallization of forsterite from a fused melt is extremely rapid with the formation of large, well-formed crystals, which may be either of the interlocking or friable type depending on conditions and rate of cooling.

Basic roof construction for basic, open-hearth furnace installations has long been a dream of the steel industry, and higher operating temperatures for these furnaces, though desirable, have been prohibited because of the melting point of silica brick now used in roof construction. Basic-type superrefractories are needed also in many other applications. The basic character of forsterite, as well as its high melting point, has prompted this investigation of its preparation and properties.

PART I, DIRECT REDUCTION OF OLIVINE

II. Materials and Process

(*A*) *Olivine:* Mineralogically the group term "olivine" includes orthosilicates of divalent bases crystallizing in the orthorhombic system.[4] The group is represented by the formula (Mg, Fe, Mn, Ca)(Mg, Fe, Mn, Zn, Pb)SiO_4, with the following recognized end compounds: Forsterite, Mg_2SiO_4; fayalite, Fe_2SiO_4; tephroite, Mn_2SiO_4; monticellite, $CaMgSiO_4$; glaucochroite, $CaMnSiO_4$; and larsenite, $PbZnSiO_4$.[5]

The mineral commonly called olivine consists of an isomorphous combination of forsterite (Mg_2SiO_4) and fayalite (Fe_2SiO_4), which within the range of 5 to 25% of fayalite is termed chrysolite.[6] In addition to secondary minerals formed by alteration, such as serpentine and chlorite, olivine is commonly associated with several primary minerals, including chromite, bronzite, and enstatite. A typical olivine analysis is presented in Table I.

Olivines from several Appalachian sources were examined, but those containing appreciable alteration products were eliminated because of their higher silica-to-magnesia ratio inasmuch as the surplus silica is difficult to remove. Loss on ignition served as a

* Received June 24, 1943.
Published by permission of the Director, Bureau of Mines, U. S. Department of the Interior; the work was done under cooperative agreement with the Tennessee Valley Authority.

† Robert R. Ralston, electrochemical engineer; McDonald S. Nelson, assistant electrothermal engineer; George W. Leever, electrician; Dan F. Allen, junior physical science aide; Earl F. Nichols, principal electrothermal technician.

[1] Hewitt Wilson and K. G. Skinner, "Review of Four Years of Research on Refractory Properties of Pacific Northwest Olivine," *Jour. Amer. Ceram. Soc.*, **23** [5] 136–38 (1940).

[2] C. E. Hunter, "Forsterite-Olivine Deposits of North Carolina and Georgia," *N. C. Dept. of Conservation and Development Bull.*, No. 41, 117 pp. (1941).

[3] N. L. Bowen and O. Andersen, "Binary System MgO–SiO_2," *Amer. Jour. Sci.*, **37**, 487–500 (1914).

[4] A. N. Winchell, Elements of Optical Mineralogy: II, Description of Minerals, 3d ed., p. 186 ff. John Wiley & Sons, Inc., New York, 1933. 459 pp.; *Ceram. Abs.*, **13** [8] 221 (1934).

[5] E. S. Larsen and H. Berman, "Microscopic Determination of the Nonopaque Minerals," *Geol. Surv. Bull.*, No. 848, 254 pp., 1934; 2d ed., p. 239; *Ceram. Abs.*, **13** [7] 196; [8] 221 (1934).

[6] (*a*) A. N. Winchell, Microscopic Characters of Artificial Inorganic Solid Substances or Artificial Minerals, 2d ed., p. 291. John Wiley & Sons, Inc., New York, 1931. 403 pp.; *Ceram. Abs.*, **11** [5] 323; [8] 468 (1932).
(*b*) E. S. Dana, System of Mineralogy, 6th ed., pp. 449–56. John Wiley & Sons, Inc., New York. 1134 pp.
(*c*) E. H. Kraus, W. F. Hunt, and L. S. Ramsdell, Mineralogy: Introduction to Study of Minerals and Crystals, 3d ed., p. 346. McGraw-Hill Book Co., Inc., New York, 1936. 638 pp.; *Ceram. Abs.*, **16** [5] 160 (1937).

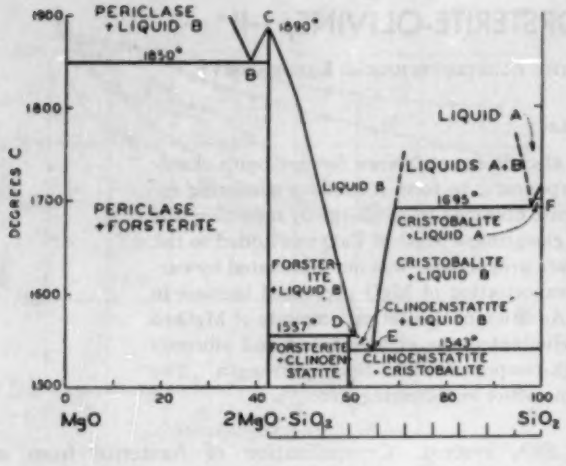

FIG. 1.—MgO–SiO_2 system (after Bowen and Andersen,[3] revised by Greig).

TABLE I

OLIVINE COMPOSITION AND CALCULATED REDUCTION

	Reported analysis (%)*	Assumed actual composition (%)	Constituents to be reduced (%)	Carbon required for reduction (parts)
SiO_2	42.6	42.6	7.9	3.2
Fe_2O_3	8.0			
FeO		7.2	7.2	1.2
Al_2O_3	1.5	1.5		
CaO	0.1	0.1		
MgO	46.6	46.6		
Ignition loss	1.4	1.4		
Cr_2O_3	†	0.5‡	0.5	0.1
NiO	†	0.2‡	0.2	0.1
	100.2	100.1		4.6

* Analysis supplied by John Boyd, chief chemist, United Feldspar and Minerals Corp., Spruce Pine, N. C.

† Not reported.

‡ Small amounts of Cr_2O_3 and NiO have been found consistently in North Carolina olivines by analysts of the Mineral Testing Laboratory, Tennessee Valley Authority, Norris, Tenn.

useful criterion of the degree of alteration because the commonly occurring products (serpentines, talc, etc.) are hydrated.

(*B*) *Carbon:* Crushed graphite electrode waste derived from petroleum coke containing less than 0.3% of ash was used for reduction.

(*C*) *Iron Turnings:* Iron and steel shavings from a local machine shop were added to some of the early melts to assist in collecting and settling the ferrosilicon droplets resulting from the reducing process. This metal addition, however, was ineffective in small-scale furnacing and was discontinued.

(*D*) *Furnace Reactions:* To form forsterite, the 46.6 parts of magnesia present in 100 parts of olivine would require 34.7 parts of silica (Table I), leaving an excess of 7.9 parts of silica. If not otherwise combined, this excess silica is capable of producing 26.4 parts of clinoenstatite in the product by reaction with the forsterite.

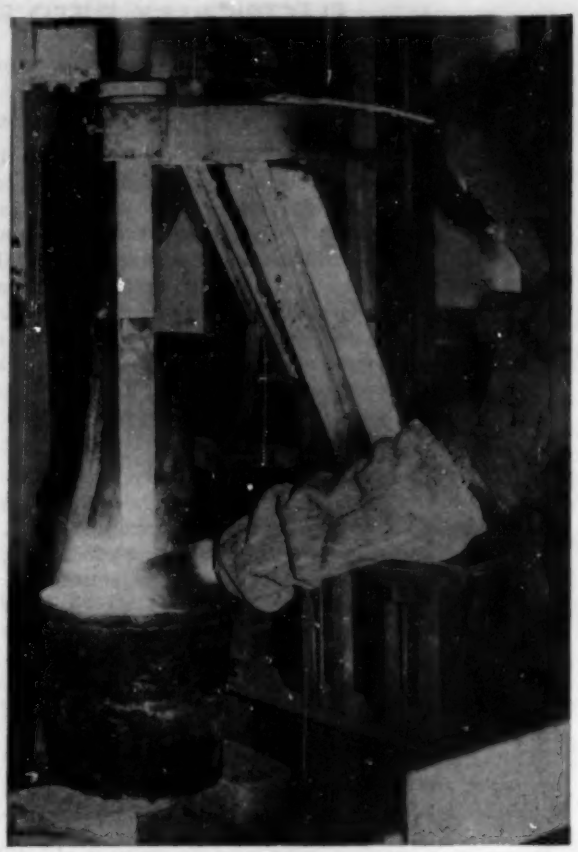

FIG. 2.—Arc furnace in which smallest samples were melted and reacted; capacity, about 50 lb.

Clinoenstatite has an incongruent melting point of 1557° ± 2°C. (as compared with 1890°C. for forsterite[3]); this constituent was therefore considered objectionable in refractory bodies and its elimination was undertaken.

Iron oxide was observed to be easily and completely reduced by carbon during furnacing, and the small amounts of chromium and nickel components were also believed to be reduced. Assuming that the iron present in olivine is largely ferrous, addition of 1.2% of carbon (Table I) theoretically should reduce it to the metallic state. The analysis of typical metal produced by 2% carbon additions indicated that the iron was effectively reduced and that lesser amounts of silicon were contributed to the metal by reduction of SiO_2. Fusion of olivine with 2% of carbon, however, invariably gave a product containing an appreciable amount of glass and clinoenstatite and indicated the presence of more unreduced silica than could be combined as forsterite. An increase in the carbon content of the charge to 5% lowered the amount of clinoenstatite produced but did not eliminate it. A ferrosilicon containing 10 to 20% of silicon was obtained. Further increase in the carbon resulted in no further reduction of silica.

(*E*) *Furnaces:* Olivine, alone or in combination with other batch constituents, was easily fused in several

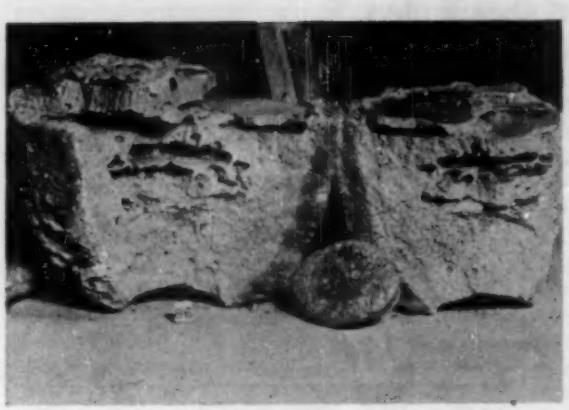

FIG. 3.—Pig of fused forsterite melted in 20- by 20-in. air-cooled furnace shell; weight approximately 300 lb.; note ferrosilicon button taken from bottom of melt.

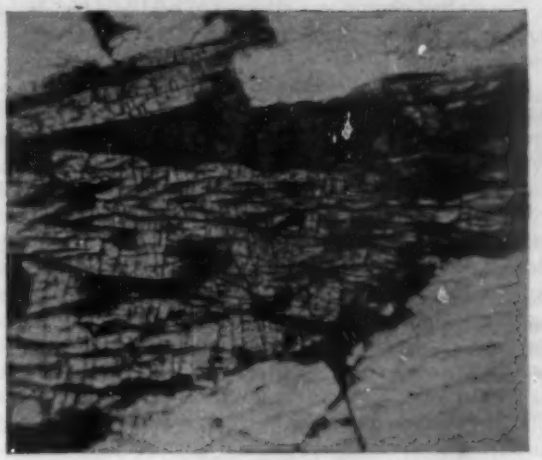

FIG. 4.—Typical cross-fractured appearance of clinoenstatite surrounded by forsterite in thin section; fusion 100, melted olivine; crossed nicols, ×50.

TABLE II

OPTICAL PROPERTIES OF FORSTERITE*

No.	Minerals present in fusion†	Alpha	Beta	Gamma
	Pure synthesized forsterite			
		1.6359	1.6507	1.6688
	Electric-furnace melt			
9	F, C	1.635	1.650	1.669
85	F, P	1.64	1.65	1.67
100	F, G, C	"	"	"
193	F, P	"	"	"
196	F, SS	"	"	"
197	F, SS, G	"	"	"
198-R	F, SS	"	"	"

* The properties of the pure synthesized forsterite are from Bowen and Schairer[7]; those of electric-furnace melt No. 9, by G. T. Faust; and melts Nos. 85, 100, 193, 196, 197, and 198-R, by T. N. McVay.

† F, forsterite; C, clinoenstatite; P, periclase; G, glass; SS, solid solution monticellite-forsterite.

types of electric furnaces, including the indirect-arc, direct-arc, and smothered-arc (or arc-resistance). The greater part of the work on olivine fusion has utilized the latter type of furnace because of its inherently high thermal efficiency and simplified structural requirements. The furnace shells were usually air cooled because the melts were small and the unreacted mix was refractory enough to protect the shell during average fusions (Fig. 2). Cylindrical steel shells, 20 in. in diameter and 20 in. deep, were used for larger melts. The electrodes contained artificial graphite and were either 2 or 3 in. in diameter.

(*F*) *Products:* The forsterite melts, in general, solidified into pigs consisting of tough, dense shells surrounding porous or cavitated zones (Fig. 3). Crystalline structure varied considerably with composition and cooling conditions. The minerals commonly present were readily detected and identified by petrographic methods. A button of metal usually formed in the bottom by gravity settling (Fig. 3), and unsettled metal when sufficiently magnetic was removed by magnetic separation.

TABLE III

HOT-LOAD RESISTANCE OF BONDED, GRANULAR FORSTERITE

No.	Composition (parts)		Specimens tested (No.)	Temp. at shear under 25 lb./in.² (°C.) Min.	Max.	Avg.
0	Original olivine	100	2	1500	1500	1500
1	Forsterite*	100	10	1408	1497	1458
1A	Forsterite*	95				
	Raw dolomite	5	1			1321
1B	Forsterite*	95				
	Magnesia	5	1			1450
2	Forsterite*	90				
	Magnesia	6	7	1470	1500	1490
	Silica	4				
3	Forsterite*	92				
	Chrome cement†	4	8	1382	1440	1410
	Raw dolomite	4				
4	Forsterite*	90				
	Aluminous cement‡	5	8	1500	1640	1576
	Magnesia	5				
4A	Forsterite*	86.5				
	Aluminous cement‡	13.5	2	Slumped at 1585° without load		
5	Forsterite*	90				
	Aluminous cement‡	5	8	1515	1585	1554
	Calcined dolomite	5				
6	Forsterite-clinoenstatite§	95				
	Magnesia	5	8	1315	1505	1438

* Contained not more than 2 to 5% of clinoenstatite and glass.

† Commercial chrome-base refractory cement.

‡ Commercial calcium aluminate hydraulic cement.

§ Contained 10 to 15% of clinoenstatite and glass.

Although forsterite crystallized rapidly from melts of widely varying composition, the crystallization of clinoenstatite appeared to be slow and incomplete, resulting in a fibrous development of clinoenstatite microlites in glass. The existence of such material was easily detected microscopically, although accurate determination of optical properties was not possible. Figure 4 illustrates the characteristic appearance of clinoenstatite as observed in thin section.

The melted charge was allowed to cool as a pig in the furnace or it was electrocast into molds, depending on the desired use.

(*G*) *Forsterite-Clinoenstatite:* Forsterite with associated clinoenstatite was easily prepared by electric-furnace melting of olivine and simultaneous reduction of the iron-bearing components to metallic iron. Forsterite obtained by complete removal of combined iron from olivine had optical properties in agreement with those of the pure compound as determined by Bowen and Schairer,[7] regardless of other phases present in the system (Table II). Although the iron component was easily reduced, the unwanted silica was not expelled by reduction. Addition of 5% of carbon lowered the undesired SiO_2 to less than 2%. Additions of 7.5, 10, and 15% of carbon were not effective in reducing silica further, and long-continued furnacing with excess carbon did not provide a noticeable decrease in the amount of clinoenstatite. In no instance was free magnesia produced by carbon reduction of olivine.

Extrapolated data by Bowen and Schairer[8] show that pure forsterite has a melting point about 120°C. higher than an olivine containing 10% of fayalite. Removal of fayalite from the olivine therefore represents a distinct improvement in refractoriness.

(*H*) *Ferrosilicon:* Reduction of iron oxide and silica resulted in the formation of ferrosilicon which collected more or less completely in the form of a button at the bottom of the melt as shown in Fig. 3.

III. Tests

Ability to withstand load at high temperature was adopted as the basis for comparison of the various forsterite refractories. Each individual fusion was cleaned of adhering unmelted charge and was jaw crushed to pass a 4-mesh screen, although accurate particle sizing was not attempted. Standard 9-in. brick were pressed on the 9- by $4^1/_2$-in. surface at 7400 lb. per sq. in. and fired without load to various temperatures between 1600° and 1700°C. before load testing. Variations of 100° in the original firing temperature produced no correlative effect on hot load strength.

The load tests were conducted in electric furnaces described previously.[9] Samples, under a load of 25 lb. per sq. in., were heated by a spiral graphite element in a strongly reducing atmosphere at a rate of 150° per hour until failure occurred by shear. Temperature readings were obtained by sighting an optical pyrometer on the side of the brick and were assumed to be accurate within ±10°C.

IV. Results and Conclusions

Out of more than 70 compositions that were made up and given preliminary tests, ten of the most promising were selected for more extensive tests. Data on these specimens are presented in Table III. These tests included attempts to develop bonding action by recrystallization of forsterite (composition 1), by synthesis of forsterite during firing (compositions 1A, 1B, 2, and 6), and by addition of refractory cement mixtures (compositions 3, 4, 4A, and 5).

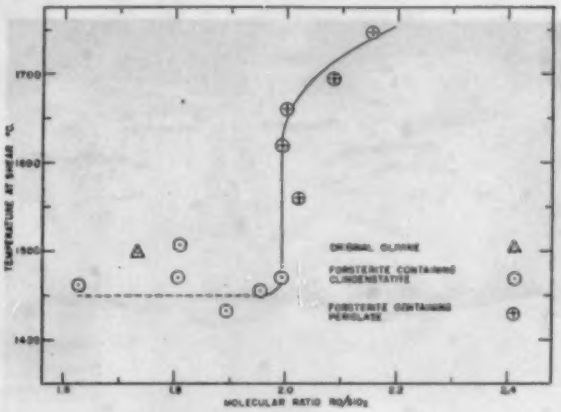

FIG. 5.—Softening temperatures versus composition of 9-in. MgO-SiO_2 brick under 25 lb. per sq. in.; olivine-magnesite fusions.

Efforts to obtain the recrystallization and synthesis of forsterite bond by continued heating alone were unsuccessful. A brick prepared by heating for 45 hours at 1500° to 1700° sheared in the load test at only 1470°C. The best refractory bonding action was obtained by the use of small amounts of calcium aluminate cement with the addition of magnesite or dolomite although these compositions were only slightly better in the load test than the original raw olivine alone.

V. Summary

(1) Forsterite containing clinoenstatite or siliceous glass did not produce acceptable refractories by any method of bonding used in these experiments.

(2) Ferrous iron was easily and completely reduced from olivine by carbon during furnacing, but silica in excess of orthosilicate proportions was only partly reduced. The surplus silica contributed clinoenstatite and glass, which lowered the high-temperature load resistance of the forsterite below that of the original olivine.

(3) Both magnesia and silica showed appreciable loss by vaporization from small arc furnaces under reducing conditions.

(4) Forsterite crystallized easily and rapidly from melts of MgO-SiO_2 compositions containing more than 45% of MgO.

(5) Pressed, granular forsterite did not recrystallize readily to provide a bond at temperatures up to 1700°C. nor did MgO and SiO_2 ingredients react to form forsterite when fired to 1700°C. No correlation between prefiring temperatures and hot load strength was observed. Long and repeated firings did not increase load resistance.

[7] N. L. Bowen and J. F. Schairer, "System MgO–FeO–SiO_2," *Amer. Jour. Sci.*, **29**, 151–217 (1935), p. 196; *Ceram. Abs.*, **15** [9] 288 (1936).

[8] See p. 163 of footnote 7.

[9] M. S. Nelson and R. R. Ralston, "Design and Operation of Electric Load-Test Furnace," *Jour. Amer. Ceram. Soc.*, **26** [February 15, No. 4] 112–16 (1942).

PART II, MgO AND CaO ADDITIONS

The phase diagram of Fig. 1 predicts that any MgO-SiO_2 composition lying between 42.7 and 61% of SiO_2 will develop a liquid phase at the incongruent melting point of clinoenstatite (1557°C.). With rapid cooling of such compositions, however, it is possible that equilibrium conditions are not achieved during cooling and that the last liquid in the melt will correspond to the eutectic composition solidifying at 1543°C. A glass phase will also appear with rapid cooling but on subsequent reheating may be converted to forsterite and clinoenstatite. Compositions containing silica in excess of forsterite proportions should therefore be expected to develop liquid when they are heated above 1557° or (under nonequilibrium conditions) as low as 1543°C. The temperature at which liquid may form is further lowered by impurities present in olivine.

Compositions of forsterite, however, containing free MgO are shown by Fig. 1 to develop liquid only when heated to 1850°C. or above. To capitalize on this advantage, the work originally undertaken has been extended to cover investigation of the effects of MgO and CaO when melted with olivine.

TABLE IV

ANALYSES OF RAW MATERIALS

	Olivine (Burnsville, N. C.)	Calcined magnesite	Dolomite (Norris dam site, Tenn.)	Limestone (Batesville, Ark.)
SiO_2	42.6	1.00	2.36	1.17
Al_2O_3	1.5	0.08		0.31
Fe_2O_3		0.03		0.23
FeO	7.2			
MnO		0.001		
CaO	0.1	1.10	27.36	54.46
MgO	46.6	93.79*	21.56	0.52
Ignition loss	1.4	4.00	41.03	42.43
	99.4	100.00	98.31	99.12

* By difference.

(1) Forsterite-Periclase Tests

Addition of calcined magnesite (Table IV) to arc-furnace fusions of olivine was therefore investigated as a means of assuring complete absence of clinoenstatite. If the silica required to combine as forsterite with all of the MgO in 100 lb. of olivine is subtracted from the total SiO_2 content, 7.9 lb. of uncombined SiO_2 remain, which would require 11.4 lb. of calcined magnesite (94% MgO) for its conversion into forsterite.

Table V shows compositions charged to each fusion as well as results of microscopic examination and load tests. The presence of free periclase in the fusion products coincided with greatly improved load resistance at high temperatures.

The plot of load-test softening temperatures versus composition (Fig. 5) emphasizes the benefit and necessity of free periclase in forsterite for high-temperature, load-bearing service. Reduction of the iron without replacement by MgO resulted in failure at a temperature below that of the original olivine. With additions of MgO insufficient in amount to convert

TABLE V

OLIVINE-MAGNESIA FUSIONS

Fusion No.	Charge composition (parts by wt.)			Mineral components of product*			No load prefiring temp. (°C.)	Temp. at shear (°C.)	Avg.
	Olivine	Carbon	Magnesia	Principal	Minor	Trace (< 1%)			
†	100	2	0	F	G		1623	1465	
							1635	1463	
							1600	1471	1462
							1600	1455	
							1700	1455	
191	100	5.2	5.2	F	G, C		1500	1470	1470
							1565	1470	
190	100	0	5.3				1605	1515	1515
218	100	5	8	F	G		1500	1430	1433
							1500	1435	
219	100	5	10	F	G		1500	1450	1455
							1500	1440	
192	100	0	11.1	F	G, C		1600	1468	1471
							1550	1475	
85	100	2.2	11.1	F	P		1500	1625	1620
								1615	
106	100	2.3	11.4	F		P	1260	1630	1660
							1600	1690	
220	100	5	12	F		G, P	1500	1540	1560
							1500	1580	
228	100	5	14	F	P		1500	1685	1695
							1500	1705	
229	100	5	16	F	P		1500	1755	1748
							1500	1740	

* Determined microscopically; F, forsterite; G, glass; C, clinoenstatite; P, periclase.
† Mixture of several early melts.

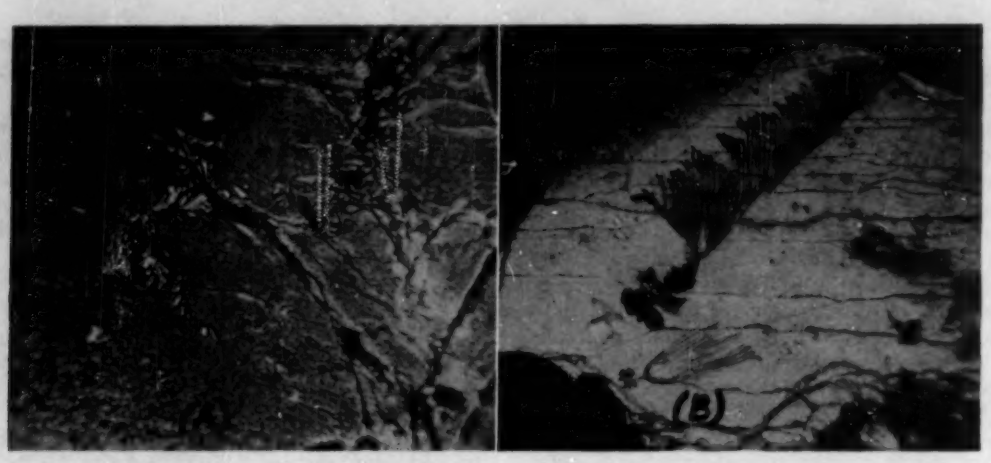

FIG. 6.—Magnesio-wüstite inclusions in forsterite resulting from MgO addition to olivine in melt No. 106; crossed nicols, ×50; (*A*) original appearance, small colorless to light brown magnesio-wüstite globules and dendrites at center; (*B*) after reheating in oxidizing atmosphere, dark brown to opaque magnesio-ferrite dendritic inclusions.

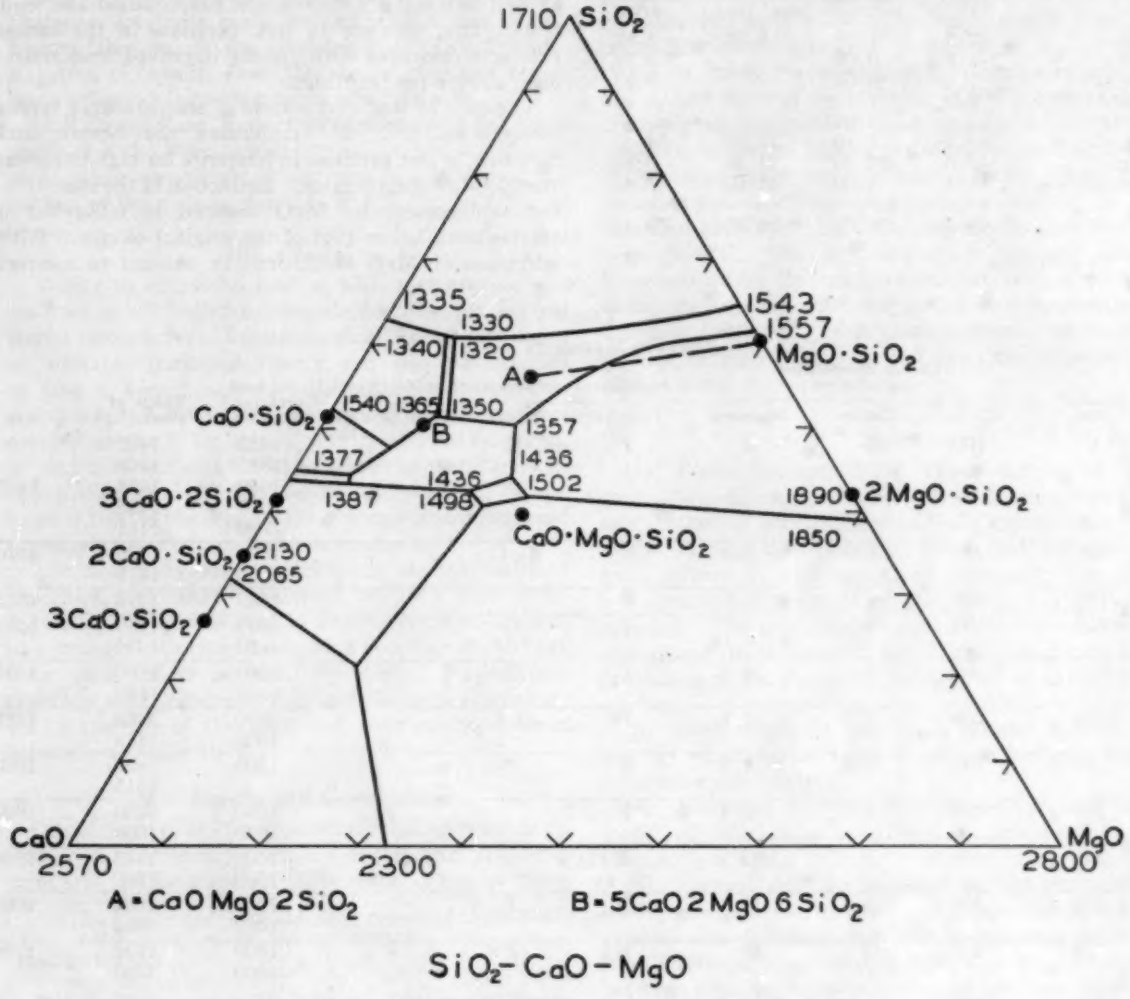

FIG. 7.—CaO–MgO–SiO_2 system (after Ferguson and Merwin[10]).

TABLE VI

OLIVINE-DOLOMITE FUSIONS

Fusion No.	Charge composition (parts by wt.)			Mineral components of products*			No load prefiring temp. (°C.)	Temp. at shear (°C.)	Avg.
	Olivine	Carbon	Raw dolomite	Principal	Minor	Trace (< 1%)			
194	100	0	11.1	F	G		1500	1375	1398
							1620	1430	
86	100	2.2	11.1	F	G		1500	1390	1388
							1500	1385	
129	100	5.9	11.1	F	G			1450	1463
							1700	1475	
108	100	2.3	11.4	F	G		1550	1385	1393
							1550	1400	
213	100	5	25	F			Deformed at 1500	1425	1420
								1415	
119	100	6.6	26.7	F	G		1250	1521	
							1250	1478	
							1700	1585	1541
							1700	1580	
196	100	0	33	F	G		1500	1400	1390
							1500	1380	
214	100	5	35	F		G	1500	1550	1550
							1500	1550	
122	100	7.7	46.2	F		P		1565	
								1565	
							1600	1610	
							1700	1620	1578
							1600	1615	
							1250	1525	
							1250	1545	
226	100	10	50	F		G, P	1500	1535	1545
							1500	1555	
225	100	5	50	F		G, P	1500	1575	1550
							1500	1525	
224	100	0	50	F		G, P	1500	1565	1550
							1500	1535	
227	100	5	75	F	P		Deformed at 1500	1510	1510
								1510	

* Components determined microscopically; F, forsterite (or forsterite-monticellite solid solution); G, glass; C clinoenstatite; P, periclase or magnesio-wüstite.

all clinoenstatite to forsterite, the temperatures at which failure occurred remained low; coincidentally, however, with the appearance of free periclase, a sharp rise in shear temperatures was obtained. Figure 5 also indicates that hot load resistance improved further as the amount of periclase was increased.

Microscopic examinations showed that the iron in olivine was not completely reduced in the presence of free magnesia in spite of a carbon content sufficient to effect total reduction of iron in the furnace charge. Instead, ferrous oxide was observed to be absorbed by the periclase to form magnesio-wüstite.* Any influence on load-bearing strength was believed to be negligible. Figure 6 illustrates the appearance of a small amount of magnesio-wüstite in a thin section of a melt to which the theoretical quantity of magnesia to produce forsterite had been added.

(2) Dolomite Additions

Dolomite likewise is a source of magnesia and has the added advantage of being more widely available in abundant quantities than magnesite. As pointed out by Ferguson and Merwin[10] and later by Seil,[11] limited amounts of CaO may (*a*) combine with the clinoenstatite ($MgSiO_3$) to form monticellite ($CaO \cdot MgO \cdot SiO_2$) or (*b*) displace MgO from forsterite (Mg_2SiO_4) to form monticellite and periclase. The phase relationships are indicated in Fig. 7.

Calculations based on a typical dolomite (Table IV) showed that 100 lb. of olivine required 40 lb. of dolomite during furnacing to convert clinoenstatite into forsterite and monticellite. Larger amounts of dolomite should result in the appearance of periclase. Separate phases in the mixture could not be identified because forsterite and monticellite[11] enter into solid solution and because the refractive indices of the monticellite solid solution and forsterite overlap. Figure 8 illustrates the typical appear-

* The term magnesio-wüstite is applied to solid solutions of magnesium oxide and ferrous oxide (wüstite) by Bowen and Schairer; see p. 151 of footnote 7.

[10] J. B. Ferguson and H. E. Merwin, "Ternary System CaO–MgO–SiO_2," *Amer. Jour. Sci.*, **48**, 81–123 (1919); p. 115 ff.; *Jour. Amer. Ceram. Soc.*, **2** [10] 844–46 (1919).

[11] G. E. Seil and Staff, "Orthosilicates of the Alkaline Earths with Special Reference to Their Uses in the Refractory Field," *Jour. Amer. Ceram. Soc.*, **24** [1] 1–19 (1941); for Bibliography with abstracts on this subject see *Ceram. Abs.*, **19** [11] 273–93 (1940).

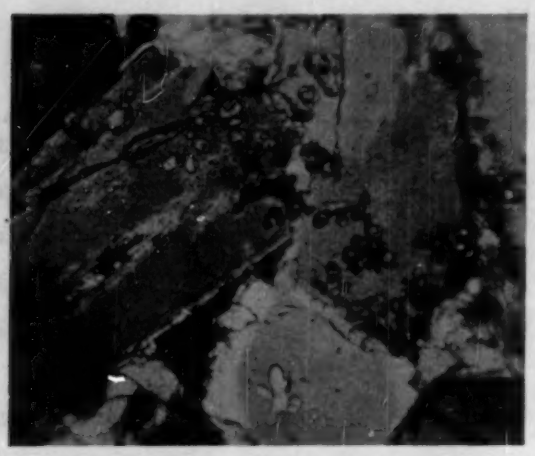

FIG. 8.—Globular periclase inclusions in forsterite resulting from dolomite addition to olivine, melt No. 224; crossed nicols, ×50.

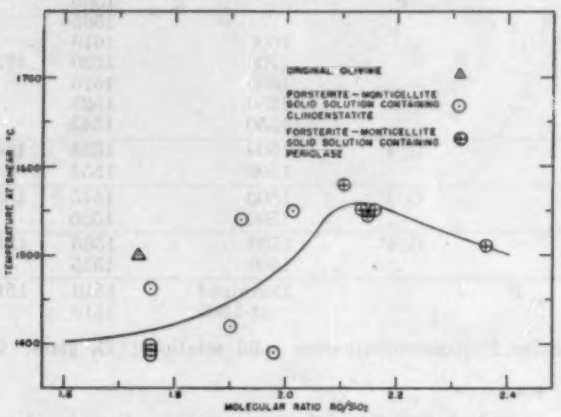

FIG. 9.—Softening temperatures versus composition of 9-in. MgO-SiO_2 brick under 25 lb. per sq. in.; olivine-dolomite fusions.

ance of periclase produced from a forsterite-dolomite melt.

Results of load tests in Table VI and Fig. 9 show that additions of dolomite to olivine melts provided little increase in refractoriness beyond that possessed by the original olivine. Melts prepared with dolomite additions and containing less than 40% were in general characterized by failure at temperatures lower than that of the original olivine. This failure is undoubtedly attributable to the silica derived from the fayalite, which contributed to the formation of low-melting metasilicate and resulted in lower load-bearing capacity than the original olivine. Dolomite additions in excess of 40% provided higher average shear temperatures, although these temperatures were decidedly lower than those containing MgO additions. The improvement in load-bearing strength indicated by Fig. 9 was probably the result of the elimination of glass rather than of the formation of more refractory compounds.

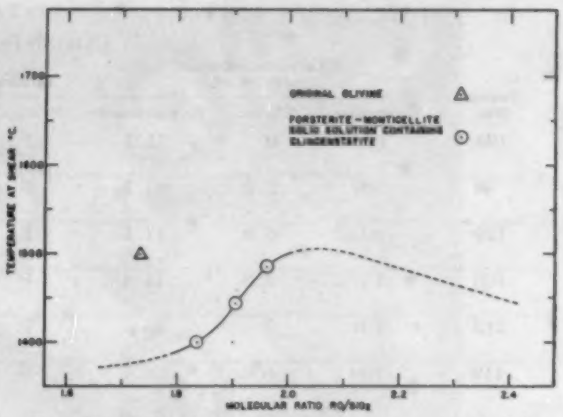

FIG. 10.—Softening temperatures versus composition of 9-in. MgO-CaO-SiO_2 brick under 25 lb. per sq. in.; olivine-limestone fusions.

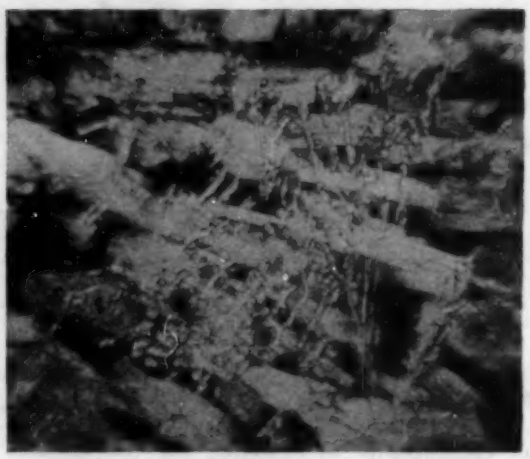

FIG. 11.—Periclase inclusions in forsterite-monticellite solid-solution phase resulting from large limestone additions to olivine, melt No. 146; crossed nicols, ×50.

(3) Limestone Additions

Because of its widespread occurrence, lime has been suggested for incorporation into the olivine charge of the melting furnace to combine with silica present in excess of forsterite proportions. Limited additions of lime would first react with clinoenstatite to form monticellite, followed by displacement of MgO from forsterite to yield monticellite and periclase. Calculation showed that 28.1 lb. of limestone (Table IV) were required for each 100 lb. of olivine in order to convert the clinoenstatite to monticellite.

As indicated by Table VII and Fig. 10, incorporation of limestone in the fusion charge caused failures either with or without load at very low temperatures. Experiments involving addition of lime were therefore discontinued. Calculations based on the charged compositions indicated that monticellite, akermanite, or dicalcium silicate should be among the products of the various fusions. Melt No. 146 was expected to con-

TABLE VII

OLIVINE-LIMESTONE FUSIONS

Fusion No.	Charge composition (parts by wt.)				Mineral components of product*			No load prefiring temp. (°C.)	Load temp. at shear (°C.)
	Olivine	Carbon	Limestone	Sand (SiO_2)	Principal	Minor	Trace (< 1%)		
221	100	5	15		F	G		Deformed at 1500	1400
222	100	5	20		F	G		Deformed at 1500	1445
223	100	5	25		F		P, G	Slumped at 1500	1485
146	100	5	91.7	5.8	F, P			Melted at 1500	

* Determined microscopically; F, forsterite (or forsterite-monticellite solid solution); G, glass; P, periclase (or magnesio-wüstite).

sist chiefly of monticellite with smaller amounts of MgO and dicalcium silicate. These minerals, however, were not identified. Figure 11 shows the characteristic appearance of monticellite-forsterite solid solutions. The grains were much smaller than forsterite, and periclase inclusions appeared as transverse filaments.

VI. Summary

(1) Addition of 16% of magnesia to fusions of olivine raised the load-failure temperature of the product from 1500° to 1750°C., or 250° above the original olivine value.

(2) The added MgO reacted with magnesium metasilicate (clinoenstatite) to produce the orthosilicate, forsterite. Additions of MgO in excess of the amount required to produce forsterite appeared in the final product as microscopic, globular inclusions of periclase.

(3) In the presence of free magnesia, the last traces of FeO were difficult to reduce and tended to remain in solid solution in the MgO. No harmful effect on refractoriness, however, was observed.

(4) Lime (CaO) (from dolomite or limestone) also combined with metasilicates to form orthosilicates and, if added in large amounts, set MgO free as periclase. The orthosilicate monticellite ($CaMgSiO_4$), however, melts at a lower temperature than clinoenstatite and therefore represents no improvement in refractoriness.

VII. Conclusions

(1) Maximum load failure at a temperature of 1750°C. or higher may be realized in electrically melted forsterite compositions by addition of magnesium oxide in excess of forsterite proportions in the melt. The presence of periclase in an otherwise homogeneous forsterite melt signifies absence of siliceous glass and clinoenstatite.

(2) Excess silica present in olivine melts is not eliminated by direct carbon reduction because of simultaneous reduction or vaporization of magnesium oxide. The excess silica is derived from olivine alteration products, such as antigorite ($3MgO \cdot 2SiO_2 \cdot 2H_2O$) and talc ($3MgO \cdot 4SiO_2 \cdot H_2O$), and from fayalite ($2FeO \cdot SiO_2$) by reduction of the iron oxide.

(3) The presence of calcium oxide in forsterite refractories is undesirable owing to the formation of low-melting calcium-magnesium silicate, low-melting ternary eutectics, and glass.

Acknowledgment

The authors are indebted to the following persons for invaluable suggestions and aid: Oliver C. Ralston and Hewitt Wilson, who inaugurated the investigation; T. N. McVay and G. T. Faust, for certain phases of the petrographic examination; A. F. Greaves-Walker and R. P. McCabe, for part of the firing and testing; and H. R. Shell and other analysts cited, for analytical data.

U. S. DEPARTMENT OF THE INTERIOR
BUREAU OF MINES
NORRIS, TENNESSEE

DUPLICATION OF CHROME-BROWN ELECTRICAL PORCELAIN GLAZES WITH NONESSENTIAL MATERIALS*

By Richard B. Fuller and Arthur S. Watts

Abstract

This condensed report covers the development of a commercial glaze using cheap, nonessential materials in maximum amount. The results meet fully the more expensive glaze which is no longer available.

As a result of wartime restrictions in the use of chromium salts, a study of the duplication of the brown glazes used on most electrical porcelain insulators was undertaken with the object of utilizing only those materials which do not involve priorities.

Before the introduction of these chrome-brown glazes, most porcelain insulator glazes were made from mixtures of slip clays with small additions of feldspar and flint. These glazes were semitransparent, reddish brown in color, and very sensitive to kiln atmosphere. A later development was a mixture of slip clays with a manganese dioxide content ranging up to 6%. This glaze was a rich chestnut brown with a brilliant surface, but it had a tendency to show crystalline mat spots where the application was thin.

The clays used were chiefly Albany and Michigan slip clays, which are being employed extensively on stoneware today. They produce a brownish black glaze at cone 7 when an excess amount of the Albany slip clay is used and a chestnut brown glaze when more Michigan slip clay is used. All these glazes develop a rust-brown surface on edges and where they are thin when the heat-treatment exceeds cone 7.

Starting with Albany slip as a base, a series was prepared using Florida kaolin, $BaCO_3$, MnO_2, Fe_2O_3, and ZnO in amounts up to 10%. When this glaze was applied to an electrical porcelain body and fired to cone 10^6, the samples showed fading in color on the edges and wherever their application was thin.

Blends of these glazes were made and fired, but nothing of promise developed except in those containing more than 6% of MnO_2 and less than 4% of ZnO, which were a dark red-brown with good covering qualities. None of these, however, was similar to the glazes to be duplicated, and all were slightly overfired at cone 10^6 except when at least 8% of Florida kaolin was added.

A base glaze was therefore prepared, consisting of 92% of Albany slip clay plus 8% of Florida kaolin, and a test series was made by adding 2% and 4%, respectively, of $BaCO_3$, MnO_2, and TAM ceramic stain. This stain contains materials which do not involve priorities. It is an extremely fine powder with a composition of ZrO_2 5.0%, SiO_2 14.5%, TiO_2 11.75%, Al_2O_3 28.15%, Fe_2O_3 24.2%, Cr_2O_3 10.15%, Na_2O 0.9%, and CaO 0.5%.

Glazes containing 2% and 4% of $BaCO_3$ are a neutral brown rather than a red-brown; those with 2% and 4% of MnO_2 retain their red-brown color but are semitransparent; and those containing 2% and 4% TAM stain are very opaque and of a deep chocolate-brown color with a good brilliant surface. Blends of the glazes containing 4% of MnO_2 and 4% of TAM stain are the most promising, especially when the TAM stain glaze predominates.

The introduction of small amounts of Michigan slip clay to replace Albany slip clay was next studied. A blend containing up to 8% of Michigan slip clay with 80% of Albany slip clay, 8% of Florida kaolin, 1% of MnO_2, and 3% of TAM stain is definitely promising, but specific gravity and thickness of glaze application must be carefully controlled if color uniformity is required.

To develop a glaze which in spraying or dipping is similar to the present electrical porcelain glaze, a typical white, electrical porcelain glaze was prepared to which 15% of TAM stain and 3% of MnO_2 were added. The clay content was also replaced with Albany slip clay. A mixture was then prepared of two-thirds of Michigan slip clay plus one-third of Albany slip clay. These glazes were blended in various proportions, applied to electrical porcelain trials, and fired at cone 10^6 in a standard electrical porcelain tunnel kiln. The most satisfactory product has the following composition:

	(%)		(%)
Potash feldspar	33.75	Whiting	11.25
Flint	15.00	TAM stain	11.25
Mich. slip clay	16.75	ZnO	1.50
Albany slip clay	8.25	MnO_2	2.25

This glaze gives excellent results on both large and small electrical porcelain products when applied at 1.33 to 1.35 of specific gravity. If the application is slightly thick, however, a faint purplish tint is apparent, which may be eliminated by reducing the MnO_2 content to 1.25 and increasing all other constituents in proportion.

In mass production, this glaze is equal in all respects to the various commercial chrome-brown insulator glazes with which it has been compared.

Department of Ceramic Engineering
Ohio State University
Columbus, Ohio

* Presented at the Forty-Fifth Annual Meeting, The American Ceramic Society, Pittsburgh, Pa., April 21, 1943 (White Wares Division). Received June 22, 1943. The material in this paper is condensed from a thesis prepared at Ohio State University in 1942.

INDEXES TO THE JOURNAL

Compiled by

THE AMERICAN CERAMIC SOCIETY

ROSS C. PURDY, *Editor*
EMILY C. VAN SCHOICK, *Assistant Editor*

Volume 26 December, 1943 No. 12

AUTHOR INDEX

The reference number in parentheses refers to the *monthly* issue of the *Journal;* the numbers following are the *page* numbers.

Andrews, A. I. See Cook, R. L.
Austin, A. E., and Bassett, L. B. Spectrochemical procedure in clay analysis, (6) 185–88.

Badger, A. E. See Rodriguez, A. R.
Bassett, L. B. See Austin, A. E.
Beam, J. R. Effect of opacifiers on fused viscosity of feldspathic glazes, (7) 205–12.
Beinlich, A. W., Jr. See Pole, G. R.
Berkelhamer, L. H. Rehydration study of clays, (4) 120–26.
Bowen, N. L. Petrology and silicate technology, (9) 285–301.

Cook, R. L., and Andrews, A. I. Fundamental study of factors influencing color of porcelain enamels, (3) 73–76.
Cooper, W. G. See Spencer-Strong, G. H.
Cortelyou, W. P. See Shell, H. R.
Currier, A. E. Influence of sodium silicate composition on its behavior with sodium carbonate as casting-slip deflocculant, (2) 67–71.

Davis, H. M. See Zerfoss, Samuel.
Deringer, W. A. Relation of hydrogen to adherence of sheet-steel enamels, (5) 151–59.

Ehlinger, J. A. See Smith, H. W., Jr.
Electrothermal Section of the Electrotechnical Laboratory. Electrically fused forsterite-olivine, I–II, (12) 405–13.

Fellows, R. L. Relation of thickness to impact resistance of porcelain enamels, (5) 160–62.
Foster, H. D. Salt glazes for structural building units, (2) 60–67.
Fuller, R. B., and Watts, A. S. Duplication of chrome-brown electrical porcelain glazes with nonessential materials, (12) 414.

Gibson, George, and Ward, Roland. Reactions in solid state: Reaction between sodium carbonate and quartz, III, (7) 239–46.
Goin, F. L. See Nicholson, T. E.
Grigorieff, W. W., and Lampman, C. M., Jr. Sealed glass bushings, (3) 83–87.

Hafner, H. C., and Jones, F. L. Adsorption of ions by leached surface films on glass, (2) 55–56; see also Jones, F. L.
Harvey, F. A. Influence of water vapor on silica brick at high temperatures, (11) 373–77.
Harvey, F. A., and Thompson, C. L. Mottled brick, facts, fancies, and fallacies, (11) 361–64.
Henry, E. C. Measurement of workability of ceramic bodies for plastic molding processes, (1) 37–39; see also Mitchell, Lane.
Herschel, W. H. See Richmond, J. C.
Holscher, H. H., Rough, R. R., and Plummer, J. H. Experimental studies of temperature gradients in glasses of various colors, (12) 398–404.
Huggins, M. L., and Sun, K.-H. Calculation of density and optical constants of glass from its composition in weight percentage, (1) 4–11.
Huggins, M. L., Sun, K.-H., and Silverman, Alexander. Vitreous state, (12) 393–98.

Johnson, A. L. Colloid chemistry in ceramics, (3) 88–92.
Jones, F. L., and Hafner, H. C. Effect of chemically formed surface films on glass solubility, (2) 56–58; see also Hafner, H. C.

Kane, L. E., and Ueltz, H. G. Possible use of ferruginous talcs in steatite dielectrics, (11) 389–92.
King, R. M. Mechanics of enamel adherence: (1) Role of cobalt oxide in metal and oxide precipitation during ground-coat firing cycle, and (2) determination of temperature and time intervals of precipitation, XIV, (2) 41–48; Influence of cobalt and nickel oxides on metal precipitation at ground-coating–iron interface, XV, (10) 358–60.
Knapp, W. J. Thermal conductivity of nonmetallic single crystals, (2) 48–55.

Lampman, C. M., Jr. See Grigorieff, W. W.
Lawrence, W. G. See Norton, F. H.
Lewis, M. O. Effects of lithia substitution for soda in vitreous enamel, (3) 77–83.
Limes, R. W. See Phelps, S. M.
Longenecker, L. S. Possible use of suspended roofs and walls in glass furnaces, (5) 167–72
Lyle, A. K. Theoretical aspects of chemical attack of glasses by water, (6) 201–204.

McDowell, J. S. Plant investigations of variables affecting color of silica brick, (11) 364–67.
McMahon, J. F. See Schurecht, H. G.
McVay, T. N., and Wilson, Hewitt. Substitution of topaz, domestic kyanite, and synthetic mullite-corundum for India kyanite, I–III, (8) 252–66; correction, (10) 340.
Mitchell, Lane, and Henry, E. C. Nature of Georgia kaolin: Evidence of chemical and colloidal analysis, I, (4) 105–12; Evidence of mineralogical analysis, II, (4) 113–19.
Moore, Henry, and Scholes, S. R. Amber glass and role of carbon, (2) 58–60.

Nicholson, T. E., and Goin, F. L. Simplified thermal-expansion rings for production control in terra cotta manufacture, (5) 163–67.
Norton, C. L., Jr. See Patton, T. C.
Norton, F. H., and Lawrence, W. G. Note on anomalous heat absorption of kaolinite, (11) 388–89.

Osborn, E. F. Compound merwinite ($3CaO \cdot MgO \cdot 2SiO_2$) and its stability relations within system CaO–MgO–SiO_2, (preliminary report), (10) 321–32.

Parmelee, C. W. See Pask, J. A.; Rodriguez, A. R.
Pask, J. A., and Parmelee, C. W. Study of diffusion in glass, (8) 267–77.
Patton, T. C., and Norton, C. L., Jr. Measurement of thermal conductivity of fireclay refractories, (10) 350–58.
Peterson, J. B. See Richmond, J. C.
Phelps, S. M., and Limes, R. W. Mottled or colored silica brick, (11) 378–87.
Plummer, H. C., and Wanner, E. F. Modular size of clay-products units, (9) 307–20.
Plummer, J. H. See Holscher, H. H.
Pole, G. R., and Beinlich, A. W., Jr. New refractory compositions resistant to molten rock phosphate, (1) 21–37.

Richmond, J. C., Peterson, J. B., and Herschel, W. H. Improved volumenometer, (4) 127–31.
Rodriguez, A. R., Parmelee, C. W., and Badger, A. E. Study of photoluminescence in glass, (5) 137–50.
Rough, R. R. See Holscher, H. H.

Scholes, S. R. See Moore, Henry.
Schurecht, H. G. Fitting glazes to ceramic bodies, (3) 93–98.
Schurecht, H. G., and McMahon, J. F. Use of aluminum metal in the ceramic industry: Effect of coating insulating firebrick with aluminum–fire-clay mixtures, II, (7) 212–17.
Seil, G. E., and Staff. Study of literature on separation of magnesia from lime in dolomite and similar materials, (7) 218–38.
Shell, H. R., and Cortelyou, W. P. Soluble sulfate content of pottery bodies during preparation, (6) 179–85.
Silverman, Alexander. See Huggins, M. L.
Smith, H. W., Jr., and Ehlinger, J. A. Direct radiant kiln firing in the ceramic industry, (4) 132–36.
Snow, R. B. Equilibrium relationships in liquidus surface in part of the MnO–Al_2O_3–SiO_2 system, (1) 11–20.
Speil, Sidney. Physical testing of talc for high-frequency ceramics, (10) 336–38.
Spencer-Strong, G. H., and Cooper, W. G. Experiments with accelerated weathering test for porcelain enamels, (8) 249–51; Gouge resistance of porcelain enamels, (1) 1–4.

Stone, R. L. Physical chemistry of firing steatite ceramics, (10) 333–36.
Sun, K.-H. See Huggins, M. L.

Thiemecke, H. Thermal and moisture expansion of ball clays and bodies fired to different temperatures, (6) 173–79.
Thiess, L. E. Vitrified cordierite bodies, (3) 99–102.
Thompson, C. L. See Harvey, P. A.
Trostel, L. J. Factors influencing staining of silica brick, (11) 368–73.

Ueltz, H. G. See Kane, L. E.

Wanner, E. F. See Plummer, H. C.
Ward, Roland. See Gibson, George.
Watts, A. S. See Fuller, R. B.
Wilson, Hewitt. See McVay, T. N.
Winckler, J. R. Spherical furnace calorimeter for direct measurement of specific heat and thermal conductivity, (10) 339–49.
Winter, Aniuta. Structural homogeneity of glass, (8) 277–84; Transformation region of glass, (6) 189–200.

Zerfoss, Samuel, and Davis, H. M. Observations on solid-phase inversions of calcium orthosilicate, constituent of dolomite-silica brick, (9) 302–307.

SUBJECT INDEX TO THE JOURNAL

Volume 26, 1943

The reference number in parentheses refers to the *monthly* issue of the *Journal;* the number following is the *page* number.

Abrasion resistance of porcelain enamels, gouge test, (1) 1.
Accelerated weathering test for porcelain enamels, (8) 249.
Acid-resistant enamels. See *Enamels.*
Adherence of enamels. See *Enamels.*
Akermanite in system $CaO–MgO–SiO_2$, (10) 321; see also *Merwinite.*
Alaskite in pottery bodies, soluble sulfate content, (6) 183.
Alkaline earth and alkaline silicates, mixture, cristobalite liquidus curves, after Kracek, (9) 292.
Alumina (Al_2O_3)–$CaO–SiO_2$, equilibrium diagram, after Rankin and Wright, (9) 295.
–MgO, portion of equilibrium diagram, melting points of steatite compositions, (10) 334.
–$MgO–SiO_2$, equilibrium diagram, after Rankin and Merwin, (9) 293; ware based on compositions of, (9) 293; "solidus" diagram, after Niggli, (9) 294.
–$MgO–SiO_2$, with flux additions, electrical and mechanical properties, (3) 99–102.
–$MgO–SiO_2$, phase diagram, composition of normal and low-loss steatite bodies, (10) 333–36.
–$MnO–SiO_2$, equilibrium relations on liquidus surface, diagram of part of system, (1) 14; isotherms and refractive index in part of system, (1) 15; pseudo-equilibrium diagram for cooling liquids, (1) 19.
–$K_2O–SiO_2$, equilibrium diagram, after Schairer and Bowen, (9) 296; petrologic and technologic significance, (9) 296.
–SiO_2, equilibrium diagram, after Rankin and Wright, (9) 288; after Bowen and Greig, (9) 289.
–SiO_2 minerals, natural, firing process, (8) 260.
–$Na_2O–CaO–SiO_2$, cross sections in, (9) 299.
Aluminum and fire clay for coating insulating firebrick, (7) 212.
Amber glass. See *Glass.*
American Standards Association, Committee A62, correlation of building materials dimensions, (9) 310.
Amorphous solid and synonymous terms, (12) 393.
Analysis of clays, trace elements in, qualitative data, (6) 186; see also *Chemical analysis* and specific types of analyses.
Andalusite in Bur. Mines test samples, composition, (8) 262; variable temperature load-test results, (8) 264.
pyrochemical and pyrophysical changes in, (8) 254; commercial deposits and chemical analysis, (8) 255.
Andrews and Howe method for preparation of lithium-containing enamels for thermal expansion measurement, (3) 79.
Annealing of glass. See *Glass.*
Antimony in enamels, and antimony-free types, gouge-resistance tests, (1) 2.
Apparatus, barometer, closed-cistern altitude mercurial, for pressure measurements, (4) 128.
Bausch and Lomb large Littrow spectrograph for clay analyses, (6) 185.
Bausch and Lomb medium quartz spectroscope for silver concentration in glass, (8) 270.
Apparatus (*continued*)
Berek compensator for glaze stress tests, (3) 94.
calculator for determination of tristimulus values from spectrophotometric data, photo, (3) 73.
calorimeter, spherical furnace, for specific heat and thermal conductivity measurements, (10) 339–49.
for crazing resistance of glazes by pressure, (3) 97.
d'Arsonval galvanometer densitometer for clay analyses, (6) 185.
electrodes, carbon types for spectrochemical analysis, (6) 186.
for enamel adherence tests, (10) 359.
for enamel resistance tests, (2) 43.
Endell body tester, modified, for plasticity of clays and bodies, (1) 37.
for equilibrium melts in system $MnO–Al_2O_3–SiO_2$, (1) 12.
for flat-plate glaze stress test, (3) 93.
furnace. See *Furnaces. Kilns.*
General Electric recording spectrophotometer for tests on porcelain enamel colors, (3) 74.
gouge-testing machine for enamels, Porcelain Enamel Institute design, (1) 1.
Hilger deviation spectrometer and "Contiflow" spotlight for fluorescence spectra studies, (5) 141; modification, (5) 142.
Hunter reflectometer for tests on lithia-containing enamels, (3) 80.
impact-testing machine, Porcelain Enamel Institute design, (5) 160.
Kraehenbuehl integrating calculator for determinating tristimulus values from spectrophotometric curves, (3) 73–74.
Michaelson interferometer for tests on strains, (8) 280.
microscopes, micrometer, for contraction or expansion of glaze stress in rings, (3) 95.
microscopes, slit ultramicroscope for $AgNO_3$ diffusion in glass, (8) 270.
for photoluminescence studies of glass, and modification, (5) 141–42.
Q meter for steatite dielectrics measurements, (10) 337.
rehydrator for clay studies, (4) 123.
Selas radiant gas burner, description and cross section, (4) 133.
spherical furnace calorimeter for specific heat and thermal conductivity measurements, diagrams and photos, (10) 340–41.
terra cotta rings for thermal expansion measurements of glazes, photo and diagram, (5) 163–64.
for thermal conductivity of crystals and glasses, (2) 50–51.
thermal conductivity tester, diagrams, (10) 351–53.
volumenometer, improved, for solid volume measurements, (4) 127.
Arrhenius equation for effect of temperature on chemical attack of glass by water, (6) 203.
Ash, synthetic coal, chemical analysis and molecular formula, (7) 213.
Austenite and ferrite, relation of enamel adherence, (5) 155.
Autoclave treatment and glaze thickness, effect on expansion and contraction of lustrous glazed rings, curves, (3) 96.
Ball clays. See *Clays.*
Barium carbonate for sulfate removal in slips, (6) 185.
Barometer, close-cistern altitude mercurial type, for pressure measurements, (4) 128.
Bauxites, rehydration-dehydration test results, (4) 123.
Beidellite, chemical analysis, (4) 107.
Bentonite, rehydration-dehydration test results, (4) 122.
Wyo., chemical analysis, (4) 107.
Berger formula on chemical attack of glass, correction of Keppeler formula, (7) 202.
Beryl in cordierite bodies, composition, color, and water absorption, (3) 100–101.
thermal conductivity curves, (2) 53.
Bibliographies and footnote references (listed according to subject of titles of *Journal* papers with the number of footnote references given for each subject); see also Footnote Citations Index listed by author names, pp. 424-29, this issue.
aluminum metal in ceramic industry, use, II, 3 ref., (7) 212–17.
calcium orthosilicate, solid-phase inversions in dolomite-silica brick, 18 ref., (9) 302–307.
clays, ball, and clay bodies, thermal and moisture expansion fired at different temperatures, 4 ref., (6) 173–79.
clays and clay bodies, plastic working properties, 4 ref., (1) 37–39.
clays, rehydration study, 16 ref., (4) 120–26.
clays, spectrochemical analysis procedure, 7 ref., (6) 185–88.
colloid chemistry in ceramics, 13 ref., (3) 88–92.
cordierite bodies, vitrified, 10 ref., (3) 99–102.
crystals, nonmetallic single, thermal conductivity, 9 ref., (2) 48–55.
dolomite and lime, magnesia separation, 461 ref., (7) 218–38.
dolomite-silica brick, solid-phase inversions of calcium orthosilicate, 18 ref., (9) 302–307.
enamels, adherence: cobalt oxide and oxide precipitation in firing, role, XIV, 11 ref., (2) 41–48; effect of cobalt and nickel oxides on metal precipitation at ground-coat interface, XV, 17 ref., (10) 358–60.
adherence of sheet-steel enamels, relation to hydrogen content, 22 ref., (5) 151–59.
gouge resistance, 1 ref., (1) 1–4.
mechanics of enamel adherence, I–XV, (10) 360.
porcelain, accelerated weathering test, 2 ref., (8) 249–51.
porcelain, color of, factors influencing, 4 ref., (3) 73–76.
porcelain, relation of thickness to impact resistance, 3 ref., (5) 160–62.
sheet-steel, relation of adherence to hydrogen content, 22 ref., (5) 151–59.
vitreous, lithia substitution for soda, 21 ref., (3) 77–83.
equilibrium relation on liquidus surface in part of $MnO–Al_2O_3–SiO_2$ system, 9 ref., (1) 11–20.
forsterite-olivine, electrically fused, 13 ref., (12) 405–13.
furnace calorimeter, spherical, for specific

Bibliographies, furnace calorimeter (*continued*)
heat and thermal conductivity measurements, 21 ref., (10) 339–49.
glass, amber, and role of carbon, 14 ref., (2) 58–60.
chemical attack by water, theory, 9 ref., (3) 201–204.
colored, temperature gradients, 12 ref., (12) 398–404.
density and optical constants, calculation, 14 ref., (1) 4–11.
diffusion, 22 ref., (8) 267–77.
photoluminescence study, 25 ref., (5) 137–50.
sealed bushings, 6 ref., (3) 83–87.
solubility, effect of chemically formed surface films, 2 ref., (2) 56–58.
structural homogeneity, 8 ref., (8) 277–84.
transformation region, 34 ref., (6) 189–200.
vitreous state, 31 ref., (12) 393–98.
glazes, feldspathic, effect of opacifiers on fused viscosity, 10 ref., (7) 205–12.
glazes, fitting to ceramic bodies, 18 ref., (3) 93–98.
glazes, salt, for structural building units, 3 ref., (2) 60–67.
hydrogen, relation to adherence of sheet-steel enamels, 22 ref., (5) 151–59.
insulating materials, cordierite, vitrified bodies, 10 ref., (3) 99–102.
insulating materials, sealed glass bushings, 6 ref., (3) 83–87.
insulating materials, talc for high-frequency ceramics, physical tests, 6 ref., (10) 336–38.
kaolin, Ga., chemical and colloidal analyses, I, 17 ref., (4) 105–13; evidence of mineralogical analysis, II, 6 ref., (4) 113–19.
kilns, direct radiant kiln firing, 1 ref., (4) 132–36.
kyanite, domestic, substitution for India kyanite, 31 ref., (8) 252–66.
lime and dolomite separation from magnesia, 461 ref., (7) 218–38.
lime–MgO–SiO_2, stability relations of merwinite, 7 ref., (10) 321–32.
lithia in enamels as soda substitute, 21 ref., (3) 77–83.
magnesia separation from lime and dolomite, 461 ref., (7) 218–38.
manganese oxide (MnO)–Al_2O_3–SiO_2, equilibrium relation on liquidus surface in part of system, 9 ref., (1) 11–20.
merwinite, stability relations in system CaO–MgO–SiO_2, 7 ref., (10) 321–32.
modular size of clay-products units, 5 ref., (9) 307–20.
mottled silica brick, 14 ref., (11) 361–64; mottled or colored silica brick, 14 ref., (11) 378–87; see also *Bibliographies, refractories, silica brick.*
mullite-corundum, synthetic, substitution for India kyanite, 31 ref., (8) 252–66.
olivine-forsterite, electrically fused, 13 ref., (12) 405–13.
opacifiers, effect on fused viscosity of feldspathic glazes, 10 ref., (7) 205–12.
petrology and silicate technology, 27 ref., (9) 285–301.
plastic working properties of ceramic bodies, workability measurements, 4 ref., (1) 37–39.
quartz and sodium carbonate, solid state reactions, 10 ref., (7) 239–46.
refractories, aluminum–fire-clay mixtures for coating insulating firebrick, II, 3 ref., (7) 212–17.
fire-clay, thermal conductivity measurements, 3 ref., (10) 350–58.
resistance to molten rock phosphate, 14 ref., (1) 21–37.
silica brick, effect of water vapor at high temperatures, 7 ref., (12) 373–77.
silica brick: mottled, 14 ref., (11) 361–64; staining factors, 10 ref., (11) 368–73; mottled or colored, 14 ref., (11) 378–87.
solid-phase inversions of calcium orthosilicate in dolomite-silica brick, 18 ref., (9) 302–307.
specific heat and thermal conductivity measurements, spherical furnace calorimeter for, 21 ref., (10) 339–49.
solid state reactions, sodium carbonate and quartz, 10 ref., (7) 239–46.
spectrochemical procedure in clay analysis, 7 ref., (6) 185–88.
steatite, firing, physical chemistry of, 3 ref., (10) 333–36.
structural materials, salt glazes for building units, 3 ref., (2) 60–67.
structural units, modular size, 5 ref., (9) 307–20.
talc for high-frequency ceramics, physical tests, 6 ref., (10) 336–38.

Bibliographies (*continued*)
terra cotta, simplified thermal expansion rings for production control, 9 ref., (5) 163–67.
thermal conductivity of nonmetallic single crystals, 9 ref., (2) 48–55.
topaz, substitution for India kyanite, 31 ref., (8) 252–66.
vitreous state, 31 ref., (12) 393–98.
volumenometer, improved, 7 ref., (4) 127–31.
Blakely test apparatus, double-pronged fork glaze test, (3) 95.
Bole and Jackson method for solid volume measurements with inclined manometer, (4) 127.
Borax in glazes for structural materials, effect on glaze thickness, (2) 64.
Boron, boron atoms in glass, optical constants, types and data, (1) 5–6.
Bouyoucos method for sedimentation of clays, (4) 109.
Brick, face, forming process, effect on body consistency, (1) 38–39; see also *Masonry* and types of *brick* under *Refractories.*
Brucite ($Mg(OH)_2$), precipitation from slurry of calcined dolomite and sea water, (7) 227.
Bureau of Mines vs. Corhart refractories test specimens, analyses, (8) 256.
refractories test specimens, composition, (8) 262–63; variable- and constant-temperature load test results, (8) 264–65.
Burning of refractories, effect on color, (11) 366–67.
of refractories, effect of sulfur gases in coal on color, (11) 367, (11) 387.
and reheating of refractories, color photo, (11) 362A–63.
of silica brick, effect of composition, and load test results, color photo, (11) 362A.
Bushings, cast glass, with sealed-in metal inserts, (3) 83–87.

Calcination method for MgO separation from dolomite, (7) 218.
Calcium orthosilicate ($2CaO \cdot SiO_2$), beta-gamma inversion (dusting) of, inhibiting effect of P_2O_5, (9) 302; inhibitors, elements studied, (9) 303–304; chemical and physical inhibition methods, (9) 305–306.
chemical properties, (9) 302; crystal structure and hydration properties, (9) 304–305.
solid solution of P_2O_5 in, thermal and optical method and evidence of, (9) 302–303.
Calcium oxide. See *Lime.*
Calcium silicate series, groups and properties, (9) 305.
Calorimeter, spherical furnace, for specific heat and thermal conductivity measurements, (10) 339–49.
Carbon in amber glass, effect on color, (2) 58–60.
Casagrande method for sedimentation and grain-size distribution in clays, (4) 109.
Casting slips. See *Slips.*
Cements, high-lime clinkers, "dusting" of, (9) 302.
Portland cement clinker, fundamental constituents, (9) 295.
Portland clinker, chemical analysis and molecular formula, (7) 213.
Ceramic industry, colloid chemistry in, use, (3) 88–92.
use of aluminum metal in firebrick coatings, (7) 212.
Chemical analysis of ball clays, (6) 173.
and colloidal analysis of Ga. clays and kaolins, (4) 105.
of manganese oxides, (1) 13.
of raw and electrodialyzed clays, (4) 106.
of sulfate and soluble salts in ball, china, and miscellaneous clays, (6) 181.
of synthetic coal ash, (7) 213.
Chemical attack of glass, formulas for soluble material in, (6) 202; Sharp formula, (6) 202.
Chemical extraction of magnesium compounds from natural impurites and miscellaneous chemical methods, (7) 220, (7) 228.
Chrome cements, specific heat and thermal conductivity data, (10) 345–47.
Chromic oxide (Cr_2O_3)–CaO series for crucible corrosion tests, (1) 25; refractory properties, (1) 27.
–ZrO_2–CaO, refractory properties, (1) 27.
Clays. See also *Kaolin.*
ball, china, and miscellaneous, rehydration-dehydration test results, (4) 122.
and china, soluble salts content, (6) 181.
Jernigan, soluble sulfate content, storage effect, (6) 184.

Clays, ball (*continued*)
Ky., Tenn., and English, chemical analyses, thermal expansion, moisture expansion and absorption, (6) 173–78.
in pottery bodies, soluble sulfate content, (6) 183.
casting processes, effect of plasticity, (3) 91.
classification, rapid rehydration-dehydration method, (4) 120.
colloidal behavior, (4) 118–19.
deflocculated slips of, comparative grain-size distribution curves, (4) 112.
dehydration and rehydration studies, (4) 120.
electrodialyzed and raw: chemical analyses, (4) 106; pH and viscosity curves, (4) 109–11.
fluorescence, Morin dye test and effect of dilute HCl leachings, (4) 108.
Ga., Pike's Peak, chemical analysis, (4) 107.
graphite dilution effect for quantitative analyses, (6) 187.
hydrogen-ion and viscosity curves, (4) 109–10.
hydrogen and sodium, coulombic forces in, diagrams, (3) 90–91.
internal standard for comparison of analyses, (6) 187.
MgO and PeO in, spectrochemical and chemical analyses, (6) 188.
nonclay impurity of, effect on rehydration and dehydration test, (4) 125.
and opacifiers in enamels, effect on gouge resistance, (1) 3.
particle-size distribution, curves, (3) 89.
plasticity, definition, (3) 89; effect on forming processes, (3) 91.
sedimentation tests, (4) 112.
spectrochemical analyses, types of electrodes and arcing techniques, (6) 185.
stream birefringence of, (4) 112.
Clayware, definitions of terms for modular unit sizes, (9) 309.
modular unit size, (9) 307; historical review, (9) 307–308; size of clay-products units, (9) 316; nominal unit face sizes, (9) 320.
thermal analyses and curves, (4) 115–16.
trace elements in, quantitative method for determination, (6) 185.
X-ray analyses, technique, apparatus, and test results, (4) 116–18.
Clinoenstatite-forsterite composition, properties, effect in refractories, (12) 408.
Cobalt oxide (CoO)–FeO, solid system, Bernard equilibrium diagram, (2) 42, (10) 359.
in metal and oxide precipitation, effect on enamel adherence, XIV, (2) 41.
Colloidal analysis of Ga. kaolins, (4) 105.
Colloid chemistry in ceramics, domestic sources of clays and treatment, (3) 88–92.
Colors, coloring oxides, effect on accelerated weathering of porcelain enamels, (8) 250–51.
color photographs, cooling, slow and rapid treatment of silica brick, (11) 382A.
mottling of silica brick, appearance and color, (11) 378A.
silica brick, heat-treatment effects, (11) 378A, (11) 382A.
silica brick, varying effects of composition, burning treatment, and load test, (11) 362A.
wollastonite, iron, and alumina mixtures in silica brick, heat-treatment effect, (11) 382A.
green and blue particles, effect of variable size, (3) 74–75; effect of variable percentages, (3) 76.
mottled, stained, or colored silica brick. See *Colors, color photographs;* also *colored, mottled,* and *stained* items under *Refractories.*
for porcelain enamels, spectrophotometric data, modified Kraehenbuehl integrating calculator, (3) 73; General Electric recording spectrophotometer, (3) 74.
Compton theory of thermal conductivity, curves and formula, (2) 49.
Copper glasses. See *Glass, copper.*
Copper salts in glass, effect on diffusion rate, (8) 275–76.
Cordierite bodies, electrical and mechanical test results and thermal expansion curves, (3) 101–102.
flux additions, composition, color, water absorption, and electrical and fired properties, (3) 100–102.
vitrified, of system MgO–Al_2O_3–SiO_2, effect of flux additions and vitrification range at cones 13 to 15, (3) 99–102.

Corhart electrocast mullite-corundum. See *Refractories, mullite-corundum.*
Corrosion test for resistance of refractories to molten rock phosphate, (1) 21–37.
Corundum, thermal conductivity curves, (2) 53.
Coulombic forces associated with hydrogen and sodium clays, diagram, (3) 90–91.
Crazing of glazes, firing under reducing conditions, effect, (3) 97.
of glazes, types, kiln, moisture, frost, thermal shock, and parallel, (3) 97–98.
of salt glazes, test, (2) 64–65.
Cristobalite liquidus curves for alkaline earth and alkali silicate mixtures, after Kracek, (9) 292.
Crucibles, corrosion-resistant, composition, fired physical properties, phosphatic materials for, and test results, (1) 23–25.
Crystalline substance vs. vitreous solid, (12) 394.
Crystallization process for magnesia production, (7) 219–20.
of merwinite, stability relations in system $CaO–MgO–SiO_2$, (10) 321.
Crystals, single nonmetallic, thermal conductivity studies, Endô and Compton theories, apparatus, test method, results, (2) 48–55.

Definitions, magnesiowüstite, (12) 411.
module and related terms for modular unit sizes, (9) 309.
petrology, (9) 285.
plasticity, (3) 89.
and symbols of density and optical constants, (1) 5.
vitreous state, (12) 393; vitreous solid, amorphous solid, supercooled liquid, glass, and plastic, (12) 393.
workability and plasticity, differentiation, (1) 37.
Deflocculants for casting slips, effect of sodium silicate and sodium carbonate, (2) 67–71.
Dehydration test on clays, (4) 124.
Dendrite theory of metal adherence, (2) 41, (5) 151.
Detroit rocking furnace for tests on corrosion resistance to molten rock phosphate, (1) 34–35.
Diaspore for refractories, physical properties and uses, (8) 256; raw material and firebrick cost quotations, (8) 257.
rehydration-dehydration test results, (4) 123.
Diatomaceous earth brick, specific heat and thermal conductivity data, (10) 345–47.
Diatomite filters, adsorption data, (6) 180.
Dielectric measurements, Q meter for, on steatite bodies, (10) 337; see also *Steatite.*
for talc, tabular data, (11) 391.
Diffusion, coefficients, Fick's law, and other formulas, (8) 267.
method for glass, correcting for true diameter of diffusion, (8) 270.
of silver in glass, formula for weight of diffused silver, (8) 269.
Diopside ($CaMgSi_2O_6$)–leucite–silica equilibrium diagram, after Schairer and Bowen, (9) 300.
Disannealing of glass, effect on refractive index, (6) 189.
Dolomite, magnesia separation from lime, methods and bibliography, (7) 218–38.
and magnesite ores, concentration, flotation methods, (7) 219.
-olivine fusions, data, (12) 411.
in pottery bodies, soluble sulfate content, (6) 183.
Dusts, multicione, chemical analysis and molecular formula, (7) 213.
Dynamic method for glass expansion vs. temperature measurements, curves, (6) 190.

Electrically fused forsterite-olivine, (12) 305.
Electrical porcelain. See *Porcelain, electrical.*
Electrical tests on steatite dielectrics, Bell Telephone Laboratory results, (11) 390.
Electrocast mullite-corundum. See *Refractories, mullite-corundum.*
Electrochemical separation of MgO from sea water and brines, (7) 227.
Electrodes, types and diagrams, and arcing techniques, (6) 186.
Electrodialyzed clays, raw Ga., analyses, (4) 106.
Electrolytes in casting slips, effect of varying amounts, (2) 67.
Electrolytic theory of adherence of sheet-iron ground coats, (5) 151.
Enamels acid-resistant, antimony-bearing and antimony-free, gouge-resistance data, (1) 2.
acid-resistant and nonacid-resistant, effect of weathering, actual vs. accelerated, (8) 250; see also *Enamels, porcelain.*
adherence: cobalt oxide in metals, effect, oxide precipitation during ground-coat firing and precipitation intervals of time and temperature, XIV, (2) 41; cobalt and nickel oxides, effect on metal precipitation in ground-coat interface, XV, (10) 358.
dendrite and oxide theories, (2) 41, (5) 151.
of ground coats, iron oxide effect, (5) 156.
relation to austenite and ferrite, (5) 155.
resistance, test apparatus and data on Co_3O_4- and Ni_2O_3-containing enamels, (10) 359.
resistance, test apparatus and resistance data, (2) 43–44.
on sheet iron, effect of varying quantities of hydrogen, (5) 158.
of sheet-steel ground coats, theories, (4) 151.
bubbles in, gouge test and effect of clays and opacifiers on structure, (1) 1–3.
chipping and coating thickness, relation to impact resistance, (5) 160.
cobalt and cobalt-free on iron, and cobalt on copper, adherence, (5) 154.
cobalt-free: adherence, photo, (5) 143; effect of furnace atmosphere, photomicrograph, (5) 157; relation of stock thickness, (5) 158.
cobalt in metal and oxide precipitation during firing, and determination of time and temperature intervals, (2) 42–43.
dendrite theory of metal adherence, (2) 41, (5) 151.
electrolytic theory of adherence of sheet-iron ground coats, (5) 151.
gouge resistance, application weight effect, and effect of clays and opacifiers, (1) 2–3.
gripping theory of adherence of sheet-iron ground coats, (5) 151.
ground-coat–iron interface, effect of Co and Ni oxides on metal precipitation, (10) 358.
ground-coat, preoxidation advantages, (5) 153.
hydrogen theory of adherence of sheet-iron ground coats, (5) 151.
impact resistance, relation of coating thickness, (5) 160.
metals for, precipitation intervals of time and temperature, effect, XIV, (2) 41; metal precipitation at ground-coat interface, effect of cobalt and nickel oxides, XV, (10) 358, (10) 360.
oxide theory of adherence: effect of "ferrous oxide" and magnetic iron oxide, (2) 41; effect on sheet-iron ground coats, (5) 151.
porcelain, accelerated weathering test, (8) 249.
atmospheric vs. accelerated weathering effects, (8) 249–50.
blue and green colors for, spectrophotometric data, integrating calculator for, (3) 73; use of General Electric recording spectrophotometer, (2) 74.
bubble formation in, effect on spalling, (8) 250–51.
coloring oxides in, effect on accelerated weathering, (8) 250–51.
gloss, actual vs. accelerated weathering effects, (8) 250; effect of coloring oxides, (8) 251.
gouge-resistance tests, (1) 1.
spalling of colored acid- and nonacid-resistant types, (8) 250–51.
resistance. See *Enamels, adherence.*
thickness of coating, relation to impact resistance, (5) 160.
vitreous, lithia as soda substitute in, effect on fusibility, gloss, opacity, gouge resistance, surface abrasion, and thermal expansion, (3) 77–83.
Endell body tester, modified, for plasticity measurements on clays and bodies, (1) 27.
Endellite and Mo. halloysite, relations, citation, (4) 119.
Endô theory of thermal conductivity, curve and formula, (2) 49.
Equilibrium diagrams, alumina (Al_2O_3), MgO, CaO, and FeO, eutectic positions in, (9) 291.
$Al_2O_3–SiO_2$ system: after Shepherd, Rankin and Wright, (9) 288; after Bowen and Greig, (9) 289.
binary systems, eutectic positions of technologic significance, (9) 291.
Equilibrium diagrams (*continued*)
cristobalite liquidus curves for alkaline earth and alkaline silicate mixtures, after Kracek, (9) 292.
ferrous oxide (FeO)–CoO, solid system, after Bernard, (2) 42, (10) 359.
join $3CaO·MgO·2SiO_2$–$2CaO·MgO·2SiO_2$, data on merwinite and akermanite mixtures, (10) 329.
leucite–diopside–silica system, after Schairer and Bowen, (9) 300.
lime (CaO)–Al_2O_3–SiO_2 system, solidus, after Rankin and Wright, (9) 295.
lime (CaO)–FeO–SiO_2 system: after Bowen, Schairer, and Posnjak, (9) 297; mixtures of metasilicate ratio, after Bowen, Schairer, and Posnjak, (9) 298.
lime (CaO)–MgO–SiO_2 system, binary equilibrium relations in join $2CaO·SiO_2$–$2CaO·MgO·2SiO_2$, (10) 328.
courses of crystallization in part of system, (10) 330.
after Ferguson and Merwin, (12) 410.
field of $3CaO·MgO·2SiO_2$, (10) 322.
field of merwinite and composition studies, (10) 324.
magnesia (MgO)–Al_2O_3–SiO_2 system, after Rankin and Merwin, (9) 293; "solidus" diagrams, after Niggli, (9) 294.
magnesia (MgO)–Al_2O_3 system, portion of, and melting points of steatite compositions, (10) 334; theoretical melting curves of talc, clay, and $MgCO_3$ bodies, (10) 335.
magnesia (MgO)–SiO_2 system, after Bowen, Andersen, and Greig, (9) 290.
magnesia (MgO)–SiO_2 system, after Bowen and Andersen (revised by Greig), (12) 406.
magnesia (MgO)–SiO_2 system, immiscible region in, (9) 291.
magnesia (MgO)–SiO_2 system, melting interval of talc (metatalc), (10) 335.
manganese oxide (MnO)–Al_2O_3–SiO_2 system, (1) 14; isotherms in part of system, (1) 15; refractive index of glasses formed, (1) 15; pseudoequilibrium diagram for cooling liquids, (1) 19.
melting curves of steatite bodies, theoretical, (10) 335.
of plagioclase feldspars after Bowen, (9) 299.
potassium oxide (K_2O)–Al_2O_3–SiO_2 system, after Schairer and Bowen, (9) 296.
silica minerals, pressure-temperature diagram indicating stability relations, after Fenner, (9) 287.
soda (Na_2O)–CaO–SiO_2 system, compositions of glasses superimposed on portion of diagram for photoluminescence studies, (5) 140.
"solidus" diagrams, definition and discussion, (9) 295.
Equilibrium studies, glass, speed distribution curves, (6) 194.
manganese oxide (MnO)–Al_2O_3–SiO_2 system: relations on liquidus surface, (1) 11; apparatus for equilibrium melts, (1) 12; melts to establish equilibrium and data on quintuple points, (1) 16–19.
phase equilibrium data on silicate compositions in region of orthosilicate join in ternary system CaO–MgO–SiO_2, (10) 321–22.
stable refractive index as function of temperature, curve, (6) 195.
Excitation method, arcing techniques and electrode types for, (6) 186.
Expansion test method, laboratory, (1) 32.

Feldspar, chemical analysis, (3) 82.
plagioclase, equilibrium diagram, after Bowen, (9) 299.
and ZnO in cordierite bodies, composition, color, and water-absorption data, (3) 100–101.
Feldspathic glazes. See *Glazes.*
Ferric oxide in steatite body, effect on dielectric constant, (11) 391–92.
Ferrite and austenite, relation of enamel adherence, (5) 155.
Ferrous oxide (FeO)–CaO–SiO_2 system, equilibrium diagram after Bowen, Schairer, and Posnjak, (9) 297; discussion of system, (9) 298; equilibrium diagram for mixtures of metasilicate ratio in system, after Bowen, Schairer, and Posnjak, (9) 298.
in clays, spectrochemical and chemical analyses, (6) 188.
–CoO, solid system, Bernard equilibrium diagram, (2) 42, (10) 359.
Ferruginous talcs. See *Talcs.*

Fettke and Stewart formula for diffusion rates and solution in slag attack of refractories, (8) 269; modified formula, (8) 269.
Fick's law of diffusion in liquids, (8) 267; test of law, (8) 273.
Filter pressing, sulfate vs. water distribution, (6) 184; effect of repeated filter pressing, (6) 184–85.
Filters, diatomite, adsorption data, (6) 180.
sulfate calculation of filtrates, (6) 182; soluble sulfate content of filter cakes and filtrates, (6) 183.
Filtration method for soluble sulfate content of clays, (6) 180.
Firing (burning) of silica brick. See *Burning; Refractories.*
radiant gas method, (4) 132; see also *Furnaces: Kilns.*
Fizeau interferometric method for thermal expansion measurements and Saunders improved procedure, (3) 79.
Flint in pottery bodies, soluble sulfate content, (6) 183.
Flotation method for magnesite and dolomite ores, (7) 219.
Fluorescence of clays, dilute HCl leachings, (4) 108.
of copper-ruby glass, composition, (5) 145; effect of Cu_2O and SnO as activators, curves, (5) 147–48.
effect of $AgNO_3$ diffusion, (8) 271; effect of other silver salts and of nonsilver salts, (8) 274.
of glasses, effect of uranium salts, (5) 140–49.
of soda-lime-silica, soda-boric oxide, and soda-borosilicate glasses, (5) 144–45.
Forsterite, bonded granular, hot-load resistance data, (12) 407.
globular periclase inclusions in, effect of dolomite additions, photomicrograph, (12) 412.
magnesio-wüstite inclusions in, photomicrographs, (12) 410.
-monticellite solid solution phase in olivine-limestone fusion, photomicrograph, (12) 412.
-olivine, electrically fused, (12) 405.
optical properties, (12) 407; fused forsterite, pig of and ferrosilicon button, photo, (12) 407.
-periclase, tests, (12) 409.
Frits, colored, blue and green, effect of color and frit particle size, application weight, and amount of colorant, (3) 74–76.
lepidolite and spodumene content, chemical analysis and calculated frit compositions, (3) 81–82.
Frost crazing of glazes, (3) 98.
Fuller's earth, fluorescence of dilute HCl leachings, (4) 108; raw and electrodialyzed, viscosity and grain-size distribution, curves, (4) 111; thermal analysis curves and X-ray data, (4) 116–18.
rehydration-dehydration test results, (4) 123.
Furnaces. See also *Kilns.*
arc, for melting olivine, photo, (12) 407.
Detroit rocking, for corrosion resistance tests on molten rock phosphate, (1) 34–35.
for electric melting and casting GE 1075 glass, description and line drawing, (3) 85.
glassmelting, colored glass, temperature-gradient study, (12) 399.
continuous, triple-fired, slab reheating type, diagram, (5) 169.
oil-burning glass tank, proposed design, (5) 172.
suspended roofs and walls in, construction advantages and limitations, (5) 167.
tank, cross section and sprung crown, diagram, (5) 168.
tank, suspended shadow wall, outside and top views, photos, (5) 170.
for simulative and reheat tests on insulating firebrick, (7) 214.
spherical furnace calorimeter, for specific heat and thermal conductivity measurements, (10) 339; diagram and photos, (10) 340–41.
for temperature gradient studies of colored glass, diagram, (12) 399.
Fusibility of feldspar in enamels, (3) 78.

Gas burner, radiant, direct-type, description and cross section, (4) 133.
Gases in kiln atmosphere, composition, (11) 375.
Gas expansion vs. liquid absorption for solid volume measurements, method, (4) 127.
Geophysical Laboratory, studies on compound merwinite and its stability relations in system $CaO–MgO–SiO_2$, (10) 321.
Georgia clays and kaolins. See *Clays; Kaolin.*
Glacial phosphoric acid, hydrogen bridges, (12) 397.
Glass, alkali content extracted as NaOH, effect of time and temperature, (6) 201, (6) 203.
amber, carbon vs. sulfur and other reducing agents, effect on color, (2) 59; effect of Fe_2O_3 and Na_2O, (2) 59.
annealing, disannealing effect on refractive index of borosilicate glasses, (6) 189.
annealing: expansion coefficient vs. refractive index of poorly annealed samples, curves, (8) 282–83; changes in properties, significance, (8) 282–83.
annealing, rapid method, (6) 196.
barium crown, dense, static method test results, curves, (6) 199.
borosilicate crown, disannealing effect on refractive index, (6) 189.
borosilicate crown: refractive index and expansion coefficient from quenched samples, (6) 191; static method, curves, (6) 199.
borosilicate crown, transformation speed, effect of pressure, (8) 284.
bottles, time-chemical attack curves of Bacon and Burch, (7) 203; chemical durability curves of Bacon and Burch, Herman, and Owens and Emanuel, (6) 204.
bushings, sealed, manufacture and tests, (3) 83–87.
cast, for sealed glass bushings, production and tests, (3) 83–87.
chemical attack, formulas for soluble material in, (6) 202.
chemical attack by water, time-temperature function, theories, (6) 201.
colored, chromium compounds in, analyses and temperature gradients, (12) 402.
chromium greens, light cobalt blue, selenium pink, cerium titanium topaz, and dark purple, analyses, temperature gradients, and curves, (12) 402–404.
colorants, analyses, (12) 400.
furnace for temperature gradient study, diagram, (12) 399.
order of radiation on cooling, (12) 399.
commercial, temperature data for tank gradients, and curves, (12) 402–404.
copper-bearing: fluorescence, curves, (5) 147; fluorescence vs. temperature, tabular data and curves, (5) 148; intensity curves, (5) 148.
copper-bearing, phosphorescence decay, curves, (5) 147.
copper-ruby, compositions, fluorescence studies, (5) 145.
definition, relation of synonymous terms, (12) 393.
definitions and symbols of density and optical constants, (1) 5.
deformation of surface, immersion method for measurement, (8) 280.
density, conversion of equations and constants for calculation, (1) 4.
density and optical constants, calculation from weight percentage composition, (1) 4.
devitrified glass, presence in quenched products along $2CaO·SiO_2$ and $2CaO·MgO·2SiO_2$ join, (10) 323; data for mixtures on $3CaO·MgO·2SiO_2$ and $2CaO·MgO·SiO_2$ join, (10) 325; data for mixtures in system $CaO–MgO–SiO_2$, (10) 326.
diffused, silver ($AgNO_3$) concentration vs. time, curves, (8) 272; concentrations vs. depth of penetration, curve, (8) 273.
diffusion coefficients, (8) 267.
diffusion: Fick's law and other formulas, (8) 267; modified formula of Fettke and Stewart, (7) 269; test of Fick's law, (8) 273.
diffusion of silver, review, (8) 268; silver content in glass vs. depth of penetration, curve, (8) 268.
diffusion vs. time and temperature: effect of AgCl, Ag_2SO_4, $AgNO_3$, and Ag_2O, curves, (8) 271; effect of AgCl, $AgNO_3$, $TlSO_4$, $CuCl_2$, and $CuSO_4·5H_2O$, (8) 272.
disannealing, effect on refractive index, (6) 189.
dispersion, variation of, as function of heat-treatment, (8) 278.
durability, time-temperature effect, (6) 201.
dynamic method for expansion vs. temperature measurements, curves, (6) 190.
equilibrium state vs. time, curves, (6) 194.
expansion coefficient, variation of, as function of heat-treatment, curve, (8) 278; test on poorly annealed sample, (8) 282.
Fernico and Corning 705-AO, thermal contraction curves, (3) 84.
ferrous-ferric, temperature gradient curves, (12) 401.
flint, commercial, chemical composition for diffusion studies, (8) 269.
flint, decolorized and undecolorized, temperature gradient studies, curves, analyses, and temperature gradients, (12) 400–402.
flint, powdered, dense sample, release of Pb and K, relative rate during passage of dilute nitric acid, (2) 56.
fluorescence, effect of $AgNO_3$ diffusion, (8) 271; effect of other silver salts and of nonsilver salts, (8) 274.
fluorescence, literature review, (5) 139.
fluorescence spectra, apparatus and modified type, (5) 141–42.
GE 1075 and No. 42 Ni-Fe alloy, contraction curves, (3) 85.
heat-treatment, variation of refractive index, expansion coefficient, and dispersion as function of, curves, (8) 278.
hydrated silica film on surface, effect on adsorption of ions, (2) 55.
hydrogen bridges in, examples, (12) 397.
iron oxide in, effect on color, (2) 59.
iron oxide series: temperature gradient studies, reduction and oxidation curves and data, (12) 400–401; effect on colors, curves, (12) 401.
leached surface films on, adsorption of ions, (2) 55.
lead-borosilicate, GE 1075, and No. 42 nickel-iron alloy for sealed glass bushings, (3) 83; contraction curves, (3) 85.
Liesegang rings, $AgNO_3$ as diffusion source, (8) 275.
optical, refractive index measurements, curves, (6) 192.
optical, solubility of, effect of chemically formed surface films, (2) 56–57.
oxides in, density and optical constants, data, (1) 6.
oxide substitutions in (K, Mg, Na, Li, Zn, Ba, Sr, Al, A, Zr, and Ti), effect on fluorescence, (5) 144.
oxide types, structure studies, (12) 395; relation of composition to structure, (12) 396.
partial dispersion ratios, calculation, (1) 11.
phosphate, silicate, and borate, fluorescence of, curves, (5) 145.
photoluminescence in, studies, (5) 137.
potash-lime-silica, with copper, phosphorescence of, data and curves, (5) 147.
Pyrex-brand, helium diffusion through, curves from static method measurements, (6) 190.
quenched samples method: for glass transformation region measurements, (6) 191; for refractive index and thermal expansion measurements, (6) 191–92.
radio-tube bulbs, defects, mechanical strains in, (8) 282–83.
refractive index, conversion of equations and constants for calculation, (1) 7–10.
furnace measurements, method, (6) 196–97.
measurement methods, single-prism, three-prism, dynamic, and static, (6) 197–99.
variation of, effect of time, distribution curve after 16 months, (8) 283.
variation of, as function of temperature, (6) 190.
variation of, as function of temperature and of heat-treatment, (8) 277–78.
sealed glass bushings, manufacture and tests, (3) 83–87.
silicate, interatomic forces in, (12) 394.
silver concentration gradient, appearance of colored rings, (8) 273.
silver in, content vs. penetration, curve, (8) 268; diffusion coefficients of Ag into glass, (8) 269.
silver nitrate diffusion in, effect, (8) 270–71; effect of other silver and nonsilver salts, (8) 274.
single-prism method, dynamic measurements of changes in refractive index, curves, (6) 197.
soda-boric oxide, soda-borosilicate, and soda-lime-silica, fluorescence studies and curves, (5) 144–45.
soda in, effect on color, (2) 59.
soda-lime, ground, for slag, chemical analysis and molecular formula, (7) 213.

Glass (*continued*)
soda-lime-silica and light barium crown, effect of leaching and baking on rate of leaching by acid solutions, (2) 57.
oxide substitutions in, effect of fluorescence, curves, (5) 144.
parent compositions superimposed on Na_2O–CaO–SiO_2 equilibrium diagram, (5) 140.
uranium in: preparation, (8) 140; fluorescence variation in, discussion and curves, (5) 142–43.
uranium substitutions in: effect on fluorescence spectra, (5) 142–43; effect of silica substitutions, (5) 143.
solubility of, effect of chemically formed surface films, (2) 56.
spectrophotometric curves for silver nitrate diffusion, effect of time and temperature, (8) 273.
stable refractive index curves as function of temperature, (6) 195.
states of, effect of glass composition, transformation rates, and rapid method of annealing, (6) 192–96.
stones in, effect of temperature gradient in tanks, (12) 398.
strains in: defects in rapidly cooled glass, causes, (8) 280; strains vs. physiochemical state, (8) 283; Michaelson interferometer for tests, (8) 290.
strains in, vs. refractive index, curves, (6) 191.
structural homogeneity, study of mechanical strains, (8) 277.
structure vs. composition, relation, diagrammatic representation, (12) 396.
in system MnO–Al_2O_3–SiO_2, refractive index, diagram, (1) 15.
tanks, effect of colors on temperature gradients, (12) 398.
temperature and time effects on chemical attack by water, equation for, (6) 201.
thermal conductivity of, curves and data on Pyrex-brand, high-soda, and fused silica types, (2) 52–54.
thermal expansion coefficients, method of quenched samples for study, (6) 192.
three-prisms method for refractive index measurements, (6) 198.
time-chemical attack curves on bottles, (6) 203.
transformation rate, speed as function of temperature, curves, (6) 193; speed distributions, time and temperature effects, curves, (6) 194.
"transformation region" vs. "transformation point" in 10^{-4} poise range, evidence for, (6) 189.
transformation speed, effect of pressure, curves, (8) 284.
transformations in, spontaneous, (8) 282.
uranium-bearing, fluorescence at varying temperatures, curves, (5) 146.
water attack, chemical effect, time-temperature function, theories of, (6) 201.
Glazes, borax in, effect on thickness, (2) 64.
chemical composition and viscosity factors, (7) 206–207.
chrome-brown, for electrical porcelain, nonessential substitute materials, (12) 414.
commercial salt glazes, crazing tests and photomicrographs, (3) 64–65.
crazing, reducing firing conditions, effect, (3) 97.
crazing types, kiln, moisture, frost, thermal shock, and parallel, (3) 97–98.
dry, thickness of, measurements, diagram, (3) 97.
feldspar, flint, kaolin, whiting, tin, and zinc oxides, Zircopax, and Opax, chemical compositions, (7) 206–209; viscosity data at cone 12, (7) 208.
feldspathic, effect of opacifiers on fused viscosity, (7) 205.
glaze fit or glaze stress, test methods, flat-plate, strength, deflection of glazed bars, microscopic, and ring, (3) 93–96.
isoviscosity triaxial diagrams, effect of composition changes, (7) 208–11.
oxidizing vs. reducing conditions, effect, (2) 63–64.
salt, glass formation, batch formulas, solubility, and thermal expansion, (2) 61.
salt, NaCl in, effect on glaze thickness, (2) 63.
salt, for structural building units, laboratory test data, (2) 60.
satin, stress measurements, curves, (5) 166.
stress measurements, terra cotta thermal expansion rings for, (5) 163.
terra cotta, dry thickness measurements, (3) 96.
test cones, viscosity, method of measurement before and after firing, photos, (7) 206–207.
thickness, effect on resistance to moisture crazing, thermal shock crazing, and expansion and contraction of rings, curves, (3) 96.
tin vs. tinless, with high calcium, feldspar, and silica content, effect on fused viscosity, diagrams and discussion, (7) 209–10.
tin-Zircopax-Opax in, with high calcium, feldspar, and silica content, viscosity of, diagram and discussion, (7) 211–12.
viscosity factors, (7) 206–207.
zinc vs. zinc-free, fused viscosity, diagrams, (8) 209; isoviscosity triaxial diagrams, (8) 210.
Gloss of porcelain enamels, effect of actual and accelerated weathering conditions, (8) 250; effect of coloring oxides, (8) 251.
Glucose, hydrogen bridge structure, (12) 397.
Gouge resistance of porcelain enamels. See *Enamels.*
Gouge tests for vitreous enamel, lithia content vs. gouge resistance, effect on surface abrasion, specular gloss, apparent reflectance, and solubility, curves, (3) 80–81.
Graphite dilution of clays, effect of, analytical curves, (6) 187.
Grog from sanitary ware vs. terra cotta grog, expansion curves, (5) 166.

Hagar and Schofield method for flat-plate stress test, and diagram, (3) 93.
Halloysite, chemical analysis, fluorescence of dilute HCl leachings, (4) 107–108.
and endellite, relation, citation, (4) 119.
hydrogen-ion and viscosity curves, (4) 112.
rehydration-dehydration test results, (4) 123.
X-ray analyses and tests, (4) 117–19.
Harrison method for surface abrasion resistance of lithia-containing enamels, (3) 80.
Harrison and Moore method for accelerated weathering of porcelain enamels, (8) 249–51.
Heat absorption of kaolinite, anomalous behavior, (11) 388.
Hydration method for magnesia recovery from brucitic dolomite, (7) 219.
Hydrogen in iron, reversible solubility under pressure, curves, (5) 154.
solubilities, curves, after Smithells, (5) 152.
theory of adherence of sheet-iron ground coats, (5) 151.
varying quantities of, effect on adherence, (5) 158.
Hydrogen bridges in glass, examples, (12) 397.

Igneous rocks, oxide composition, average, (9) 286.
Illite, Illinois, chemical analysis, (4) 107.
Immersion method for glass deformation tests, (8) 280.
Impact test and apparatus for chipping resistance of porcelain enamels, (5) 160.
India kyanite, substitution of topaz, domestic kyanite, and synthetic mullite-corundum, (8) 252; see also *Refractories, kyanite.*
Inhibition, crystal-chemical vs. physical, differentiation, (9) 306–307.
Inhibitors, chemical and physical inhibition, suggested mechanism, (9) 305.
elements investigated and effect on calcium orthosilicate, (9) 303–304; properties of inhibited phase, (9) 304.
Insulating materials, cordierite vitrified bodies, (3) 99–102.
sealed glass bushings, production and tests, (3) 83–87.
thermal conductivity and specific heat data, (10) 347.
Insulating refractories. See *Refractories.*
Insulators, high-frequency, talc for, physical tests, (10) 336.
Ion-exchange method for magnesium salts production, (7) 227.
Iron oxide in ground-coat enamels, effect on adherence, (5) 156.
in high-frequency ceramics, effect on color and dielectric efficiency, (10) 337.
in steatite body, effect on dielectric constant, (11) 391–92.
in talc, effect on fired properties, (10) 338.
Isoviscosity triaxial diagrams for feldspathic glazes, effect of composition changes on fused viscosity, (6) 208–11.

Jander equation for reactions in solid state, (7) 239.

Kaolin. See also *Clays.*
electrolytes in, effect on grain-size distribution and pH, curves, (4) 112.
Fla., monodisperse fractions, thermal absorption study, (11) 388.
fluorescence of dilute HCl leachings, (4) 108.
Ga.: nature, chemical and colloidal analyses, (4) 105–13; mineralogical analysis, (4) 113–19; thermal analyses and curves, (4) 115–16.
heat absorption, anomalous behavior, (11) 388.
N. C. and Fla., in pottery bodies, soluble sulfate content, (6) 183.
rehydration-dehydration test results and curves, (4) 122–24.
sedimentary, of Ga., chemical and colloidal analyses, summary, (4) 113.
X-ray analyses and tests, (4) 117–19.
Zettlitz, chemical analysis, (4) 107.
Kaolinite, colloid study of, (3) 88.
Keppeler and Thomas equation for effect of time and temperature on water attack of glass, inaccuracies in, (6) 202.
Kiln crazing of glazes, (3) 97.
Kilns. See also *Furnaces.*
continuous, midget straight-type, photo, (4) 136.
direct radiant, gas-fired, basic principles, photos, and application, (4) 132–34.
laboratory salt-glazing, diagram and tests, (2) 62.
Kraehenbuehl integrating calculator for determination of tristimulus values from spectrophotometric curves, (3) 73–74.
Kyanite, India, domestic kyanite as substitute, (8) 252; see also *Refractories.*

Leaching method for magnesite separation from dolomite, (7) 219.
Lepidolite, chemical analysis and use in melted frit composition, (3) 82.
Leucite–diopside–silica system, equilibrium diagram, after Schairer and Bowen, and discussion, (9) 300–301.
Liesegang rings in glass sample, $AgNO_3$ as diffusion source, (8) 273.
Lime (CaO)–Al_2O_3–SiO_2, equilibrium diagram, after Rankin and Wright, (9) 295.
in dolomite, magnesia separation, methods and bibliography, (7) 218–38.
–FeO–SiO_2, equilibrium diagram after Bowen, Schairer, and Posnjak, (9) 297; discussion of system, (9) 298; equilibrium diagram for mixtures of metasilicate ratio in system, after Bowen, Schairer, and Posnjak, (9) 298.
–MgO–SiO_2, stability relations of merwinite in, (10) 321.
in silica brick, staining or coloring effect, (11) 371.
–Na_2O–Al_2O_3–SiO_2, cross sections in, (9) 299.
–Na_2O–SiO_2 glasses, portion of equilibrium diagram, (5) 140.
–ZrO_2–Cr_2O_3, refractory properties, (1) 27.
Limestone-olivine fusions, curve and tabular data, (12) 412–13; limestone additions to olivine melt, photomicrograph, (12) 412.
Lithia as soda substitute in vitreous enamels, effect on physical properties, (3) 77–83.
Lithium fluoride, thermal conductivity curves, (2) 53–54.
Lithium materials, commercial types, in vitreous enamels, melt compositions and batch formulas, (3) 77–78.
Load test for silica brick. See *Refractories.*
Luminescence. See *Photoluminescence.*

MacGee method for solid volume measurements, (4) 127.
Magnesia (MgO)–Al_2O_3, equilibrium diagram of portion of system, melting points of steatite compositions, (10) 334.
–Al_2O_3–SiO_2, equilibrium diagram, after Rankin and Merwin, and ware based on compositions of, (9) 293; "solidus" diagrams, after Niggli, (9) 294.
–Al_2O_3–SiO_2 with flux additions, properties, (3) 99–102.
–CaO–SiO_2, equilibrium diagram, after Ferguson and Merwin, (12) 410.
–CaO–SiO_2, stability relations of merwinite in, (10) 321.
lime-free product, CO_2 and CO method for production, (7) 220–21; dolomite separation, method, (2) 221–27.
lime separation from, in dolomite, methods and bibliography, (7) 218–38.

Magnesia (*continued*)
magnesia insulation (85%), specific heat and thermal conductivity data, (10) 345–47.
-olivine fusion data, (12) 409.
physical and chemical extraction processes, (7) 218–28.
from sea water and brines, electrochemical methods of separation, (7) 227.
-SiO_2, equilibrium diagram, after Bowen, Andersen, and Greig, (9) 290; immiscible region in, after Marsh, (9) 291.
-SiO_2, melting diagram, after Bowen and Andersen (revised by Greig), (12) 406.
-SiO_2, melting interval of talc (metatalc), (10) 335.
Magnesiowüstite, appearance, (12) 411.
Magnesite and dolomite ores, concentration, flotation methods, (7) 219.
separation from dolomite, classification and calcination methods, (7) 218; hydration and leaching methods, (7) 219.
Magnesium in clays, spectrochemical and chemical analyses, (6) 188.
Magnesium salts, crystallization process, (7) 219–20; production, ion-exchange method, (7) 227.
Manganese oxide (MnO)–Al_2O_3–SiO_2 system: equilibrium relations on liquidus surface, (1) 11; diagram in part of system, and refractive index of glasses, (1) 15; isotherms, diagram, (1) 15; pseudoequilibrium diagram for cooling liquids, (1) 19.
chemical analyses and tests, (1) 13.
Maps, Ga., geologic and topographic divisions, (4) 106.
India, kyanite deposits, (8) 253.
Masonry, modular sizes of clayware units, (9) 307; basis for coordination, (9) 313.
Merwinite ($3CaO \cdot MgO \cdot 2SiO_2$)–akermanite ($2CaO \cdot MgO \cdot 2SiO_2$) join, data for mixtures of and ternary invariant points, (10) 324–25, (10) 331; mixtures of, equilibrium diagram of join, (10) 329.
-akermanite, solid solution in, evidence, (10) 327; courses of crystallization, (10) 328–30.
field of, in equilibrium diagram showing part of system CaO–MgO–SiO_2, (10) 330.
stability relations within system CaO–MgO–SiO_2, (10) 321.
Metals for enamels, adherence, presence of gas at interface, (5) 153.
precipitation intervals of time and temperature, effect, XIV, (2) 41; metal precipitation at ground-coat interface, effect of cobalt and nickel oxides, XV, (10) 358.
preoxidation, advantages for adherence of enamel ground coats, (5) 153.
sheet steel for enamels, relation of hydrogen content to adherence, (5) 151.
Methods, American Ceramic Society, moisture expansion and absorption of ball clays, (6) 178–79.
dynamic, for glass expansion vs. temperature measurements, curves, (6) 190.
electrochemical, for magnesia separation from sea water and brines, (7) 227.
filtration, for soluble sulfate content of clays for pottery bodies, (6) 180.
Fizeau interferometric, for thermal expansion measurements and Saunders improved procedure, (3) 79.
formation of silicate ions, (7) 243.
gouge resistance of porcelain enamels, (1) 1.
Hagar and Schofield, flat-plate glaze stress test, and diagram, (3) 93.
Harrison and Moore accelerated weathering test for porcelain enamels, (8) 249–51.
Harrison test for surface abrasion resistance of lithia-containing enamels, (3) 80.
immersion, for glass deformation tests, (8) 280.
leaching, for magnesite separation from dolomite, (7) 219.
for manganese oxides, chemical analyses and tests, (1) 13.
microscopic, for glaze stress tests, and diagram, (3) 94–95.
Morin dye test for fluorescence of clays, (4) 108.
New South Wales test for acid resistance of lithia-containing enamels, (3) 81.
Pole and Taylor, static method for reaction rates, (7) 239.
of quenched samples for glass transformation region, refractive index, and thermal expansion measurements, (6) 191–92.
refractories load tests, (1) 35, (8) 261–63.
ring test, for glaze stress, micrometer microscope for measurements, (3) 95.
single-prism, for refractive measurements of glass, (6) 198.
Methods (*continued*)
Stull and Johnson, for measuring solid volumes, (4) 127.
thermal conductivity, Compton and Endō curves and formulas, (2) 49.
three prisms, for refractive index measurements on glass, (6) 198.
Washburn and Bunting, for porosity and volumenometer design, (4) 127.
Microscopes, micrometer, for measurements of glass stress in rings, (3) 95.
slit ultramicroscope for $AgNO_3$ diffusion in glass, (8) 270.
Microscopic method for glaze stress tests and diagram, (3) 94–95.
Microscopic studies of colors in silica brick, (11) 385–86.
Mineralogical analysis of Ga. kaolins, (4) 113.
Minerals, single crystals of, thermal conductivity tests, apparatus and results, (2) 48–55.
with stability range on liquidus surface in system MnO–Al_2O_3–SiO_2, cristobalite and tridymite, mullite, corundum, rhodonite, tephroite, galaxite, and spessartite, (1) 11; melting data on quintuple points, (1) 19.
Modular Service Association, unit masonry sizes, studies, (9) 307.
Moisture crazing of glazes, (3) 97.
Moisture expansion and absorption of ball clays and bodies, (6) 178.
Molding, plastic process, workability measurements, (1) 37.
Molds, cast-iron and graphite, for metal-to-glass sealed bushings, photo, (3) 86.
Molten rock phosphate, refractories resistance tests, (1) 21.
Monticellite, studies in system CaO–MgO–SiO_2, (10) 321.
Montmorillonite and kaolinite-illite clays, effect of rehydration, and dehydration-rehydration curves and data, (4) 120–25.
Texas, in pottery bodies, soluble sulfate content, (6) 183.
thermal and X-ray analyses, (4) 115–19.
Morgan and Blakely modifications of Steger glaze-fit test, (3) 94.
Morin dye test for fluorescence of clays, (4) 108.
Mottled brick. See *Refractories, silica brick.*
Mullite in nature, use in refractories, (9) 289–90.
Mullite "bundle", thermal conductivity curves, (2) 53–54.
Mullite-corundum brick. See *Refractories, mullite-corundum.*

Nagleschmidt method for intermittent heating, dehydration curves, (4) 121.
National Bureau of Standards test for gouge resistance of lithia-containing enamels, (3) 79.
Nepheline syenite in cordierite bodies, composition, color, and water absorption, (3) 101.
Neumann rule for refractive index vs. birefringence variation, (6) 191.
New South Wales test for acid resistance of lithia-containing enamels, (3) 81.

Olivine, composition and calculated reduction, (12) 406.
-dolomite fusions, data, (12) 411.
and limestone, fusion curve and data, (12) 412–13; limestone additions, photomicrograph, (12) 412.
-magnesia, fusion data, (12) 409.
-magnesite fusions, softening temperature curve, (12) 408.
Opacifiers and clays in enamels, effect on gouge resistance, (1) 3.
in glazes, tin-Zircopax-Opax with high calcium, feldspar, and silica content, viscosity of, diagram and discussion, (7) 211–12.
Opax in glazes, effect on fused viscosity, composition, diagram and discussion, (7) 207, (7) 211–12.
Optical constants and density of glass, composition of, from weight percentage composition, (1) 4.
Organic polymers, structure, (12) 397.
Orthoclase, melting point, in equilibrium diagram of leucite–diopside–silica, after Schairer and Bowen, (9) 300.
Orthosilicates, presence in quenched products along $2CaO \cdot SiO_2$ and $2CaO \cdot MgO \cdot 2SiO_2$ join, (10) 323; data for mixtures along $3CaO \cdot MgO \cdot 2SiO_2$ and $2SiO_2 \cdot MgO \cdot 2SiO_2$ join, (10) 325; data for mixtures in system CaO–MgO–SiO_2, (10) 326.
Oxide precipitation in ground-coat firing cycle, role of cobalt in, (2) 42.
Oxides, color, effect on accelerated weathering of porcelain enamels, (8) 250–51.
Oxide theory of enamel adherence, (2) 41.

Parallel crazing of glazes, (3) 98.
Periclase, thermal conductivity curves, (2) 53–54.
Petrology, definition, (9) 285.
igneous, significance and research in, (9) 295.
and silicate technology, (9) 285.
Phase rule. See *Equilibrium diagrams; Equilibrium studies.*
Phases. See *Systems.*
Phosphates, molten rock, corrosion resistance of refractory crucibles to, (1) 21; chemical analyses of phosphatic material, (1) 24.
Phosphorescence and compositions of K_2O–CaO–Na_2O glasses with copper, (5) 147.
decay of, in copper-bearing glasses, (5) 147.
Phosphoric acid, glacial, hydrogen bridge structure, (12) 397.
Phosphorus pentoxide (P_2O_5), solid solution of, in calcium orthosilicates, thermal and optical studies, (9) 302.
Photoluminescence in glass, study, (5) 137.
spectrographic apparatus for tests, "Contiflow" spotlight, Hilger constant deviation spectrometer, and process for, (5) 141.
Plagioclase feldspars, equilibrium diagram, after Bowen, (9) 299.
Plastic and synonymous terms, (12) 393.
Plasticity of clays, definition, (3) 89; effect on plastic- and slip-forming processes, (3) 91.
Plastic molding, processes, workability of ceramic bodies, for, measurement, (1) 37.
Pole and Taylor static method for reaction rates, (7) 239.
Polymers, organic, structure, (12) 397.
Polyvinyl alcohol, hydrogen bridges in structure, (12) 397.
Porcelain, electrical. See also *Insulating materials.*
electrical, chrome-brown glazes with non-essential materials, (12) 414.
electrical, cordierite bodies of system MgO–Al_2O_3–SiO_2, effect of flux additions, vitrification range, (3) 98–102.
electric, high-frequency ceramics, physical tests of talc for, (10) 336.
Porcelain Enamel Institute, gouge testing machine, (1) 1.
impact test for laboratory specimens of porcelain enamel sheet iron and steel, (5) 160.
reflectance test for opaque white porcelain enamels with Hunter reflectometer, (3) 80.
standard rolling-ball gouge test, (1) 1.
tentative screen test for porcelain wet-milled enamels, (3) 78.
Porcelain enamels. See *Enamels.*
Porous specimens, solid volume measurements, (4) 130.
Potassium oxide (K_2O)–Al_2O_3–SiO_2 system, equilibrium diagram, after Schairer and Bowen, (9) 296; petrologic and technologic significance, (9) 296.
Pottery, soluble sulfate content, during preparation, analyses, (6) 179.
Pottery bodies, batch composition and soluble sulfate content, (6) 183.

Q meter and Q values for dielectric measurements on steatite bodies, (10) 337–38.
Quartz, particle size, effect on reaction rate, (7) 242.
and sodium carbonate, reaction rates and methods of determination, (7) 239–46.
specific heat curves, (10) 345; commercial insulation and quartz, curves, (10) 346.
thermal conductivity, curves, (2) 53.
Quartzites, Medina and Baraboo, chemical analyses and load-test data, (11) 376; effect of steam-treatment, (11) 377.
Quenched samples method for glass transformation region measurements, (6) 191.
for refractive index and thermal expansion measurements of glass, (6) 192.

Radiant firing, direct, in ceramic industry, method and photos, application, (4) 132–34.
Radiation, frequency of, equation for, (5) 138.
Radio-tube bulbs, mechanical strains in, test method, (8) 282–83.

Reaction kinetics of sodium carbonate and quartz mixtures, (7) 242–43.
Reaction rates vs. reaction products, effect of sample size, flow rate of nitrogen, and time and temperature, (7) 240–41.
Reducing agents, carbon vs. sulfur, effect on amber glass, (2) 58.
Refractories, alumina in silica brick, mottling effect, (11) 363.
alumina-silica minerals in, firing process, (8) 260.
aluminum–fire-clay coatings, reheating shrinkage at cones 6 to 18, (7) 214.
andalusite: pyrochemical and pyrophysical changes in, (8) 254; commercial deposits and chemical analyses, (8) 255; composition of Bur. Mines test samples, (8) 262; variable-temperature load test results, (8) 264.
bauxite in, properties and costs, (8) 257.
burning, color effects from, (11) 366–67.
of natural alumina-silica minerals, results, (8) 258–60.
and reheating effect and color photo, (11) 362A–63.
of silica brick, effect on composition, load test results, color photo, (11) 362A.
of silica brick, effect of lime content and of reburning in air, (11) 385.
sulfur gases in coal, color effects from, (11) 367, (11) 387.
calcium orthosilicates for, behavior and application, (9) 306.
chrome-magnesia, effect of rock phosphate, corrosion test data, (1) 36.
chrome ore in, properties and costs, (8) 257.
coated and uncoated firebrick, changes in length, curve, (7) 214.
colored. See also *Refractories, silica brick.*
chemical composition of, effect, (11) 384–85.
colors in, reversible nature, (11) 363.
plant tests on variables in, (11) 364.
sulfur gases from coal, effect, (11) 367; sulfur effect, (11) 387.
synthetic color-forming compounds, tests, (11) 386.
constant-temperature load test vs. standard A.S.T.M. test curve, (8) 263; description and results, (8) 264–65.
corrosion tests on molten rock phosphate, (1) 28; on electric-furnace phosphate and basic open-hearth slags, (1) 29–30.
corrosion tests, physical and chemical properties of test brick, laboratory expansion tests, Detroit rocking furnace tests, load tests, (1) 30–35.
cracking of insulating firebrick, effect of aluminum–fire-clay coatings, photo, (7) 216.
crucibles for small-scale tests on molten-rock phosphate, (1) 21; large-scale tests, (1) 27.
crushing strength, effect of cooling-treatment, (11) 383.
diaspore, physical properties and uses, (8) 256; raw material and firebrick costs, (8) 257.
dolomite and lime, calcium orthosilicate behavior, (9) 306.
dolomite-silica brick, solid-phase inversions of calcium orthosilicate, (9) 302.
driers for, effect on colors in silica brick, (11) 366.
firebrick, super-refractories costs, (8) 257.
firebrick, thermal conductivity stability, effect of reheating, curves, (10) 355; dense firebrick, hot and cold face temperatures, curves, (10) 357.
fire clay for, physical properties and costs, (8) 256.
fire-clay, thermal conductivity of, (10) 350.
forming processes, effect on body consistency, data, (1) 38–39.
furnace calorimeter, spherical, for specific heat and thermal conductivity direct measurements, (10) 339.
fused, electrically fused forsterite-olivine, (12) 305.
heat-capacity curves for various types, (10) 345.
insulating firebrick, aluminum–fire-clay coatings, effect, (7) 212; shrinkage in reheating test, effect, (7) 214.
insulating firebrick, A.S.T.M. specification for bulk density, (7) 213.
insulating firebrick, for high-temperature use, composition, (10) 346.
insulating materials, commercial, thermal conductivity curves, (10) 346; thermal conductivity and specific heat data, (10) 347.
insulating materials, thermal conductivity results with tester, (10) 357.
Refractories (*continued*)
iron oxide content, effect on colors, (11) 365.
iron oxide in silica brick, mottling effect, (11) 362; iron plus wollastonite, color effect, color photo, (11) 382A; data, (11) 386–87.
kaolin, thermal conductivity test, (10) 350.
kyanite and corundum, calculated percentage content, (8) 260.
kyanite, domestic: sources and analyses of Va. and N. C. samples, (8) 253–54; Bur. Mines test samples, (8) 262; with mullite-corundum and S.C. topaz, summary, (8) 266.
kyanite, India: sources, properties, and domestic materials substitutes, (8) 252–53; map of deposits, (8) 253; costs quotations, (8) 257.
kyanite, India: test samples, effect of repeated heatings, curves, (8) 258–59; chemical analyses, (8) 260; commercial calcined materials, properties, (8) 261; Bur. Mines test samples, (8) 262; variable- and constant-temperature load-test results, (8) 264–65.
lateral heat loss and heat flow, temperature measurement, (10) 354.
lightweight, slag resistance to aluminum coatings, diagram, (7) 215.
lime-alumina ratio, effect on color in, (11) 365–66.
lime in silica brick, effect on coloration or staining, (11) 371.
lime in silica brick, mottling effect, (11) 362; color photo, (11) 362A.
load tests, (1) 35, (8) 261–63.
load tests, color photos and test, (11) 362A, (11) 364.
load tests, effect on coated and uncoated samples, curve and discussion, (7) 215–17.
load tests: variable temperature curves, (8) 261, (8) 263; time-temperature curves, (8) 263; variable temperature load-test curves on experimental refractories and commercial India kyanite, (8) 265.
magnesia-CaO-SiO_2 brick, softening temperatures vs. composition, curve, (12) 412.
classifying methods, (7) 218.
insulation (85%), specific heat and thermal conductivity data, (10) 345–47.
properties and costs, (8) 257.
separation from lime in dolomite, methods and bibliography, (7) 218–38.
-SiO_2 brick, softening temperature curves, (12) 408.
-SiO_2 brick, softening temperatures vs. composition, olivine-dolomite fusion, curve, (12) 412.
for molten rock phosphate resistance tests, (1) 21.
mottled, mottling of. See *Refractories, silica brick.*
mullite-corundum: bonded electric furnace Bur. Mines samples, (8) 262; combined with topaz and domestic kyanite, (8) 262; variable- and constant-temperature load tests, summary of results, (8) 264–66.
mullite-corundum, electric-furnace, production, properties, casting process, analyses, (8) 255–56; cost quotations, (8) 257.
mullite in, use, (9) 289–90.
olivine, calcined magnesite, dolomite, and limestone, analyses, (12) 409.
resistance to molten rock phosphate, compositions, (1) 21.
shrinkage of exposed (uncoated) faces in reheat tests and spalling effect, (7) 215–16.
shrinkage, volume and linear, effect on aluminum–fire-clay coatings at cones 6 to 18, (7) 214.
silica brick, bleached specimens, reignition effect, (11) 370.
chemical composition and properties, Dodd data, (11) 375.
chemical composition of stained samples, tests in air and in CO_2-air mixtures, (11) 369.
color photographs, brick samples, variation effects of CaO, Al_2O_3, percentage of fines, burning treatment, reheating, and load test, (11) 362A.
color photographs, effect of time during heat-treatment, slow and rapid cooling, and of wollastonite with iron, and Al_2O_3 additions, (11) 382A.
color photographs, mottling, color and appearance, effect of heat-treatment, (11) 378A.
Refractories, silica brick (*continued*)
colors in, microscopic studies, (11) 385–86.
colors in, reversible nature, color photos, (11) 362A–63.
composition, drying, and firing, effects on color, (11) 365–66.
cooling rates in heat-treatment test, curves, studies, and color photos, (11) 380–82A; effect on mottled brick, color photo, (11) 382–82A.
cream color, effect of lime content, (11) 367.
cream and dark, thermal expansion curves, (11) 380.
dicalcium ferrite as colorant in silica brick, (11) 368.
heat-treatment and effect of time, color photos, (11) 378A.
iron and CaO in, hydrochloric acid extraction, (11) 385.
lime content, effect at cone 17 and reburning in air, (11) 371.
lime in, mottling effect and color photo, (11) 362–62A.
load-test data, (11) 379.
load tests, color photos and test, (11) 362A, (11) 364; steam-treatment, effect on weight, (11) 376–77.
mottled, color photos and heat-treatment studies, (11) 378A, (11) 380.
mottled, effect of lime, Al_2O_3, and thermal history and color photos, (11) 361–62A.
mottled and normal types, properties, (11) 378–79.
mottling: chemical composition, (11) 362; effect on brick properties, (11) 363–64.
stained, removal by reburning in air, (11) 370–71.
staining test: in air and CO_2-air mixtures, (11) 369; in reducing atmosphere and in SO_2-air mixture, (11) 370; effect of sulfur gases in kiln atmosphere, (11) 372.
steam-treatment, effect on weight, (11) 376–77.
sulfur effect: on color formation, (11) 367, (11) 387; mottling effect, (11) 363.
synthetic compounds in, effect on color, (11) 386–87.
thermal conductivity tests, effect, photos, (10) 354–55.
time effect during heat-treatment at 900°C., study and color photo, (11) 381–82A.
water-vapor effect at high temperatures, (11) 373.
wollastonite in, effect of heat-treatment on color, (11) 386–87; color photo, (11) 382A.
wollastonite in stained portions, (11) 371.
silica-CaO-MgO brick, softening temperatures vs. composition, curve, (12) 412.
silica-MgO brick, softening temperatures vs. composition, olivine-dolomite fusion, curve, (12) 412.
silica for, properties and costs, (8) 256–57.
silicon carbide, properties and costs, (8) 257.
slag resistance, effect of aluminum coatings on lightweight brick, (7) 215.
slag test, chemical analyses and molecular formulas for multiclone dust, Portland cement clinker, ground glass, and synthetic coal ash, (7) 213.
spalling and reheat tests, effect on coated and uncoated firebrick, (7) 216.
specific heat test method, formulas, data, and calculations (10) 343–44.
stained, studies, (11) 368–73; see also *Refractories, silica brick.*
steam-treatment, effect on weight, (11) 376–77.
sulfur effect on color formation, (11) 367, (11) 382, (11) 387.
sulfur in silica brick, mottling effect, (11) 363.
superduty fire-clay lining, in Detroit rocking furnace, effect of rock phosphate, (1) 36.
superduty, thermal conductivity tests, (10) 350.
thermal conductivity, diagram and curve for insulating firebrick, (10) 352.
thermal conductivity and specific heat tests with spherical furnace calorimeter, (10) 339–41.
thermal conductivity tester, diagram, (10) 351; asbestos strips under test samples, diagram, (10) 352; initial and final arrangement for test, (10) 353.
thermal-expansion studies and curves on cream and dark-colored brick, (11)

Refractories, thermal expansion (*continued*)
379–80; effect of color on thermal expansion, study and curves, (11) 383.
time-temperature relations, effect on colors in, (11) 367.
topaz, Bur. Mines samples, composition and variable- and constant-temperature load-test results, (8) 262–65.
with electric furnace mullite-corundum and domestic kyanite, summary, (8) 265–66.
firing, effect of repeated firings, curves and properties of calcined topaz, (8) 258–61.
and kyanite, domestic, cost quotations, (8) 257.
S.C., deposits, development, and chemical analyses, (8) 254–55.
variables affecting color of silica brick, plant tests, (11) 364–67.
wollastonite as matrix material in groundmass of stained silica brick, effect, (11) 371.
wollastonite and wollastonite mixtures in silica brick, color photo of heat effect, (11) 382A, (11) 386–87.
zirconium oxide-Cr_2O_3-CaO compositions, refractory properties, (1) 27.
Rehydration-dehydration test, rapid, for clays, (4) 125; effect of nonclay impurities, (4) 125.
Ring test for glaze stress, micrometer microscope for measurements, (3) 95.
for glaze stress, use of terra cotta thermal expansion rings, (5) 163.
Rock phosphate, molten, resistance of refractory compositions, (1) 21.
Rock phosphate corrosion of refractories, tests, (1) 28.
Rolling-ball gouge test, Porcelain Enamel Institute, (1) 1.

Salt glazes. See *Glazes.*
Sapphire, thermal conductivity curves, (2) 53.
Saunders improved procedure for thermal expansion measurements, (3) 79.
Scratch resistance of porcelain enamels, gouge tests, (1) 1.
Sea water and brines, magnesia separation, methods, (7) 227.
Selas radiant gas burner, description and cross section, (4) 133.
Selenium and sulfur, vitreous, structure, (12) 394.
Semivitreous bodies. See *Vitreous bodies.*
Serin and Ellickson formula for solid state reactions, (7) 239.
Sharp formula for chemical attack of glass, (6) 202.
Sheet steel for enamels. See *Enamels; Metals.*
Silica (SiO_2)–Al_2O_3–CaO, equilibrium diagram, after Rankin and Wright, (9) 295.
–CaO–FeO, equilibrium diagram, after Bowen, Schairer, and Posnjak, and discussion, (9) 297–98; equilibrium diagram for mixtures of metasilicate ratio in system, after Bowen, Schairer, and Posnjak, (9) 298.
–CaO–MgO, merwinite in, stability relations, (10) 321.
crystalline and vitreous, structure, dimensional representation, (12) 394.
–leucite–diopside, equilibrium diagram, after Schairer and Bowen, and discussion, (9) 300–301.
–MgO–Al_2O_3, equilibrium diagram, after Rankin and Merwin, and ware based on compositions of, (9) 293; "solidus" diagrams, after Niggli, (9) 294.
–MgO–Al_2O_3, with flux additions, electrical and mechanical properties, (3) 99–102.
–MgO–CaO, equilibrium diagram, after Ferguson and Merwin, (12) 410.
–MgO, diagram of melting interval of talc and metatalc, (10) 335; SiO_2–MgO–Al_2O_3, phase diagram and composition of normal and low-loss steatite bodies, (10) 333–36.
–MgO, equilibrium diagram, after Bowen, Andersen, and Greig, (9) 290; immiscible region in, after Marsh, (9) 291.
–MgO, equilibrium diagram, after Bowen and Andersen (revised by Greig), (12) 406.
–MnO–Al_2O_3, equilibrium relations on liquidus surface, (1) 11; diagram in part of system, isotherms, and refractive index of glasses formed, (1) 14–15; pseudo-equilibrium diagram for cooling liquids, (1) 19.
Silica (*continued*)
–K_2O–Al_2O_3, equilibrium diagram, after Schairer and Bowen, technologic and petrologic significance, (9) 296.
–Na_2O–CaO–Al_2O_3, cross sections in, (9) 299.
–Na_2O–SiO_2 glass, portion of equilibrium diagram, (5) 140.
vitreous, structure of, and effect of sudden cooling, (12) 395.
Silica brick. See *Refractories, silica brick.*
Silica minerals, pressure-temperature diagram of stability relations in, (9) 298.
Silicate glasses. See *Glass, silicate.*
Silicate ions, formation methods, (7) 243.
Silicates, binary systems of, partial and complete immiscibility, equilibrium diagram, after Marsh, (9) 291; petrologic significance of immiscible relation, diagram, (9) 292.
compositions in region of orthosilicate join in ternary system CaO–MgO–SiO_2, phase equilibrium data, (10) 321–32.
of soda, properties, (2) 68; see also *Sodium silicate.*
structures, relation of composition, dot composition, (12) 396.
Silver compounds as source of diffusion in glass, (8) 270; see also *Glass.*
Single-prism method for glass refractive index measurements, (6) 198.
Slags, multicione dusts, Portland cement clinker, soda-lime glass, and synthetic coal ash, chemical analyses and molecular formulas, (7) 213.
Slag test for electric-furnace phosphate slags, (1) 29; for basic open-hearth slags, (1) 30.
Slips, barium carbonate as precipitant for sulfate, effect, (6) 185.
casting, deflocculants for, effect of sodium silicate and sodium carbonate, (2) 67; electrolyte additions, effect on casting properties, (2) 68–70.
casting, effect of plasticity, (3) 91.
slip clays, Mich. and Albany, in chrome-brown electrical porcelain glazes, (12) 414.
sulfate calculations and soluble sulfate content, (6) 182–83.
Soapstone for steatite dielectrics, chemical analyses, firing data, (11) 390–91.
Soda (Na_2O)–CaO–Al_2O_3–SiO_2, cross sections in, (9) 299.
–CaO–SiO_2 glasses portion of equilibrium diagram, (5) 140.
vs. lithia in vitreous enamels, effect of fusibility, (3) 77–83.
Sodium carbonate in casting slips with Na_2SiO_3, effect as deflocculant, (2) 67.
and quartz, reaction rates, methods, (7) 239–46.
Sodium silicate in casting slips, effect of Na_2CO_3 additions, (2) 67.
"Solidus" diagrams, definition, (9) 294; diagram for CaO–Al_2O_3–SiO_2 system, after Rankin and Wright, (9) 295.
of MgO–Al_2O_3–SiO_2 system, after Niggli, (9) 294.
Solubility of glass, effect of chemically formed surface films, (2) 56.
Soluble salts in ball and china clays and miscellaneous materials, (6) 181.
in pottery bodies, in raw materials, and in batch composition, (6) 182.
Spalling of porcelain enamels, bubble formation in, effect, (8) 250–51.
and reheat tests, furnace diagram, (7) 214.
Spectra, origin, Bohr "stationary states," (5) 138.
Spectrochemical analysis of clays, (6) 185.
Spectrograph, Bausch and Lomb large Littrow, for clay analyses, (6) 185.
Bausch and Lomb medium quartz, for silver concentration in glass, (8) 270.
Spectrophotometry, General Electric recording spectrophotometer for color panel tests, (3) 74.
Kraehenbuehl calculator for determination of tristimulus values from spectrophotometric data, (3) 73.
Spodumene, chemical analysis, use in melted frit compositions, (3) 82.
in cordierite bodies, composition, color, and water absorption data, (3) 100–101.
Staining of silica brick. See *Refractories, silica brick.*
Steam-treatment for silica brick, effect on weight, (11) 376–77.
Steatite bodies, chemical specifications and physical properties of high-lime talcs, (10) 336; physical tests, (10) 337.
Steatite bodies (*continued*)
decomposition and softening rate, (10) 333; composition modifiers, effect, theoretical melting curves, diagram, (10) 335.
Fe_2O_3 in, effect on properties, (10) 336.
firing, physical and chemical studies, (10) 333; firing range and effect of firing rate, (10) 336.
melting points of, portion of equilibrium diagram for system MgO–Al_2O_3, (10) 334.
Steatite dielectrics, ferruginous talcs in, use, (11) 389.
Q meter for measurement, (10) 337.
Steger method for glaze-fit test, Morgan and Blakely modifications, (3) 94.
Structural materials, modular sizes of clayware units, (9) 307; basis for coordination, (9) 313.
salt glazes for building units, laboratory tests, (2) 61.
Stull and Johnson method for solid volume measurements, (4) 127.
Sulfates, barium carbonate as precipitant in slips, (6) 185.
soluble, in pottery bodies during preparation, (6) 179; batch composition percentage and aging effect, (6) 183.
vs. water distribution in filter pressing, (6) 184.
Sulfur and selenium, vitreous, structure, (12) 394.
Sulfur gases from coal, effect on silica brick colors, (11) 363, (11) 367; effect on staining, (11) 370–72; effect on mottling, (11) 382–83.
Supercooled liquid and synonymous terms, (12) 393.
Surface films, chemically formed on glass, effect on solubility, (2) 56.
leached, on glass, ion adsorption by, (2) 55.
Suspended roofs and walls in glass tank furnaces, advantages and limitations, (5) 167.
Systems. See also *Equilibrium diagrams; Equilibrium studies.*
Al_2O_3–SiO_2, equilibrium diagram, after Shepherd, Rankin, and Wright, (9) 288; after Bowen and Greig, (9) 289.
binary, diagram of eutectic position in Al_2O_3, MgO, CaO, and FeO, (9) 291.
CaO–Al_2O_3–SiO_2 equilibrium diagram, after Rankin and Wright, (9) 295.
–Fe_2O_3–SiO_2, dicalcium ferrite as colorant in silica brick, (11) 368.
–FeO–SiO_2, discussion, (9) 298; equilibrium diagram, after Bowen, Schairer, and Posnjak, (9) 297; diagram for mixtures of metasilicate ratio in system, after Bowen, Schairer, and Posnjak, (9) 298.
–MgO–SiO_2, courses of crystallization in, (10) 328; diagram, (10) 330.
–MgO–SiO_2, data for mixtures: along join $2CaO \cdot SiO_2$–$2CaO \cdot MgO \cdot 2SiO_2$, (10) 323; along join $3CaO \cdot MgO \cdot 2SiO_2$–$2CaO \cdot MgO \cdot 2SiO_2$, (10) 325; phases present in quenched product, (10) 326.
–MgO–SiO_2, equilibrium diagram, after Ferguson and Merwin, (12) 410.
–MgO–SiO_2, stability relations of merwinite in, (10) 321.
FeO–CaO, solid system, equilibrium diagram, after Bernard, (2) 42, (10) 359.
MgO–Al_2O_3–SiO_2, effect of flux additions and vitrification range, (3) 99–102.
–Al_2O_3–SiO_2, equilibrium diagram, after Rankin and Merwin, (9) 293; ware based on compositions, (9) 293; Niggli diagram of possibilities of joining compounds in system, (9) 294.
–Al_2O_3–SiO_2, phase diagram studies, composition of normal and low-loss steatite bodies, (10) 333–36.
–SiO_2, equilibrium diagram, after Bowen, Andersen, and Greig, (9) 290; immiscible region in, after Marsh, (9) 291.
–SiO_2, melting diagram, (12) 406.
–SiO_2, melting interval of talc (metatalc), (10) 335.
MnO–Al_2O_3–SiO_2, equilibrium relationships on liquidus surface (1) 11–20.
one-component, stability relations of silica minerals, pressure-temperature diagram, (9) 287.
K_2O–Al_2O_3–SiO_2, equilibrium diagram, after Schairer and Bowen, (9) 296; technologic and petrologic significance, (9) 296.
silicate, immiscible relations in, petrologic significance, (9) 292.
Na_2O–CaO–Al_2O_3–SiO_2, cross sections in, (9) 299.

Talc, ferruginous, white-firing, and Manchurian, chemical analyses, (11) 390; washed vs. unwashed samples, (11) 391.
for high-frequency ceramics, physical tests, (10) 336.
high-lime, chemical specifications and physical properties for steatite bodies, (10) 336–37.
iron-bearing vs. ferruginous, shrinkage, absorption, and color tests, (11) 389–92.
metatalc, melting interval, equilibrium diagram in system $MgO–SiO_2$, (10) 335.
white-firing, effect of Fe_2O_3 on dielectric constant, (11) 391–92.
Tanks, glassmelting. See *Furnaces, glassmelting, tanks.*
Temperature gradients in colored glasses, (12) 398; see also *Glass, colored.*
Tennessee Valley Authority, refractory compositions, resistance to molten rock phosphate, (1) 21.
Terra cotta, glaze stress measurements, simplified thermal expansion rings for control, (5) 163; composition for expansion rings, (5) 165.
Thallium salts in glass, diffusion data, effect on color and fluorescence, (8) 274–75.
Thermal absorption of kaolinite, anomalous behavior, (11) 388.
Thermal analysis of Ga. kaolin, (4) 115–16.
Thermal conductivity of crystals, single nonmetallic, Endō and Compton theories, test method, (2) 48–55.
of refractories. See *Refractories.*
of single crystals, quartz, corundum, beryl, tourmaline, and topaz, directional effect, (2) 55.
tester, diagram and use, (10) 351–54.
Thermal expansion of ball clays and vitreous bodies, data and curves, (6) 174–78.
of lithia-containing frits, Andrews and Howe method of preparation, Fizeau interferometric method, and Saunders improved procedures, (3) 79.
Thermal-expansion rings for terra cotta production control, (5) 163.
Thermal-shock crazing of glazes, (3) 98.
Three-prisms method for glass refractive index measurements, (6) 198.
Tin oxide in feldspathic glazes, effect on fused viscosity, (7) 210.
Topaz, thermal conductivity curves, (2) 53–54; see also *Refractories, topaz.*
Tourmaline, thermal conductivity curves, (2) 53.
Transformation of glass. See *Glass.*
Triaxial isoviscosity diagrams of feldspathic glazes, effect of composition changes, (7) 208–11.

Uranium salts, fluorescing action in glass, (5) 140–49.

Vanadium salts, diffusion data, (8) 274–75.
Viscosity of casting slips, deflocculants for, curves, (2) 67–71.
fused, of glasses and glazes, measurement methods, (7) 205; see also *Glazes.*
Vitreous bodies, composition and thermal expansion, (6) 176.
semivitreous, composition and thermal expansion, effect of firing temperature, (6) 175–76.
Vitreous enamels. See *Enamels.*
Vitreous silica, dimensional representation, (12) 394; structure, cooling effect, (12) 395.
Vitreous solid vs. crystalline substances, (12) 394.
Vitreous state, definition, relation to vitreous solid, amorphous solid, supercooled liquid, glass, and plastic, (12) 393.
Vitreous sulfur and selenium, structure, (12) 394.
Vitrified cordierite bodies of $MgO–Al_2O_3–SiO_2$, effect of flux additions and vitrification range, (3) 99–102.
Volume measurements, gas-expansion vs. liquid absorption methods, (4) 127.
Volumenometer, improved, for measuring solid volumes, (4) 127; diagram and photo, (4) 129; calibration data, (4) 130.
types, Washburn and Bunting, Pressler, MacGee, and Stull and Johnson, (4) 127; improved type, (4) 128.

Washburn and Bunting method for porosity and volumenometer design, (4) 127.
Water, Norris, constituents, (6) 181; tap and distilled, sulfate content, (6) 181.
Water vapor, effect on silica brick at high temperatures, (11) 373.
Weathering test for porcelain enamels, accelerated test, (8) 249; actual vs. accelerated, data, (8) 250; effect of coloring oxides, (8) 251.
Whiteware. See also *Pottery bodies; Vitreous bodies.*
casting slips, deflocculants for, effect of sodium silicate with sodium carbonate additions, (2) 67.
clays and bodies, workability for plastic molding measurements, (1) 37.
forming processes, effect on body consistency, (1) 38–39.
Wollastonite with iron and Al_2O_3 additions, effect of heat-treatment, color photo, (11) 382A.
as matrix material in groundmass of stained silica brick, (11) 371.
in silica brick, heat effect, color photo, (11) 382A; data, (11) 386–87.

X-ray analyses of clays, technique, apparatus, and test results, (4) 116–18.
of halloysites, (4) 117–19.
of kaolins, (4) 117–19.

Zehnder gas-expansion method for density of materials, (4) 127.
Zinc vs. zincless glazes, fused viscosity, diagrams, (7) 209; isoviscosity diagrams, (7) 210.
Zinc oxide in glazes, effect on fused viscosity, composition, (7) 207; discussion and diagram, (7) 211–12.
Zircon, thermal conductivity curves, (2) 53–54.
Zirconium oxide–CaO series, for crucible corrosion tests, (1) 25.
$–Cr_2O_3–CaO$, refractory properties, (1) 27.
Zircopax in glazes, effect on fused viscosity, glaze composition, diagram, and discussion, (7) 207, (7) 211–12.

FOOTNOTE CITATIONS INDEX TO THE JOURNAL

Volume 26, 1943

The reference number in parentheses refers to the *monthly* issue of the *Journal;* the number following is the *page* number.

Adair, J. T., analysis of electrodialyzed clays, (4) 106.
Adams, L. H., and Williamson, E. D., annealing of glass, (8) 283.
Albers-Schönberg, Ernst, Hochfrequenzkeramik (high-frequency ceramic products), (3) 99.
Alexander, Jerome, colloid chemistry, theoretical and applied, Vol. II, (8) 268.
Alexander, L. T., Faust, G. T., Hendricks, S. B., Insley, H., and McMurdie, H. F., relations of clay minerals halloysite and endellite, (4) 119.
American Ceramic Society, Standards Comm. standard methods for behavior in firing, (6) 178; Standards Report, Comm. A-15, elasticity and transverse strength apparatus, (10) 337.
American Society for Testing Materials, tentative methods of test for power factor and dielectric constant of electrical insulating materials, specification D150–41T, (10) 337.
American Standards Association, proposed American war standard for ceramic radio insulating materials, class L, specification C75/93, (10) 337.
Ammon, M. G., accelerated weathering tests on porcelain enamels, (8) 249.
Andrews, A. I., enamels, (2) 42, (5) 165.
Andrews, A. I., and Cook, R. L., relation of particle sizes of frit and color oxides to color properties of porcelain enamels, (3) 73.
Andrews, A. I., and Howe, E. E., effect of fluorine on properties of white sheet-steel enamels, (3) 79.
Andrews, A. I., and Mullady, R. E., further data on reboiling, (5) 159.
Andrews, A. I., and Swift, H. R., iron oxide in enamel glass as dissolved from metal base, (2) 41.
Austin, J. B., factors influencing thermal conductivity of nonmetallic materials, (10) 357.

Bacon, F. R., and Burch, O. G., effect of time and temperature on accelerated chemical durability tests made on commercial glass bottles, I–II, (6) 201; data on alkali extracted as NaOH, (6) 201, (6) 203.
Badger, A. E., effect of gaseous atmospheres on vitrification of ceramic bodies, (11) 374; seeds in soda-lime glass, (5) 152.
Bahlen, W. E., new type vacuum seal, (3) 83.
Bailey, James, scratch-resisting power of glass and its measurement, (3) 80.
Bancroft, W. D., applied colloid chemistry, (8) 277.
Bannister, F. A., relation between density and refractive index of silicate glasses with application to determination of imitation gem stones, (1) 6.
Barrett, R. L., and McCaughey, W. J., system $CaO–SiO_2–P_2O_5$, (9) 303.
Bates, P. H., and Klein, A. A., properties of calcium silicates and calcium aluminates in normal Portland cement, (9) 303.
Becker, A., and Salmang, H., gases in glass, gas and moisture content of glasses, II, (5) 156.
Bekkedahl, N., application of thermodynamics to chemistry of rubber, (6) 190; forms of rubber as indicated by temperature-volume relation, (6) 190.
Bell, W. C., evaluation of glaze-fit test methods, (3) 94, (5) 163.
Bemis, A. F., evolving house, rational design, Vol. III, A (9) 308.
Benrath, H. E., Glasfabrikation, (2) 58.
Berger, E. (Edwin), changes of equilibrium in glass and effect of prior heat-treatment on physical properties, (6) 189; contributions to theory of glass formation and glassy state, (6) 189; fundamental principles underlying chemical corrosion of glass, (2) 56, (6) 202.
Berger, E., Thomas, M., and Turner, W. E. S., determination of transformation point of same optical glasses in three different laboratories, (6) 189–90.
Berkmann, Sophia, and Egloff, Gustav, emulsions and foams, (8) 272.
Bernard, Jaques, decomposition du protoxide de fer et de ses solutions solides, (2) 42, (10) 358.
Besborodov, M. A., and Abelchuk, N. O., fluorescence tests for identification of striae and cords, (5) 137.
Beuken, L., measurement of thermal conductivity of insulating brick, (10) 340.
Biltz, Wilhelm, Weibke, Friedrich, and Schrader-Traeger, Lisolotte, Molrefraktionen und Molvolumina von Gläsern (molecular refractions and molecular volumes of glasses), (1) 8.
Birch, F., and Clark, H., thermal conductivity of rocks and dependence on temperature and composition, (2) 48.
Birch, R. E., phase-equilibrium data in manu-

facture of refractories, (9) 306, (11) 362, (11) 368, (11) 386.
Biscoe, J., and Warren, B. E., X-ray diffraction study of soda-boric oxide glass, (5) 149.
Blakely, A. M., life history of a glaze, measurement of stress in cooling glaze, II, (3) 94, (5) 163.
Bleininger, A. V., and Kinnison, C. S., viscosity of porcelain bodies, (7) 205.
Blodgett, K. B., use of interference to extinguish reflection of light from glass, (2) 57.
Bogue, R. H., digest of literature on constitution of Portland cement clinker, (9) 302.
Bole, G. A., and Jackson, F. G., simple control porosimeter, (4) 127.
Bonhoeffer, K. F., and Hartek, P., Grundlagen der Photochemie, (5) 150.
Bork, A., Färbung des Glases durch Kohle und Sulfide, (2) 58.
Bouyoucos, G. J., comparison between pipette method and hydrometer method for making mechanical analyses of soil, (4) 109.
Bowen, N. L., colored phases in silica brick, (11) 371; diffusion in silicate melts, (8) 269; melting phenomena of plagioclase feldspars, (9) 300; voglite, isomorphous with wollastonite, (9) 299.
Bowen, N. L., and Andersen, Olaf, binary system $MgO–SiO_2$, (9) 290, (12) 405.
Bowen, N. L., and Greig, J. W., system $Al_2O_3–SiO_2$, (1) 11, (9) 289.
Bowen, N. L., Greig, J. W., and Zies, E. G., mullite, a silicate of alumina, (9) 289.
Bowen, N. L., and Schairer, J. F., properties of pure synthesized forsterite, (12) 407; system $MgO–FeO–SiO_2$, (10) 335, (12) 408.
Bowen, N. L., Schairer, J. F., and Posnjak, E., system $CaO–FeO–SiO_2$, (9) 298.
Bowles, Edgar, kyanite in eastern Ala., (8) 253.
Boyd, John, analyses of olivine compositions, (12) 406.
Boyd, W. B., recovery of kyanite from north Ga. schist, (8) 253.
Bradley, A. J., crystal structures of rhombohedral forms of selenium and tellurium, (12) 395.
Bradley, R. S., Schroeder, F. W., and Keller, W. D., study of refractory properties of topaz, (8) 254.
Bragg, W. H., and Gibbs, R. E., structure of α- and β-quartz, (12) 395.
Brandenberger, E., crystal structure and chemical foundations of stereochemistry of crystalline compounds in Portland cement, (9) 304; X-ray characteristics of various modifications of dicalcium silicate, Ca_2SiO_4, (9) 304.
Brodig, M. A., isomorphism and allotrophy in compounds of type A_2XO_4, (9) 305.
Brode, W. R., chemical spectroscopy, (8) 277.
Budnikov (Budnikoff), P. P., silica refractories that give double service, (11) 379.
Burch, O. G., communication on obtaining colorless glasses, (2) 60.
Burch, O. G., and Babcock, C. L., effect of glass color on setting rates in manufacture of glass bottles, (12) 398.
Burdick, M. D., studies on system lime–ferric oxide–silica, (9) 303, (11) 372.
Burgess, B. C., topaz development as source of alumina, (8) 254.
Burke, J. B., fluorescence and absorption, (5) 139.
Burwell, J. T., unit cell and space group of monoclinic sulfur, (12) 395.
Busse, W. F., physical structure of elastic colloids, (12) 395.
Büssem, W., X rays and cement chemistry, (9) 304.

Carpenter, G. L., and Harle, T. F., vacuum calorimeter for high temperatures, (10) 339.
Carter, W. K., and King, R. M., mechanics of enamel adherence, enamels on copper, nature of adherence, III, (10) 360.
Casagrande, A., Aräometer Methode zur bestimmung der Kornverteilung von Boden (areometer method for determining grain distribution in soils and other materials), (4) 109.
Charrin, V., lithium in ceramics, (3) 77.
Chesters, J. H., and Parmelee, C. W., measurement of reaction rates at high temperatures, (1) 32.
Close, Paul, and Bacon, F. R., colorant analyses of glass, (12) 400.
Coblentz, W. W., Emerson, W. B., and Long, M. B., spectroradiometric investigation of transmission of various substances, (12) 399.
Cohn, B. E., thermoluminescence in glasses which contain two activators, (5) 139.
Cohn, W. M., crystal modifications of zirconia, clear, fused zirconia produced in sun furnace, (12) 395; determination of specific heats and heat tone from time-temperature curves, (10) 339; Herstellung von Zirkondioxydglas mit Hilfe des Straubelschen Sonnenspiegels (development of zirconium glass with Straubel sun mirror), (12) 395.
Compton, A. H., physical study of thermal conductivity of solids, (2) 48.
Curie, M., phosphorescent glasses, decay of phosphorescence, (5) 137.
Curtis, H. A., Copson, R. L., Brown, E. H., and Pole, G. R., fertilizer from rock phosphate, (1) 21.

D'Adrian, A. L. D., lepidolite in enamels, (3) 77.
Dake, H. C., Fleener, F. L., and Wilson, B. H., quartz family minerals, (11) 381.
Dana, E. S., system of mineralogy, (12) 405.
Davis, H. E., and Lueders, R. L., simplification of ring method for determining glaze stresses (3) 95, (5) 163.
Day, A. L., Shepherd, E. S., and Wright, F. E., lime-silica series of minerals, (9) 302.
Debye, P., Vorträge über kinetische Theorie der Materie und Elektrizität, (2) 48.
Deer, W. A., and Wager, L. R., two new pyroxenes of system clinoenstatite, clinoferrosilite, diopside, and hedenbergite, (9) 299.
Deutschbein, O., Fluoreszenz seltener Erden in Gläsern, (5) 140.
Dietzel, A., and Meures, K., adjustment of enamels to sheet steel, (2) 42.
Dinger, C., Kind, A., Shütz, W., and Dietzel, A., determination of thermal conductivity at high temperatures, (10) 340.
Dobischek, D., Darstellung und Eigenschaften lumineszenzfähiger Gläser unter besonderer Berücksichtigung von Zinksilikatphosphoren, (5) 140.
Dodd, A. E., action of water vapor on silica brick at high temperatures and possible industrial significance, (11) 373.
Dolbear, S. H., ed., industrial minerals and rocks, (8) 251.
Dorn, J. E., and Harder, O. E., theory of diffusion in solids, (8) 277.
Duff, R. D., and Pfeifer, O. W., results on commercial tank gradients, (12) 403.
Dunn, J. A., aluminous refractory materials, cyanite, sillimanite, and corundum, in northern India, (8) 252.
Dyckerhoff, W., formation and properties of calcium silicate, (9) 302.

Eckert, F., and Schmidt, E., Einfluss von Cer und Arsen auf des photochemische Verhalten von Silikatgläsern, (5) 139.
Edwards, Cyril, testing refractory materials, (11) 373.
Eitel, Wilhelm, physikalische Chemie der Silikate, (8) 277.
Eitel, W., and Lange, B., determining radiating power of glass, (12) 398.
Eitel, W., and Skaliks, W., Doppelkarbonate der Alkalien und Erdkalien (double carbonates of alkalis and alkaline earths), (1) 8.
Endell, Kurd, diffusion phenomena in silicate fusions at high temperatures, (8) 269.
Endell, Kurd, Fendius, H., and Hofmann, U., base exchangeability of clays and forming problems in ceramics, (1) 37.
Endell, Kurd, Heidtkamp, Günther, and Hax, Ludwig, Flüssigkeitsgrad von kalksilikaten, kalkferriten, und basischen Siemens-Martin-Schlacken bis 1625°, (11) 372.
Endô, Y., theory of conductivity, (2) 48.
Eucken, A., Temperaturabhängigkeit der Wärmeleitfähigkeit fester Nichmetalle, (2) 53; Wärmeleitfähigkeit keramischer feuerfester Stoffe, (2) 48.

Faust, G. T., optical properties of forsterite, (12) 407.
Fay, M. A., effects of adsorbed ions on workability of clay, (1) 37.
Fedotieff, P. P., and Lebedeff, A., Absorptionspektra von gefärbten Gläsern, (2) 58.
Fenner, C. N., differential thermocouple technique on inversion of cristobalite, (4) 115; stability relations of silica minerals, (9) 287.
Ferguson, J. B., and Merwin, H. E., ternary system $CaO–MgO–SiO_2$, (10) 321, (12) 411.
Fettke, C. R., microscopic analyses of mottled brick, (11) 365; report on examination of brick samples, (11) 385.
Fettke, C. R., and Stewart, W. E., slagging action of western Pa. coals on different types of refractories in small pulverized coal installation, (8) 260.
Finkelnburg, W., Kontinuierliche Spektren, (5) 150.
Fizeau, L., use of interferometer for expansion measurement, (3) 79.
Flagg, Ernest, basis of Greek design, (9) 316.
Flint, E. P., and Wells, L. S., system lime–boric acid–silica, (9) 303.
Foster, H. D., résumé of technical studies of salt glazing, (2) 61.
Foster, W. R., system $NaAlSi_2O_6–CaSiO_3–NaAlSiO_4$, (9) 300.
Fries, Carl, Jr., topaz deposits near Brewer Mine, Chesterfield Co., S. C., (8) 255.
Fuwa, K., glasses colored by carbonaceous matter, I–III, (2) 58.

Garrison, A. D., surface chemistry of clays and shales, (4) 120.
Gehlhoff, G., Schneekloth, W., and Thomas, M., currents and temperatures in glass tanks, (12) 399.
Gehlhoff, G., and Thomas, M., temperature measurement in glass furnaces, (12) 399.
Geiger, M., Kayser's Handbuch der Spektroskopie, (5) 139.
Geisinger, E. E., and Berlinghof, K., effect of furnace gases on glass enamels, (5) 152.
Geller, R. F., and Insley, Herbert, thermal expansion of some silicates of elements in Group II of Periodic System, (3) 99.
German, S. L., effect of steam on silica brick for coke ovens, (11) 374.
Gerold, E., influence of glaze on physical properties of porcelain, (3) 93.
Gibbs, R. C., effect of temperature on absorption and fluorescence, (5) 139.
Gibbs, R. E., structure of α-quartz, (12) 395; variation with temperature of intensity of reflection of X rays from quartz and its bearing on crystal structure, (12) 395.
Gibson, G. E., and Giauque, W. F., third law of thermodynamics, evidence from specific heats of glycerol that entropy of glass exceeds that of crystal at absolute zero, (6) 189.
Gibson, G. E., Latimer, W. M., and Parks, G. S., entropy changes at low temperatures, (6) 189.
Gilard, P., and Dubrul, L., coloration of glass by staining, III, (8) 269.
Gilard, P., Dubrul, L., and Crespin, D., fluorescence du verre, (5) 137.
Gilard, P., Dubrul, L., Jamar, F., and Crespin, D., fluorescence of glass, (5) 137.
Glaser, O., thermal and microscopical investigations of cupola slag systems $MnO–Al_2O_3–SiO_2$, $MnS–MnSiO_3$, and $CaS–CaSiO_3$, (1) 11.
Glastechnische Tabellen, (12) 399.
Glazebrook, R., dictionary of applied physics, Vol. I, (10) 340.
Goldschmidt, V. M., geochemical distribution laws of the elements, laws of crystal chemistry, VII, (9) 304.
Golla, Hans, red-spotted silica brick, (11) 361, (11) 384.
Goranson, R. W., and Adams, L. H., method for precise measurement of optical path difference, especially in stressed glasses, (3) 94.
Gorgeu, A., cited on synthesis of apessartite, (1) 14.
Grace, Robert, analysis of electrodialyzed clays, (4) 106.
Graham, R. P., and Sullivan, J. D., workability of clays, (1) 37.
Graton, L. C., reconnaissance of some gold and tin deposits of southern Appalachians, (8) 254.
Greaves-Walker, A. McK., and King, R. M., mechanics of enamel adherence, studies on adherence of enamels to cast iron, IV, (10) 360.
Green, S. E., spherical shell method of determining thermal conductivity of thermal insulator, (10) 340.
Greene, C. F., placer mining kyanite in Ga., (8) 253.
Greig, J. W., formation of mullite from kyanite, andalusite, and sillimanite, (8)

254; immiscibility in silicate melts, (9) 290.
Greig, J. W., Shepherd, E. S., and Merwin, H. E., annual report of director of the Geophysical Laboratory, (9) 286.
Grim, R. E., modern concepts of clay minerals, (3) 88; properties of clay, (4) 114; relation of composition to properties of clays, (4) 120.
Grim, R. E., and Bradley, W. F., investigation of effect of heat on clay minerals illite and montmorillonite, (4) 107, (4) 120.
Grim, R. E., and Bray, R. H., mineral constitution of ceramic clays, (4) 120.
Gruner, J. W., personal communication on chemical analysis of fuller's earth, (4) 107.
Gummer, W. K., system $CaAl_2Si_2O_8$–$CaSiO_3$–$NaAlSiO_4$, (9) 300.

Hägg, G., vitreous state, (12) 395.
Halberstadt, Joseph, diffusion of silver and copper in glass, (8) 268.
Hall, F. P., influence of chemical composition on physical properties of glazes, (2) 66.
Halle, K., Preston, Eric, and Turner, W. E. S., distribution of temperature in molten masses of colored and colorless glass, (12) 399.
Handrek, H., importance of glazes for safe porcelain insulators, (3) 93; review of European special materials, (3) 99.
Hanna, H. H., study of most fusible mixtures of K_2O, CaO, Al_2O_3, and SiO_2, (7) 205.
Hardy, A. C., handbook of colorimetry, (3) 73.
Harman, C. G., and Badger, A. E., method of improving appearance of silica brick, (11) 362, (11) 368, (11) 378.
Harrison, G. R., M.I.T. wave-length tables, (6) 188.
Harrison, H. C., and Bassett, L. B., emission spectroscopy and its application in investigation and solution of problems in ceramics, (6) 186.
Harrison, W. N., tentative tests for abrasion resistance, (3) 80.
Harrison, W. N., and Moore, D. G., weather resistance of porcelain enameled iron structural units, (8) 249.
Harrison, W. N., and Shartsis, L., experimental work on crushing resistance of enamels, (3) 79.
Harvey, F. A., personal communication on analyses of lime in dark and colored portions of silica brick, (11) 366.
Harvey, F. A., and McGee, E. N. testing coke-oven refractories, (11) 361.
Hasler, M. F., and Harvey, C. E., quantitative spectrochemical methods for zinc die-casting analysis, (6) 186.
Hauser, E. A., colloid chemistry in ceramics, (3) 88.
Hauser, E. A., and Hirshon, S., behavior of colloidal suspensions with electrolytes, (3) 92.
Hauser, E. A., and Johnson, A. L., plasticity of clays, (3) 89.
Hauser, E. A., and Reed, C. E., development of new method for measuring particle-size distribution in colloidal systems, (3) 89.
Heath, Frederick, Jr., modular masonry, (9) 308; standard unit of dimension for masonry, (9) 308.
Hendricks, S. B., and Alexander, L. T., minerals in soil colloids, description and methods for identification, I, (4) 107, (4) 120.
Hendricks, S. B., Nelson, R. A., and Alexander, L. T., hydration mechanism of the clay mineral montmorillonite saturated with various cations, (4) 121.
Henry, E. C., plasticity and workability of ball clays, (1) 37.
Henry, E. C., and Taylor, N. W., acid and base binding capacities and viscosity relations in certain whiteware clays, (4) 108.
Herman, A., factors influencing autoclave chemical durability tests of glass containers, (6) 203.
Herold, P. G., personal communication on Mo. halloysite analysis, (4) 107.
Herty, C. H., Jr., physical chemistry of steel making, (1) 11.
Hess, F. O., and Brown, Leslie, perfect firing of fine chinaware in radiant-heat kiln, (4) 132.
Heuer, R. P., kyanite refractories, (8) 252.
Heydweiller, A., and Kopfermann, F., knowledge of electrolysis of glass, (8) 268.
Higgins, W. W., and Deringer, W. A., investigation of fish-scale phenomena, (5) 156.
Hodkin, F. W., and Cousen, A., textbook of glass technology, (2) 59, (3) 77.
Hoff, H., and Klärding, J., correlation between gas and fish-scale formations in enameling, (5) 154.
Holscher, H. H., measurement and significance of enamel thickness, (5) 162.
Housley, W. L., and King, R. M., mechanics of enamel adherence, application of theory of dendritic adherence to development of white ground coats for sheet steel, XI, (10) 360.
Howarth, J. T., Maskill, W., and Turner, W. E. S., rate of reaction between silica and sodium carbonate at different temperatures and processes of vitrification, (7) 239.
Howe, E. E., observations on adherence phenomena of sheet-iron ground coats, (5) 151.
Howe, E. E., and Fellows, R. L., effect of manganese, nickel, and cobalt on adherence and reboiling properties of ground-coat enamel, (5) 152.
Hüttig, G. F., and Herrmann, E., increase of solubility of alumina contained in kaolin due to preheating different gases, (4) 120.
Hugett, J., application de l'analyse thermomagnetique l'étude des oxydes et des minerals de fer, (2) 42.
Huggins, M. L., crystal structure of quartz, (12) 395; density of silicate glasses as function of composition, (1) 4, (12) 397; dispersion of silicate glasses as function of composition, (1) 4, (12) 397; hydrogen bridges in organic compounds, (12) 397; refractive index of silicate glasses as function of composition, (1) 4, (12) 397; symposium on glass, silicate glasses, calculation of densities, refractive indices, and dispersions from glass compositions, (1) 4.
Huggins, M. L., and Sun, K.-H., calculation of density and optical constants of a glass from its composition in weight percentage, (12) 397.
Huggins, M. L., Sun, K.-H., and Davis, D. O., dispersion of silicate glasses as function of composition, II, (1) 4, (12) 397.
Hugill, W., and Rees, W. J., influence of iron oxide and iron sulfides on rate of quartz conversion in commercial silica brick manufacture, (11) 368, (11) 378.
Hull, A. W., and Burger, E. E., glass-to-metal seals, (3) 84.
Hull, A. W., Burger, E. E., and Navias, L., glass-to-metal seals, II, (3) 84.
Hull, A. W., Moore, R. W., and Dell, O. H., sealed glass bushings for electrical apparatus, (3) 83.
Hundeshagen, Franz, Bestimmung des Eisengehaltes in Blei-Mennige für Kristallglas, Kritik der in der Technik üblichen Analysenverfahren, (2) 59.
Hunter, C. E., forsterite-olivine deposits of N. C. and Ga., (12) 405.
Hunter, R. S., multipurpose photoelectric reflectometer, (3) 80.

Industrial Minerals and Rocks, (8) 253.
International Critical Tables, isothermal surfaces of crystal, Vol. V, (2) 49; curve for platinum, Vol. V, (10) 345; inversion temperature values, Vol. VI, (10) 342.
Iwase, Keizo, and Nisioka, Usaburo, equilibrium diagrams of three binary systems, (1) $CaO \cdot SiO_2 \cdot TiO_2$–$MgO \cdot TiO_2$, (2) $CaO \cdot MgO \cdot 2SiO_2$–$MnO \cdot TiO_2$, and (3) $CaO \cdot SiO_2$–$2CaO \cdot Fe_2O_3$, (11) 372.

Jäckel, G., Neuzeitliche Absorptionsgläser, (5) 139.
Jander, Wilhelm, reactions in solid state at high temperatures, reaction rates of endothermic reactions, I, (7) 239.
Jebsen-Marwedel, H., and Becker, A., Farbstich von Glas ohne Entfärbung, (2) 58.
Johnson, A. L., and Norton, F. H., fundamental study of clay: mechanism of deflocculation in the clay–water system, II, (3) 92; casting as base-exchange phenomenon, III, (3) 92.
Jost, Wilhelm, diffusion and chemical reactions in solid state, (8) 267.

Kalnarskii, I. S., effects of lime addition and of granulometric composition on properties of Dinas brick, (11) 362.
Karrer, E., kinetic theory of elasticity of highly elastic gels, (12) 395.
Kautz, Karl, further data on enamel adherence, (2) 42, (5) 151; observations on function of adherence-promoting oxides in ground-coat enamels, (2) 42, (5) 152; random experiments on enamel adherence, (5) 158.
Kaye, G. W. C., and Higgins, W. F., thermal conductivity of metal crystals, bismuth, I, (2) 53.
Kelley, W. P., Jenny, H., and Brown, S. M., hydration of minerals and soil colloids in relation to crystal structure, (4) 120.
Keppeler, Gustav, Berichte der technisch-wissenschaftlichen Abteilung des Verbandes keramischer Gewerke in Deutschland, (4) 121.
Keppeler, Gustav, and Thomas, M., time dependence of water attack on glass, (6) 202.
Kerr, P. F., decade of research on nature of clay, (3) 88, (4) 120.
Kethley, T. W., analyses of raw Ga. clays, (4) 106.
King, R. M., mechanics of enamel adherence: (A) apparatus for firing enamels under accurate control of temperature, pressure, and atmosphere, (B) studies in firing enamels under reduced pressures, VIII, (10) 360; "iron oxide layer" in sheet-steel ground coats, X, (5) 151, (10) 360; chemical and X-ray examination of metallic precipitates from enamels containing iron and cobalt oxides, XII, (10) 360; review of theoretical explanations for formation of metal particles in cobalt ground coats and pertinent experiments, XIII, (2) 41, (10) 360; (1) role of cobalt oxide in metal and oxide precipitation during ground-coat firing cycle, and (2) determination of temperature and time intervals of precipitation, XIV, (10) 358, (10) 360.
Kitaigorodskii, I. I., and Solomin, N. W., rate of setting of glass during working, (12) 398.
Klinkhardt, H., measurement of true specific heats at high temperature by heating with thermionic electrons, (10) 336.
Klug, H. P., X-ray study of red monoclinic selenium, proof of existence of two red monoclinic varieties of selenium, (12) 395.
Kocher, A. L., rational design, A (9) 309.
Kracek, F. C., cristobalite liquidus in alkali oxide–silica systems and heat of fusion of cristobalite, (9) 292; personal communication on presence of disilicate and quartz in Na_2O–SiO_2, (7) 239; system sodium oxide–silica, (7) 239.
Kraner, H. M., and McDowell, S. J., talc as principal body ingredient in vitrified ceramic bodies, (10) 333.
Kraus, E. H., Hunt, W. F., and Ramsdell, L. S., mineralogy, introduction to study of minerals and crystals, (12) 405.
Krause, O., and Jäckel, E., talc (steatite)-containing bodies of three-component system $MgO \cdot Al_2O_3 \cdot SiO_2$, (3) 99.
Kröger, Carl, and Fingas, Ernst, action of quartz and alkali silicates on alkali carbonates, (7) 239.
Kubaschewski, O. v., diffusion of silver into glass, (8) 268.

Ladd, C. E., preliminary report on part of clays of Ga., (4) 106.
Lafon, Pierre, anomalies in expansion of glasses, (6) 189.
Lamy, A., sur le verre de thallium, (1) 6.
Larsen, E. S., and Berman, H., microscopic determination of nonopaque minerals, (12) 405.
Lebedeff, A. A., annealing optical glass, (6) 190; curve for variation of refractive index as function of heat-treatment, (8) 278; polymorphism and tempering of glass, (6) 190.
LeChatelier, H., allotropy of glass, (6) 189; viscosity of glass, (6) 189.
Lee, H. C., personal communication on liquidus surface field of merwinite in system CaO–MgO–SiO_2, (10) 322.
Lenard, P., Schmidt, F., and Tomaschek, R., Handbuch der Experimentalphysik, Phosphoreszenz und Fluoreszenz, Vol. 23, (5) 150.
Lester, W. R., fluorescence of certain colored glasses, (5) 137.
Lewis, G. N., valence and structure of atoms and molecules, (12) 394.

Lillie, H. R., changes in atomic arrangements of glass during cooling, (6) 190; viscosity-time-temperature relations in glass at annealing temperature, (6) 190.
Littleton, J. T., critical temperatures in silicate glasses, (6) 190.
Litzow, K., tension measurements of glazed ware by polarization microscope, (5) 163.
Long, B., propriétés physiques et la fusion du verre, (2) 58, (6) 190.
Lord, J. O., summary of observations and facts concerning phenomenon of reboiling, (5) 152.
Lord, J. O., and Rueckel, W. C., mechanics of enamel adherence, technique of preparing enamel metal sections for microscopic analysis, I, (10) 360.
Lux, Elizabeth, and Krause, Otto, red-stained silica brick, (11) 361.
Lyle, A. K., relation between storage and accelerated chemical durability tests for several glass compositions, (6) 201.

MacGee, A. E., several gas-expansion porosimeters, (4) 127.
Malinovszky, A., raw and white ground coats, (3) 77.
Marsh, J. S., principles of phase diagrams, (9) 291.
Mason, L. R., analysis of India kyanite samples, (8) 260.
Mattson, V. L., kyanite operations of Celo Mines, Inc., (8) 253; progress in commercial development in south Atlantic states, (8) 253.
Mayer, Max, and Havas, Béla, coefficient of expansion of enamels and chemical compositions, (5) 165.
McCartt, K. C., personal communication on sulfate content of Jernigan ball clay, (6) 182, (6) 184.
McDowell, J. S., discoloration of silica brick, (11) 361.
McIntyre, G. H., vitreous enamel frits, (3) 77.
McMillan, L. B., heat transfer through insulation in moderate and high-temperature fields, statement of existing data, (10) 340.
McVay, T. N., optical properties of forsterite, (12) 407.
Mehmel, M., structures of halloysite and metahalloysite, (4) 117.
Mellor, J. W., comprehensive treatise on inorganic and theoretical chemistry, Vol. IV, (9) 306; discoloration of refractories by "iron," (11) 362, (11) 368, (11) 378.
Memnonova, T. V., and Zil'berfarb, L. M., spottiness of silica brick, (11) 362, (11) 368, (11) 386.
Menzer, G., Kristallstruktur des Granat, (1) 4.
Merritt, G. E., application of interferometer to measurements of thermal dilatation of ceramic materials, (3) 79; interference method of measuring thermal expansion, (3) 79.
Metz, A., Zeiss dilatometer for investigating glasses, (3) 102.
Meyer, K. H., and Go, Y., sur le soufre filiforme et sa structure, (12) 395.
Meyer, K. H., Susich, G. v., and Valko, E., Plastische Eigenschaften der organischen Hochpolymeren und ihre kinetische Deutung, (12) 395.
Minerals Yearbook, review of 1937, (8) 255; review of 1938, (8) 255; review of 1940, (8) 243.
Minton, R. H., use of substitutes for tin oxide in glazes, (7) 205.
Monack, A. J., and Beeton, E. E., analysis of strains and stresses in glass, I–IV, (3) 94.
Mondain-Monval, P., and Galet, P., anomalies of physical properties of the vitreous state, amorphous sulfur and selenium, (6) 189.
Montgomery, R. J., and Office, L. R., notes on laboratory testing of silica brick, (11) 368, (11) 378.
Moore, R. W., glass fabrication process and mold, (3) 86.
Morey, G. W., composition of glass, (8) 277; properties of glass, (7) 205, (9) 292, (12) 395.
Morey, G. W., and Ingerson, Earl, pneumatolytic and hydrothermal alteration and synthesis of silicates, (1) 14.
Moser, H., measurement of true specific heats of silver, nickel, β-brass, quartz, and vitreous silica between 50° and 700°C. by refined method, (10) 339.
Munyan, A. C., supplement to sedimentary kaolins of Ga., (4) 106.

Nagelschmidt, G., identification of minerals in soil colloids, (4) 120.
Navias, Louis, effect of lithium oxide on thermal expansion of glass, (3) 77; glass-to-metal seals, (3) 85.
Nelson, M. S., and Ralston, R. R., design and operation of electric load-test furnace, (8) 263, (12) 408.
Neumann, C., and Dietzel, A., Farbkörper in den sogenannten kohlegelben Gläsern (coloring agent in so-called carbon yellow glasses, coloring glass with colloidal carbon), I, (2) 58; II, (2) 59.
Newman, F. H., and Searle, V. H. L., general properties of matter, (8) 277.
Nicholls, P., determination of thermal conductivity of refractories, (10) 357.
Nichols, E., and Merritt, E., studies in luminescence, (5) 139.
Niggli, P., Magma und seine Produkte, (9) 294.
Norton, C. L., Jr., apparatus for measuring thermal conductivity of refractories, (10) 350.
Norton, F. H., critical study of differential thermal method for identification of clay minerals, (3) 89, (4) 107, (4) 115, (8) 256; refractories, (1) 34.
Norton, F. H., and Johnson, A. L., fundamental study of clay, preparation of purified kaolinite suspension, I, (4) 110.
Norton, F. H., and Speil, S., measurement of particle sizes in clays, (3) 89.

Osborn, E. F., system $CaSiO_3$–diopside–anorthite, (10) 321.
Osborn, E. F., and Schairer, J. F., ternary system pseudowollastonite–akermanite–gehlenite, (10) 321.
Owens, J. S., and Emanuel, E. C., variable factors in accelerated autoclave chemical durability tests, (6) 203.

Page, J. B., unreliability of benzidine color reaction as test for montmorillonite, (4) 120.
Pardee, J. T., Glass, J. J., and Stevens, R. E., massive low-fluorine topaz from Brewer Mine, S. C., (8) 254.
Parks, G. S., and Huffman, H. M., studies on glass, transition between glassy and liquid states of some simple organic compounds, I, (6) 189.
Parks, G. S., Thomas, S. B., and Gilkey, W. A., glass, heat capacity data for some complex organic glasses and liquids, V, (6) 189.
Parmelee, C. W., and Ehman, R. G., effects of addition of zinc oxide and cadmium oxide on simple glasses, (1) 6.
Parmelee, C. W., and Fréchette, V. D., heat-of-wetting values of unfired and fired clays, (4) 121.
Parmelee, C. W., and Thurnauer, Hans, some effects of additions of compounds of zirconium, titanium, aluminum, and barium to a talc body, (3) 101.
Parmelee, C. W., and Westman, A. E. R., effect of steam on transverse strength of fire-clay brick, (11) 374.
Paschkis, V., and Baker, H. D., method of determining unsteady-state heat transfer by means of electrical analogy, (10) 339.
Pauling, Linus, nature of chemical bond and structure of molecules and crystals, (3) 88.
Peck, A. B., changes in constitution and microstructure of andalusite, cyanite, and sillimanite at high temperatures and their significance in industrial practice, (8) 254; note on andalusite from Calif., new use and some thermal properties, (8) 255.
Pelouze, yellow coloration in commercial glasses, (2) 58.
Perrier, A., and Roux, H., furnace calorimeter, (10) 339.
Phelps, S. M., properties of insulating refractories, behavior under load at high temperatures, I, (7) 213; studies of effect of chlorine, sulfur dioxide, and carbon monoxide on various refractories, (11) 361, (11) 382.
Phelps, S. M., and Limes, R. W., mottled silica brick, (11) 361, (11) 368.
Phelps, S. M., and Petrie, E. C., mottled silica brick, (11) 361, (11) 368.
Phemister, James, Nurse, R. W., and Bannister, F. A., merwinite as an artificial mineral, (10) 322.
Pierce, W. C., and Nachtrieb, N. H., photometry in spectrochemical analysis, (6) 187.
Pierce, W. C., Torres, Raminez, and Marshall, W. W., qualitative spectrographic analysis in arc with graphite electrodes, (6) 186.
Pole, G. R., calcination of topaz ore in a rotary kiln, (8) 254; calcium oxide-chromium oxide refractories, (1) 27; calcium oxide-chromium oxide-zirconium oxide refractories, (1) 27; calcium oxide-zirconium refractories, (1) 27.
Pole, G. R., and Beinlich, A. W., Jr., testing refractories against molten calcium metaphosphate, (1) 27.
Pole, G. R., and Moore, D. G., expansion characteristics of kyanite and kyanite-clay mixtures when heated, (8) 252.
Pole, G. R., and Taylor, N. W., kinetics of solid-phase reaction of certain carbonates with mullite, silica, and alumina, (7) 239.
Porcelain Enamel Institute, impact test for laboratory specimens of porcelain enamel, sheet iron, and steel, (5) 160; reflectance test for opaque white porcelain enamels, (3) 80; standard rolling-ball gouge test, (1) 1; tentative screen test for wet-milled porcelain enamels, (3) 78; test for resistance of porcelain enamels to gouging, (3) 78.
Poste, E. P., analyses of India kyanite samples, (8) 260.
Pressler, E. E., simple brick porosimeter, (4) 127.
Pringsheim, P., Fluoreszenz und Phosphoreszenz im Lichte der neueren Atomtheorie, (5) 150; general discussion on luminescence, (5) 138.
Pringsheim, P., and Schlivitch, S., Fluoreszenz von praesodymium- und neodymium-glas, (5) 139.
Pulfrich, O., negative values of phosphate glasses, (8) 277.
Purdy, R. C., porcelain glazes, (7) 205.

Ralston, O. C., iron oxide reduction equilibria, (11) 372.
Randall, J. T., and Rooksby, H. P., X-ray diffraction and structure of glasses, (12) 395.
Rankin, G. A., and Merwin, H. E., ternary system MgO–Al_2O_3–SiO_2, (9) 293.
Rankin, G. A., and Wright, F. E., ternary system CaO–Al_2O_3–SiO_2, (9) 295, (9) 302.
Read, E. B., chemical analyses of mottled silica brick, (11) 384.
Rees, W. J., bonding of silica brick, (11) 361; discussion of Dodd's paper, (11) 373; further note on influence of iron oxide in promoting inversion of silica, (11) 379; mottled silica brick, (11) 361, (11) 378; silica refractories, (11) 378.
Rencker, E., thesis on temperature intervals in glass, (6) 190.
Reusch, H. J., and Wartenberg, H. v., melting diagram of refractory oxides, calcium oxide, (1) 23.
Rexer, J., Lumineszenz von Gläsern, (5) 140.
Riddle, F. H., personal communication on Calif. sillimanite mine, (8) 255.
Rigby, G. R., and Green, A. T., thermal expansion characteristics of some calcareous and magnesian minerals, (3) 102.
Rollefson, G. K., and Burton, M., photochemistry and mechanism of chemical reactions, (5) 150.
Ross, C. S., and Kerr, P. F., halloysite and allophane, (4) 117; kaolin minerals, (4) 107; tests on *d* values of clay minerals, (4) 119.
Rowland, D. H., recent improvements in high-voltage insulator design, (3) 93.
Rueckel, W. C., personal communication on staining of silica brick in coke ovens, (11) 372.
Rueckel, W. C., and King, R. M., mechanics of enamel adherence, effect of composition and firing atmosphere on adherence of ground-coat enamel, II, (10) 360.

Sampson, J. R., and Tucker, W. B., mineral resources of Imperial County, State of Calif., (8) 253.
Samsoen, M. O., research on vitreous state, (6) 189.
Saunders, J. B., improved interferometric procedure with application to expansion measurements, (3) 79.
Sawyer, J. P., Jr., and Whittemore, J. W., characteristics of Va. kyanite, (8) 253.
Saxe, C. W., and Buckner, O. S., bonding strengths of a number of clays between normal temperatures and red heat, (4) 121.

Sayers, R. R., Bur. Mines tests on corrosion of refractory brick, (1) 35.
Schachtschabel, P., über Dehydratisierung und Rehydratisierung des Kaolins (dehydration and rehydration of kaolins), (4) 121.
Schairer, J. F., system $CaO–FeO–Al_2O_3–SiO_2$, results of quenching experiments on five joins, I, (1) 20, (9) 300, (10) 321.
Schairer, J. F., and Bowen, N. L., acknowledgment to equilibrium diagram of system $K_2O–Al_2O_3–SiO_2$, (9) 295; binary system $CaSiO_3$–diopside and relations between $CaSiO_3$ and akermanite, (10) 321; system leucite–diopside–silica, (10) 321.
Schairer, J. F., and Osborn, E. F., system $CaO–MgO–FeO–SiO_2$, preliminary data on join $CaSiO_3–MgO–FeO$, I, (10) 321.
Schloemer, Alfons, Phosphoreszenz bei Gläsern, (5) 140.
Schmidt, G. C., Beiträge zur Kenntnis der Fluoreszenz, (5) 139.
Schofield, H. Z., study of replacement of Cornwall stone by talc and feldspar in wall-tile body, (3) 93.
Schulze, Gunther, experiments concerning diffusion of silver in glass, (8) 268.
Schurecht, H. G., how to overcome crazing in ceramic glazes, (3) 97; methods for testing crazing of glazes caused by increases in size of ceramic bodies, (3) 97, (5) 163; reaction of slag with refractories, surface reactions of slags with refractories, I, (7) 213; reactions of slag with refractories, refractory coatings produced with metallic aluminum, II, (7) 217.
Schurecht, H. G., and Fuller, D. H., some effects of thermal shock in causing crazing of glazed ceramic ware, (3) 98.
Schurecht, H. G., and Pole, G. R., effect of water in expanding ceramic bodies of different compositions, (3) 97; method of measuring strains between glazes and ceramic bodies, (3) 95, (5) 163; some special types of crazing, (3) 97.
Schurecht, H. G., and Wood, K. T., use of borax and boric acid together with salt in salt glazing, (2) 64.
Schwalbe, F. G., control for luminous flame firing in glass furnaces, (12) 398; depth of heat penetration in molten glass with luminous and nonluminous flames, (12) 398.
Schwartzwalder, Karl, and King, R. M., mechanics of enamel adherence, petrographic, metallographic, and X-ray study of enamel-metal contact zones, VI, (2) 42, (5) 151, (10) 360.
Schwarz, F., clays and fuller's earths, isobar dehydration and absorption of water of clays, IV, (4) 120.
Searle, A. B., encyclopedia of ceramic industries, Vol. III, (11) 379.
Sears, F. W., improved calculator for obtaining tristimulus values from spectrophotometric curves, (3) 73.
Seger, H. A., collected writings, (7) 205.
Sell, G. E., Heck, F. G., and Heiligman, H. A., specific heats of chrome and magnesia refractories, (10) 339.
Sell, G. E., and Staff, bibliography on orthosilicates of the alkaline earths with special reference to their use in the refractory field, (9) 302; orthosilicates of alkaline earths with special reference to use in the refractory field, (9) 305, (12) 411.
Selzer, Robert, valuation of silica brick according to external nature, (11) 361.
Serin, B., and Ellickson, R. T., determination of diffusion coefficients, (7) 239.
Sharp, D. E., time factor in durability tests, (6) 202.
Shearer, H. K., report on bauxite and fuller's earth of coastal plain of Ga., (4) 107.
Shearer, W. L., and Wyckoff, W. R., thermal expansions of whiteware materials and bodies over a wide temperature, (5) 163.
Shell, H. R., analyses of electric-furnace mullite corundum, (8) 256.
Shelton, S. M., thermal conductivity of some iron and steels over temperature range 100° to 500°C., (2) 52.
Shepherd, E. S., Rankin, G. A., and Wright, F. E., binary systems of alumina with silica, lime, and magnesia, (9) 288.
Shute, R. L., and Badger, A. E., effect of iron oxide on melting of glass, (12) 399.
Shvetsov, V. N., colored spots in silica brick, (11) 361.
Singer, Felix, and Cohn, W. M., new ceramic bodies, composition and expansion behavior, I–II, (3) 99.
Sitz, G., system $CaO–Fe_2O_3–SiO_2$ in relation to its significance for metallurgical slags, (11) 372.
Slattery, M. K., crystal structure of metallic selenium and tellurium, (12) 395; crystal structure of metallic tellurium and selenium and of strontium and barium selenide, (12) 395.
Smith, P. L., chipping resistance of enamels, (5) 160; development of two tentative standard tests, (5) 160.
Smith, R. W., sedimentary kaolins of Ga., (4) 106.
Smithells, C. J., gases and metals, (5) 152.
Snell, C. A., and Ward, R., reactions in solid state, reaction between monazite and sodium carbonate, (7) 245.
Snow, R. B., and McCaughey, W. J., equilibrium studies in system $FeO–Al_2O_3–SiO_2$, (1) 20.
Sortwell, H. H., high-fire porcelain glazes, (7) 205.
Sosman, R. B., properties of silica, (6) 178, (9) 287, (10) 345.
Speil, Sidney, and Wilson, Hewitt, improved mercury balance volumeter, (8) 260.
Spencer-Strong, G. H., and Cooper, W. G., gouge resistance of porcelain enamels, (3) 79.
Spencer-Strong, G. H., and King, R. M., mechanics of enamel adherence: study of enamel-metal contact zones by chemical methods, V, (2) 43, (5) 151, (10) 360; equilibrium studies in some systems of enamel glass and cobalt, nickel, and iron oxides, IX, (2) 43, (10) 360.
Spencer-Strong, G. H., Lord, J. O., and King, R. M., mechanics of enamel adherence, further studies of enamel-metal contact zones by microscopic and metallographic methods, VII, (5) 151, (10) 360.
Spivak, J., system $NaAlSiO_4–CaSiO_3–Na_2SiO_3$, (9) 300.
Springer, L., cited on effect of carbon in glass on color, (2) 58.
Staley, H. F., electrolytic reactions in vitreous enamels and relation to adherence of enamels to steel, (5) 151; some relations of composition to solubility of enamels in acids, (3) 77.
Stefan, I., cited on Fick equation, (8) 268.
Steger, W., measuring tension in fired ceramic mixes, (3) 94; strain in glazed ware and its detection, (3) 94, (5) 163.
Stillwell, C. W., crystal chemistry, (5) 150.
Stojaroff, A. J., variation of refractive index of glasses at high temperatures, (6) 195.
Strock, L. W., spectrum analysis with carbon arc cathode layer, (6) 186.
Stuckert, L., lithium oxide enamels highly resistant to acids as components of glazes and different opacifiers, (3) 77.
Stuckey, J. L., and Amero, J. J., physical properties of massive topaz, (8) 254.
Stull, R. T., and Johnson, P. V., properties of pore system in brick and their relation to frost action, (4) 127.
Sun, K.-H., and Silverman, Alexander, tantalum glass, $K_2O–Ta_2O_5–SiO_2$ series, (1) 6.
Swank, H. A., and Mellon, M. G., calculator for obtaining tristimulus values from spectrophotometric data, (3) 73.

Tammann, G., behavior of glasses in their softening interval, (6) 189; Glaszustand (glass state), (6) 191.
Tammann, G., and Boehme, W., temperature dependence of dielectric constants of some glasses in softening range, (6) 189.
Taylor, H. S., treatise on physical chemistry, Vol. II, (8) 277.
Taylor, N. W., and Dear, P. S., elastic and viscous properties of several soda-silica glasses in annealing range of temperature, (6) 190.
Taylor, N. W., and Lin, C.-Y., effect of various catalysts on conversion of quartz to cristobalite and tridymite at high temperatures, (6) 178.
Taylor, N. W., McNamara, E. P., and Sherman, J., elastico-viscous properties of soda-lime-silica glass at temperatures near "transformation point," (6) 190.
Taylor, N. W., and Rast, William, diffusion of helium and of hydrogen through Pyrex-brand chemically resistant glass, (6) 190.
Tennessee Valley Authority, Minerals Testing Lab., olivine analysis, (12) 406.
Thiemecke, Harry, thermal and moisture expansion of kaolins and bodies fired to different temperatures, (6) 173.
Thiene, Hermann, Glas, Vol. I, (8) 277.
Thiess, L. E., influence of glaze composition on mechanical strength of electrical porcelain, (3) 93; steatite ware as ceramic furnace material, (3) 99.
Thilo, E., and Rogge, Gerhard, chemical investigation of silicates, thermal transformation on anthrophyllite, $Mg_7Si_8O_{22}(OH)_2$, polymorphism of magnesium metasilicate and mechanism of transformation of anthrophyllite and talc on heating, VIII, (10) 333.
Thompson, C. L., and Wilcox, H. G., high-temperature gas-fired test furnace, (11) 376.
Thurnauer, Hans, cordierite gives low thermal expansion in ceramic bodies, (3) 99; review of ceramic materials for high-frequency insulation, (3) 99, (10) 337.
Thurnauer, Hans, and Badger, A. E., dielectric loss of glass at high frequencies, (10) 337.
Tilley, C. E., wollastonite solid solutions from Scawt Hill, County Antrim, (9) 299.
Tomaschek, R., applications of phosphorescence spectra to investigation of structure of solids and solutions, (5) 140.
Tomaschek, R., and Deutschbein, O., Erschliessung der Glasstruktur aus Fluoreszenzbeobachtungen, (5) 140.
Tool, A. Q., analytical representation concerning glass in its glass annealing range, (8) 270.
Tool, A. Q., and Eichlin, C. G., absorption of heat in glass, (6) 189.
Tool, A. Q., Tilton, L. W., and Hill, E. E., heat-treatment of glass, its refractivity and density, (6) 193.
Tool, A. Q., Tilton, L. W., and Saunders, J. B., effect of heat-treatment on refractive index of glass, (6) 193.
Tool, A. Q., and Valasek, J., concerning annealing and characteristics of glass, (6) 189.
Trömel, G., investigations in three-component system $CaO–P_2O_5–SiO_2$ and their significance for production of Thomas slag, (9) 303.
Trostel, L. J., quartz as a devitrification product of vitreous silica, (9) 287 (reference to be substituted for Trostel and Wynn reference on same page).
Trostel, L. J., and Wynn, D. J., determination of quartz (free silica) in refractory clays, (9) 287 (for a correction on this reference, see Trostel, L. J.).
Tscheischwilli, L., Büssem, W., and Weyl, W., Metakaolin, (4) 108.
Turner, W. E. S., and Winks, F., casing of colorless by cobalt blue glass, thermal expansion, I, (12) 398; thermal expansion of glass, general form of expansion curve, I, (6) 190.
Twells, Robert, Jr., field of porcelain glazes maturing between cones 17 and 20, (7) 205; further studies of porcelain glazes maturing at high temperatures, (7) 205; progress report on use of andalusite as a refractory, (8) 255.

Van Dusen, M. S., thermal conductivity of heat insulators, (10) 340.
Vasenin, F. I., phase equilibrium in system $CaO·Cr_2O_3–CaO·Al_2O_3$, (1) 24; reciprocal action of CaO and Cr_2O_3 on heating, I, (1) 24.
Veatch, Otto, second report on clay deposits of Ga., (4) 106.
Veatch, Otto, and Stephenson, L. W., preliminary report on geology of coastal plain of Ga., (4) 106.
Vielhaber, L., lithium in enamels, (3) 77.
Vogt, J. H. L., Silikatschmelzlösungen, (9) 298.

Wainer, Eugene, and Dubois, E. M., spectrographic analysis of enamel frits, (6) 186.
Warburg, E. v., diffusion of metal in glass, (8) 268.
Ward, R., and Struthers, J. D., reactions in solid state, reactions between barium carbonate and ferric oxide in presence of oxygen, I, (7) 240.
Waring, C. E., and Robison, G., experimental details for precision high-temperature control utilizing the Hull circuit, (7) 240.
Warren, B. E., X-ray diffraction of vitreous silica, (12) 395.
Warren, B. E., and Biscoe, J., structure of silica glass by X-ray diffraction studies, (12) 395.
Warren, B. E., and Burwell, J. T., structure of rhombic sulfur, (12) 385.

Wartenberg, H. v., and Gurr, W., melting diagrams of refractory oxides, zirconium oxides, (1) 23.
Wartenberg, H. v., and Reusch, H. J., melting diagram of refractory oxides, aluminum oxide, IV, (1) 34.
Wartenberg, H. v., Reusch, H. J., and Saran, E., melting diagram of refractory oxides, calcium oxide, (1) 23.
Washburn, E. W., and Bunting, E. N., porosity, determination: by gas-expansion method, VI, (4) 147; of highly vitrified bodies, VII, (4) 127.
Waterton, S. C., and Turner, W. E. S., properties of mixed alkali-lime-silica glasses containing lithia, soda, potash, and rubidia, (3) 77.
Watkins, J. H., kyanite in Graves Mountain, Ga., (8) 253.
Watts, A. S., study of Bristol glazes compounded on eutectic basis, (7) 205.
Weckerle, Hermann, Anfärbung von Gläsern durch Kupfer, Selen, und Schwefel, (2) 58.
Weigert, G., optische Methoden der Chemie, (5) 150.
Weinland, C. E., celite-type high-temperature thermal conductivity apparatus, (10) 340; method of measuring thermal conductivity at furnace temperature, (10) 340; thyratron voltage regulator for alternator, (10) 341.
Wentrup, H., formation of inclusions in steel, (1) 11.
Wessels, Herman, thermolysis, Ludwig-Soret phenomena in solid states, (8) 269.
Westman, A. E. R., and Hugill, H. R., packing of particles, (1) 35.
Weyl, W. A., Beitrag zur Fluoreszenz der Gläser, (5) 140.
Weyl, W. A., and Thümen, E., Konstitution und Farbe der Uran gläser, (5) 139.
White, W. P., calorimetry in furnaces, (10) 339.
Whiteley, J. H., inclusions in series of bath samples from electric furnace and note on sulphides, (1) 11.
Whittaker, H., effect of particle size on plasticity of kaolinite, (3) 91.
Wiehr, Hartmut, Kristallisation von einfachen Natriumsilikatgläser, (5) 140.
Wilkes, G. B., and Wood, C. V., specific heat of thermal insulating materials, (10) 347.
Wilson, E. O., plasticity of finely ground minerals with water, (3) 91.
Wilson, Hewitt, comparative load tests on silica brick, (11) 375; high-temperature load and fusion tests of firebrick from Pacific northwest in comparison with other well-known firebrick, (8) 263.
Wilson, Hewitt, and Skinner, K. C., review of four years of research on refractory properties of Pacific northwest olivine, (12) 405.
Winchell, A. N., elements of optical mineralogy, description of minerals, II, (12) 405; microscopic characters of artificial inorganic substances or artificial minerals, (12) 405.
Winter (Winter-Klein) Aniuta, causes and effects of phenomena when glass is quenched, I-II, (6) 191; transformation region of glass, (8) 277.
Wood, R. W., physical optics, (5) 150.
Wray, G. W., and Brand, C. M., comparative tests of chinaware using two forms of testing machines, (10) 337.
Wyckoff, R. W. G., crystal structure of high-temperature (β) modification of quartz, (12) 395; Kriterien für hexagonale Raumgrupten und die Kristallstruktur von β-Quartz, (12) 395.

Young, J. C., and Finn, A. N., comparison of two recent studies on refraction and dispersion of glasses, (1) 4; effect of composition and other factors on specific refraction and dispersion of glasses, (1) 6.

Zachariasen, W. H., atomic arrangement in glass, (12) 395.
Zapffe, C. A., and Faust, C. L., metallurgical aspects of hydrogen in electroplating, (5) 155.
Zapffe, C. A., and Sims, C. E., hydrogen embrittlement, internal stress, and defects in steel, (5) 152; relation of defects in enamel coatings to hydrogen in steel, (5) 151.
Zapffe, C. A., and Yarne, J. L., relation of surface oxidation to certain defects in enamel coatings on steel, III, (5) 151.
Zehnder, H., principle of gas-expansion method, (4) 127.

OFFICIAL PERSONNEL OF DIVISIONS AND CLASSES, 1943–1944

	Design	Enamel	Glass	Materials and Equipment	Refractories	Structural Clay Products	White Wares
Trustee	C. W. Read	R. L. Fellows	G. W. Morey	J. E. Eagle	J. B. Austin	Frederick Heath, Jr.	F. P. Hall
Chairman	W. A. Weldon	D. G. Bennett	J. F. Greene	E. M. Rupp	C. L. Thompson	L. R. Whitaker	J. R. Beam
Vice-Chairman	Theodore Lenchner	H. D. Carter	K. C. Lyon	J. R. Kauffman	W. R. Kerr	C. P. Austin	
Secretary	Myrtle M. French	D. G. Moore	S. R. Scholes	J. F. Day	S. M. Swain	R. L. Stone	J. W. Whittemore
Division Nominations		F. R. Porter M. J. Bahnsen E. E. Howe	E. W. Tillotson U. E. Bowes R. A. Miller	S. S. Cole J. F. McMahon	R. S. Bradley P. G. Herold	J. H. Isenhour W. C. McGolpin J. G. Seanor	Donald Hagar R. E. Gould
Papers and Program	H. E. Simpson Rexford Newcomb, Jr.	H. D. Carter	K. C. Lyon	V. J. Roehm	E. E. Callinan C. L. Norton, Jr. E. B. Read C. A. Freeman	V. W. Boeker A. C. Jackson H. K. Lynn	C. M. Lambe, Jr. E. P. McNamara
Membership	Theodore Lenchner	J. F. Hunt	R. R. Shively	D. E. Walsh	G. B. Remmey S. F. Walton W. P. Charbonnier A. R. Blackburn	R. R. Robinson A. C. Christopher	John D. Clark
Standards		R. L. Cook W. N. Harrison W. W. Higgins R. M. King F. A. Petersen	F. W. Adams H. P. Hood K. M. Henry	J. S. Breitenstein		E. F. Theobald A. W. Hough	F. P. Hall
Research		J. C. Reimers	H. R. Lillie Alexander Silverman W. R. Lester	R. R. Robinson	D. W. Ross	H. C. Plummer H. G. Schurecht	*Ball clay:* Ralston Russell, Jr. *Steatite:* Glenn Howatt
Classification and Nomenclature	Mrs. J. W. Dixon	G. H. McIntyre	E. P. McNamara	R. G. Janatka	C. M. Dodd	C. F. Wiseman R. E. Grim Morriss Corbman	A. S. Watts J. R. Beam Ralston Russell, Jr. Harry Thiemecke E. K. Koos
Rules		W. A. Deringer	S. R. Scholes	Philip Dressler	S. F. Walton	Howells Frechette	Don Postlewaite
Councillors		J. D. Tetrick Karl Kautz	F. C. Flint R. W. Wampler	V. V. Kelsey		R. A. Shipley C. F. Tefft	
Exhibitions			J. E. Frazier				
Industrial Management			C. J. Uhrmann	C. L. Cruikshank	O. L. Jones	J. C. Peck	A. A. Wells
Bibliography		J. E. Rosenberg					

	Institute of Ceramic Engineers	Ceramic Educational Council
President	H. B. DuBois	R. M. Campbell
Vice-President	R. F. Sherwood	C. M. Dodd
Secretary	Karl Schwartzwalder	E. C. Henry

JOURNAL

of

The American Ceramic Society

A Monthly Journal Devoted to the
Arts and Sciences Related to
the Silicate Industries

Volume 26, 1943

Ross C. Purdy, *Editor*
Emily C. Van Schoick, *Assistant Editor*

Committee on Publications: John D. Sullivan, *Chairman;* H. H. Blau, J. J. Canfield, R. L. Stone, H. Thiemecke, and *(ex officio)* Ross C. Purdy

Editorial and Advertising Offices: 2525 North High Street, Columbus 2, Ohio
Publication Office: Easton, Pennsylvania

THE AMERICAN CERAMIC SOCIETY TRUSTEES AND OFFICERS FOR 1943–1944

President: C. E. Bales, Ironton Fire Brick Co., Ironton, Ohio.
Vice-President: E. H. Fritz, Stupakoff Ceramic & Mfg. Co., Latrobe, Pa.
Treasurer: C. Forrest Tefft, The Claycraft Co., Columbus, Ohio
Secretary-Editor: R. C. Purdy, 2525 North High St., Columbus, Ohio
Past-President: L. J. Trostel, General Refractories Co., Baltimore, Md.
Past-President: J. T. Littleton, Corning Glass Works, Corning, N. Y.

TRUSTEES FROM INDUSTRIAL DIVISIONS*

Design: C. W. Read, Shenango Pottery Co., New Castle, Pa. (1946)
Enamel: R. L. Fellows, Chicago Vitreous Enamel Product Co., Cicero, Ill. (1946)
Glass: G. W. Morey, Geophysical Laboratory, Washington, D. C. (1944)
Materials and Equipment: J. E. Eagle, 6306 20th Ave., Green Meadows, Hyattsville, Md. (1945)
Refractories: J. B. Austin, U. S. Steel Corp., Kearny, N. J. (1946)
Structural Clay Products: Frederick Heath, Jr., Owens-Corning Fiberglas Corp., Toledo, Ohio (1945)
White Wares: F. P. Hall, Onondaga Pottery Co., Syracuse, N. Y. (1944)
Institute of Ceramic Engineers: H. G. Wolfram, Pemco Corp., Baltimore, Md. (1944)
Ceramic Educational Council: J. W. Whittemore, Virginia Polytechnic Institute, Blacksburg, Va. (1944)

* Date of expiration of term of office in parentheses.

DIVISION OFFICERS

Design
Chairman: W. A. Weldon, Locke Insulator Corp., Baltimore, Md.
Secretary: Myrtle M. French, Art Institute of Chicago, Chicago, Ill.

Enamel
Chairman: D. G. Bennett, Mellon Institute, Pittsburgh, Pa.
Secretary: D. G. Moore, National Bureau of Standards, Washington, D. C.

Glass
Chairman: J. F. Greene, Kimble Glass Co., Vineland, N. J.
Secretary: S. R. Scholes, N. Y. State College of Ceramics, Alfred, N. Y.

Materials and Equipment
Chairman: E. M. Rupp, National Engineering Co., 58 Fallis Rd., Columbus, Ohio
Secretary: J. F. Day, Donald Hagar Ceramic Materials, Zanesville, Ohio

Refractories
Chairman: C. L. Thompson, Harbison-Walker Refractories Co., Pittsburgh, Pa.
Secretary: S. M. Swain, North American Refractories Co., Cleveland, Ohio

Structural Clay Products
Chairman: L. R. Whitaker, Carolina Ceramics, Inc., Columbia, S. C.
Secretary: R. L. Stone, Dept. of Ceramic Engineering, Univ. of North Carolina, Raleigh, N. C.

White Wares
Chairman: J. R. Beam, Universal Sanitary Mfg. Co., New Castle, Pa.
Secretary: J. W. Whittemore, Virginia Polytechnic Institute, Blacksburg, Va.

OFFICERS OF THE FELLOWS

Dean: R. B. Sosman, U. S. Steel Corp., Kearny, N. J.
Associate Dean: Howells Frechette, Bureau of Mines, Ottawa, Ontario, Canada.
Secretary-Treasurer: R. M. King, Ohio State University, Columbus, Ohio

INSTITUTE OF CERAMIC ENGINEERS

President: H. B. DuBois, Consolidated Feldspar Corp., Trenton, N. J.
Vice-President: R. F. Sherwood, United Feldspar & Minerals Corp., New York, N. Y.
Secretary: Karl Schwartzwalder, A C Spark Plug Co., Flint, Mich.

CERAMIC EDUCATIONAL COUNCIL

President: R. M. Campbell, N. Y. State College of Ceramics, Alfred, N. Y.
Vice-President: C. M. Dodd, Iowa State College, Ames, Iowa
Secretary: E. C. Henry, Pennsylvania State College, State College, Pa.

LOCAL SECTIONS

Baltimore-Washington
Chairman: D. G. Moore, National Bureau of Standards, Washington, D. C.
Secretary: J. C. Richmond, National Bureau of Standards, Washington, D. C.

Central Ohio
Chairman: H. J. Orlowski, O.S.U. Engr. Expt. Sta., Columbus, Ohio
Secretary: A. C. Jackson, The Claycraft Co., Columbus, Ohio

Chicago
Chairman: Hugo Filippi, 228 N. LaSalle St., Chicago, Ill.
Secretary: J. J. Svec, Industrial Publications, Inc., 59 E. VanBuren St., Chicago, Ill.

Michigan-Northwestern Ohio
Chairman: J. F. Quirk, A C Spark Plug Co., Flint, Mich.
Secretary: W. V. Blake, Macklin Co., Jackson, Mich.

Northern California
President: W. V. Bragdon, California Faience Co., Berkeley, Calif.
Secretary: P. C. Valentine, Del Monte Properties Co., San Francisco, Calif.

Pacific-Northwest
President: Howard Mansur, Washington Brick & Lime Co., Spokane, Wash.
Secretary: J. A. Pask, Univ. of Washington, Seattle, Wash.

Pittsburgh
Chairman: E. E. Marbaker, Mellon Institute, Pittsburgh, Pa.
Secretary: H. E. Simpson, Mellon Institute, Pittsburgh, Pa.

Southern California
Chairman: R. H. Martin, Vernon Kilns, Los Angeles, Calif.
Secretary: W. O. Brandt, Gladding, McBean & Co., Los Angeles, Calif.

St. Louis
Chairman: H. H. Hanna, Pittsburgh Plate Glass Co., Crystal City, Mo.
Secretary: J. H. Ivery, Hydraulic Press Brick Co., St. Louis, Mo.

TABLE OF CONTENTS

for

Volume 26, 1943

January [No. 1], pp. 1–40

1. G. H. Spencer-Strong and W. G. Cooper: Gouge Resistance of Porcelain Enamels 1–4
2. M. L. Huggins and K.-H. Sun: Calculation of Density and Optical Constants of Glass from Its Composition in Percentage of Weight 4–11
3. R. B. Snow: Equilibrium Relationships on Liquidus Surface in Part of MnO–Al_2O_3–SiO_2 System 11–20
4. G. R. Pole and A. W. Beinlich, Jr.: New Refractory Compositions Resistant to Molten Rock Phosphate 21–37
5. E. C. Henry: Measurement of Workability of Ceramic Bodies for Plastic Molding Processes 37–39

February [No. 2], pp. 41–72

6. R. M. King: Mechanics of Enamel Adherence: XIV, (1) Role of Cobalt Oxide in Metal and Oxide Precipitation During Ground-Coat Firing Cycle, and (2) Determination of Temperature and Time Intervals of Precipitation 41–48
7. W. J. Knapp: Thermal Conductivity of Nonmetallic Single Crystals 48–55
8. H. C. Hafner and F. L. Jones: Adsorption of Ions by Leached Surface Films on Glass 55–56
9. F. L. Jones and H. C. Hafner: Effect of Chemically Formed Surface Films on Glass Solubility 56–58
10. Henry Moore and S. R. Scholes: Amber Glass and Role of Carbon 58–60
11. H. D. Foster: Salt Glazes for Structural Building Units 60–67
12. A. E. Currier: Influence of Sodium Silicate Composition on Its Behavior with Sodium Carbonate as a Casting Slip Deflocculant 67–71

March [No. 3], pp. 73–104

13. R. L. Cook and A. I. Andrews: Fundamental Study of Factors Influencing Color of Porcelain Enamels 73–76
14. M. O. Lewis: Effects of Lithia Substitution for Soda in Vitreous Enamel 77–83
15. W. W. Grigorieff and C. M. Lampman, Jr.: Sealed Glass Bushings 83–87
16. A. L. Johnson: Colloid Chemistry in Ceramics 88–92
17. H. G. Schurecht: Fitting Glazes to Ceramic Bodies 93–98
18. L. E. Thiess: Vitrified Cordierite Bodies 99–102

April [No. 4], pp. 105–36

19. Lane Mitchell and E. C. Henry: Nature of Georgia Kaolin: I, Evidence of Chemical and Colloidal Analysis 105–13
20. Lane Mitchell and E. C. Henry: Nature of Georgia Kaolin: II, Evidence of Mineralogical Analysis. 113–19
21. L. H. Berkelhamer: Rehydration Study of Clays 120–26
22. J. C. Richmond, J. B. Peterson, and W. H. Herschel: Improved Volumenometer 127–31
23. H. W. Smith, Jr., and J. A. Ehlinger: Direct Radiant Kiln Firing in the Ceramic Industry 132–36

May [No. 5], pp. 137–72

24. A. R. Rodriguez, C. W. Parmelee, and A. E. Badger: Study of Photoluminescence in Glass 137–50
25. W. A. Deringer: Relation of Hydrogen to Adherence of Sheet-Steel Enamels 151–59
26. R. L. Fellows: Relation of Thickness to Impact Resistance of Porcelain Enamel 160–62
27. T. E. Nicholson and F. L. Goin: Simplified Thermal-Expansion Rings for Production Control in Terra Cotta Manufacture 163–67
28. L. S. Longenecker: Possible Use of Suspended Roofs and Walls in Glass Furnaces 167–72

June [No. 6], pp. 173–204

29. H. Thiemecke: Thermal and Moisture Expansion of Ball Clays and Bodies Fired to Different Temperatures 173–79
30. H. R. Shell and W. P. Cortelyou: Soluble Sulfate Content of Pottery Bodies During Preparation 179–85
31. A. E. Austin and L. B. Bassett: Spectrochemical Procedure in Clay Analysis 185–88
32. Aniuta Winter: Transformation Region of Glass 189–200
33. A. K. Lyle: Theoretical Aspects of Chemical Attack of Glasses by Water 201–204

July [No. 7], pp. 205–48

34. J. R. Beam: Effect of Opacifiers on Fused Viscosity of Feldspathic Glazes 205–12
35. H. G. Schurecht and J. F. McMahon: Use of Aluminum Metal in the Ceramic Industry: II, Effect of Coating Insulating Firebrick with Aluminum–Fire-Clay Mixtures 212–17
36. G. E. Seil and Staff: Study of Literature on Separation of Magnesia from Lime in Dolomite and Similar Materials 218–38
37. George Gibson and Roland Ward: Reactions in Solid State: III, Reaction Between Sodium Carbonate and Quartz 239–46

August [No. 8], pp. 249–84

38. G. H. Spencer-Strong and W. G. Cooper: Experiments with Accelerated Weathering Test for Porcelain Enamels 249–51
39. T. N. McVay and Hewitt Wilson: Substitution of Topaz, Domestic Kyanite, and Synthetic Mullite-Corundum for India Kyanite, I–III 252–66
40. J. A. Pask and C. W. Parmelee: Study of Diffusion in Glass 267–77
41. Aniuta Winter: Structural Homogeneity of Glass 277–84

September [No. 9], pp. 285–320

42. N. L. Bowen: Petrology and Silicate Technology 285–301
43. Samuel Zerfoss and H. M. Davis: Observations on Solid-Phase Inversions of Calcium Orthosilicate, Constituent of Dolomite-Silica Brick 302–307
44. H. C. Plummer and E. F. Wanner: Modular Size of Clay-Products Units 307–20

October [No. 10], pp. 321–60

45. E. F. Osborn: Compound Merwinite ($3CaO \cdot MgO \cdot 2SiO_2$) and Its Stability Relations Within System $CaO–MgO–SiO_2$ (Preliminary Report) 321–32
46. R. L. Stone: Physical Chemistry of Firing Steatite Ceramics 333–36
47. Sidney Speil: Physical Testing of Talc for High-Frequency Ceramics 336–38
48. J. R. Winckler: Spherical Furnace Calorimeter for Direct Measurement of Specific Heat and Thermal Conductivity 339–49
49. T. C. Patton and C. L. Norton, Jr.: Measurement of Thermal Conductivity of Fire-Clay Refractories 350–58
50. R. M. King: Mechanics of Enamel Adherence: XV, Influence of Cobalt and Nickel Oxides on Metal Precipitation at Ground Coat-Iron Interface 358–60

November [No. 11], pp. 361–92

51. F. A. Harvey and C. L. Thompson: Mottled Silica Brick, Facts, Fancies, and Fallacies 361–64
52. J. S. McDowell: Plant Investigation of Variables Affecting Color of Silica Brick 364–67
53. L. J. Trostel: Factors Influencing Staining of Silica Brick 368–73
54. F. A. Harvey: Influence of Water Vapor on Silica Brick at High Temperatures 373–77
55. S. M. Phelps and R. W. Limes: Mottled or Colored Silica Brick 378–87
56. F. H. Norton and W. G. Lawrence: Note on Anomalous Heat Absorption of Kaolinite 388–89
57. L. E. Kane and H. G. Ueltz: Possible Use of Ferruginous Talcs in Steatite Dielectrics 389–92

December [No. 12], pp. 393–434

58. M. L. Huggins, K.-H. Sun, and Alexander Silverman: Vitreous State 393–98
59. H. H. Holscher, R. R. Rough, and J. H. Plummer: Experimental Studies of Temperature Gradients in Glasses of Various Colors 398–404
60. Electrothermal Section of the Electrotechnical Laboratory: Electrically Fused Forsterite-Olivine, I–II 405–13
61. R. B. Fuller and A. S. Watts: Duplication of Chrome-Brown Electrical Porcelain Glazes with Non-essential Materials 414

Author Index to *The Journal* 415–16
Subject Index to *The Journal* 416–24
Footnote Citations Index to *The Journal* 424–29